

SPOTs: A Novel Mitochondrial Response to Stress at the Outer Mitochondrial Membrane

Inaugural-Dissertation

zur

Erlangung des Doktorgrades

der Mathematisch-Naturwissenschaftlichen Fakultät

der Universität zu Köln



vorgelegt von

Li Xianhe (李显赫)

aus China

Veröffentlichung: Köln, 2023

Berichterstatter: Dr. Lena F. Pernas

(Gutachter) Prof. Dr. Thomas Langer

Prof. Dr. Hamid Kashkar

Tag der mündlichen Prüfung: 20.01.2023

Zwei Dinge erfüllen das Gemüt mit immer neuer und zunehmender
Bewunderung und Ehrfurcht, je öfter und anhaltender sich das
Nachdenken damit beschäftigt:

Der bestirnte Himmel über mir,
und das moralische Gesetz in mir.

Two things fill the mind with ever new and increasing admiration and
awe, the more often and steadily we reflect upon them:
the starry heavens above me and the moral law within me.

这个世界惟有两样东西让我们的心灵感到深深的震撼，
是头顶上灿烂的星空，
是内心崇高的道德法则。

——Immanuel Kant

Content

1. List of abbreviations.....	1
2. Abstract.....	4
3. Introduction.....	6
3.1 Mitochondrial function.....	8
3.1.1 Mitochondrial ATP production.....	8
3.1.2 Mitochondrial metabolite synthesis.....	11
3.1.3 Mitochondrial regulation of cell death.....	13
3.1.4 Innate immune signaling.....	14
3.2 Mitochondrial dynamics.....	16
3.2.1 Mitochondrial fission.....	16
3.2.2 Mitochondrial fusion.....	17
3.3 Mitochondrial structure.....	19
3.3.1 Mitochondrial structure.....	19
3.3.2 MIB—the bridge between the OMM and IMM.....	20
3.4 Mitochondrial biogenesis: insights into protein import.....	22
3.4.1 Presequence carrying mitochondrial precursors.....	22
3.4.2 Non-presequence containing mitochondrial precursors.....	23
3.4.3 Cysteine motif-containing precursors.....	23
3.4.4 OMM protein biogenesis.....	24
3.5 Mitochondrial quality control.....	26
3.5.1 Mitochondrial proteostasis.....	26
3.5.2 The ubiquitin-proteasome system (UPS) and mitophagy.....	27
3.5.3 Mitochondrial-derived vesicles (MDVs).....	28
3.6 Modulation of mitochondria during microbial infection.....	31
3.6.1 Mitochondrial dynamics during infection.....	31
3.6.2 Modulation of mitochondrial functions upon infection.....	32
3.6 <i>Toxoplasma gondii</i> : a competitor to host mitochondria?.....	34
3.6.1 <i>Toxoplasma gondii</i> : a very successful human parasite.....	34
3.6.2 The parasitophorous vacuole (PV) of <i>Toxoplasma</i>	35
3.6.3 The Host Mitochondria Association (HMA) with PVM.....	37
4. Publication.....	40
5. Discussion.....	87

6. Reference	92
7. Acknowledgements.....	112
8. Curriculum vitae	113
9. Erklärung	116

1. List of abbreviations

1C	One-carbon
APAF1	Apoptotic peptidase activating factor 1
ASP5	Aspartyl protease 5
ATP	Adenosine triphosphate
Bax	Bcl-2-associated X
BCL2	B cell lymphoma 2
CJs	Cristae junctions
CMT2A	Charcot Marie Tooth 2A
CoA	Coenzyme A
CoQ	Hydrophobic ubiquinone
CPT1	Carnitine palmitoyltransferases 1
CTP	Citrate transporters
Cyt c	Cytochrome c
DENV	Dengue virus
DHO	Dihydro-orotate
DHODH	Dihydroorotate dehydrogenase
DOA	Dominant optic atrophy
EMRE	Essential MCU regulator
ETC	Electron transport chain
ETF	Electron-transferring flavoprotein
FAD	Flavin adenine dinucleotide
FAF2	Fas-associated factor family member 2
FAO	Fatty acid β -oxidation
FAs	Fatty acids
FASN	Fatty acid synthase
Fe-S	Iron-sulphur
fMet	Factor 2 exclusively uses the N-formylated methionine
FPR	Formyl peptide receptor
GPIs	Glycosylphosphatidylinositol proteins
GPX4	Glutathione peroxidase 4
GS	Glutamine synthetase
HMA	Host mitochondrial association
HR	Heptad repeat
HSV	Herpes simplex virus
IBM	Inner boundary membrane
IFNs	Interferons
IMM	Inner mitochondrial membrane
IMP	Inner membrane protease
iMTS	Internal mitochondrial targeting signals

LC3	Microtubule-associated protein 1A/1B-light chain 3
LCV	Legionella-containing vacuole
LLO	Listeriolysin O
MAF1b	Mitochondria association factor 1B
MAPL	Mitochondrial-anchored protein ligase
MAVS	Mitochondrial antiviral signaling
MCU	Mitochondrial calcium uniporter
mDAMPs	Mitochondria-derived components
MDH1	Malate dehydrogenase
MDVs	Mitochondrial-derived vesicles
MERCS	Mitochondria-ER contact sites
Metaxin	MTX
MFN	Mitofusin
MHC I	Class I major histocompatibility complex
MIB	Mitochondrial intermembrane space bridging
MICOS	Mitochondrial contact site and cristae organizing system
MIM	Mitochondrial import machinery
MIP	Mitochondrial intermediate peptidase
MLKL	Mixedlineage kinase domainlike pseudokinase
MOMP	Mitochondrial outer membrane permeabilization
MPP	Mitochondrial processing peptidase
mtFAS	Mitochondrial fatty acid synthesis
MTHFD2	Methylenetetrahydrofolate dehydrogenase
mtHsp70	Mitochondrial heat-shock protein 70
MTS	Mitochondrial targeting sequence
MVBs	Multivesicular bodies
MYR1	Myc regulation 1
NS4B	Nonstructural protein 4B
OAA	Oxaloacetate
OAT	Ornithine amino transferase
OMM	Outer mitochondrial membrane
OXPHOS	Oxidative phosphorylation
P5C	Pyrroline-5-carboxylate
P5CS	Pyrroline-5-carboxylate synthase
PAM	Presequence translocase-associated motor
PARL	Presenilin-associated rhomboid-like protease
PC	Pyruvate carboxylase
PCK	Phosphoenolpyruvate carboxykinase
PEP	Phosphoenol pyruvate
Pi	Inorganic phosphate
PINK1	PTEN-induced kinase 1

PMF	Proton-motive force
PV	Parasitophorous vacuole
PVM	PV membrane
PYCR	Pyrroline-5-carboxylate reductase
RIG-I	Retinoic acid-inducible gene I
RIPK1/3	Receptor interacting protein kinase 1/3
RLRs	RIG-I-like receptors
ROS	Reactive oxygen species
SAM	Sorting assembly machinery
SHMT2	Serine hydroxymethyltransferase
SNX9	Sorting nexin 9
T2D	Type 2 diabetes
T4SS	Type IV secretion system
TBK1	TANK (TRAF family member-associated NF- κ B activator)-binding kinase 1
TgMAF1	Toxoplasma mitochondrial association factor 1
THF	Tetrahydrofolate
TIM	Translocase of the inner membrane
TNF	Tumour necrosis factor
TOM70	Translocase of the outer membrane 70
TPRs	Tetratricopeptides repeat motifs
UPS	Ubiquitin-Proteasome System
VacA	Vacuolating cytotoxin A
VDAC	Voltage-dependent anion-selective channel protein
VDACs	Voltage-dependent anion channels
α -KG	α -ketoglutarate
$\Delta\psi$	Electric charge

2. Abstract

Mitochondria are essential organelles with multiple functions, including energy production, metabolic homeostasis, programmed cell death, and immune signaling[1], [2]. Because of their diverse functions, mitochondria have complex quality control systems and intricate coordination cellular processes with other organelles. The outer mitochondrial membrane (OMM) is considered the gateway between mitochondria and the rest of the cell and ensures its homeostasis[3]. Although the OMM responses to artificial drugs have been described, whether the OMM responds to natural stress remains unknown.

Infection is an ideal model to study the occurrence of natural OMM stress due to effector proteins secreted by pathogens that affect the OMM. *Toxoplasma gondii* (*Toxoplasma*) is of particular interest due to the physical contact between the parasite vacuole and the OMM of the host mitochondria. To address how *Toxoplasma* affected the OMM, we infected OMM-targeted GFP expressing mammalian cells with *Toxoplasma* and observed the OMM response by live-cell imaging.

We found that mitochondria in contact with the *Toxoplasma* vacuole released large structures which we termed “SPOTs” (structures positive for OMM). SPOTs were positive for OMM but lacked markers of the inner mitochondrial membrane (IMM) and matrix and have an average size of 2.6 μm . TgMAF1 (*Toxoplasma* mitochondrial association factor 1), which is required for the contact between host mitochondria and parasite vacuole, was required for SPOT formation and led to the decrease of the OMM dynamic-related proteins Mitofusin (MFN) 1 and 2 - which mediate a nutritional defense against *Toxoplasma* by promoting mitochondrial uptake of fatty acids.

SPOT formation induced by TgMAF1 also depends on its binding to the host OMM protein TOM70 (translocase of the outer membrane 70), whose role as a receptor of mitochondrial precursor proteins is impaired by the interaction. TOM70 was beneficial for parasite growth and enabled the interaction between TgMAF1 and the OMM translocase SAM50 (sorting assembly machinery 50 kDa subunit). SAM50 is the only known component of host mitochondrial import machinery with a defined role in

bridging the OMM and IMM. In the absence of infection, the genetic ablation of SAM50 or the overexpression of an OMM-targeted protein induced the formation of SPOT structures.

Collectively, these results support a model in which OMM stress is triggered by TgMAF1 which sequesters the mitochondrial precursor receptor TOM70 and interacts with SAM50 during infection. This enables *Toxoplasma* to hijack a cellular response to OMM stress—the formation of SPOTs—and drive the constitutive shedding of the OMM. The finding of OMM remodeling during infection and infection-independent scenarios sheds light on potential cellular mechanisms that safeguard OMM function.

3. Introduction

Mitochondria were first described by Richard Altmann in 1890, termed “Bioblasts”. In 1898, Carl Benda gave the current name “mitochondrion” from Greek, “mitos” meaning thread and “chondros” meaning grains [4]. In the early 20th century, pioneering biochemical analysis revealed a function for mitochondria as the “powerhouse of the cell”. In 1967, Lynn Margulis postulated that mitochondria were once a free-living prokaryote that were engulfed by a larger prokaryote. During evolution, and in a process now termed endosymbiosis, these ancestors of mitochondria became functional parts of those cells but retained their DNA [5]. Indeed, recent phylogenetic analyses support that mitochondria are derived from an endosymbiotic α -proteobacterium that integrated into a host cell related to Asgard Archaea [6].

Mitochondrial structure is different among the other organelles in the cell because they have a unique double-membrane structure and several compartments including the OMM (outer mitochondrial membrane), IMS (inner mitochondria space), IMM (inner mitochondria membrane), and matrix. These allow mitochondria to import and target their 1000+ proteins to independent niches through the complex import systems[7]. Moreover, mitochondrial quality control systems are essential to ensure a healthy mitochondrial network through the clearance of damaged mitochondria, and turnover of dysfunctional proteins [8]. These multi-sides together sustain the mitochondrial integrity and shape itself as the key player in various cellular processes.

Previously considered to be the ‘powerhouse’ of the cell, mitochondria are now recognized as multifaceted players in metabolite synthesis, cell death, neuron degeneration, and immune signaling. These diverse functions rely on the sustained mitochondria network, which undergoes the cycles of fusion and fission to regulate the equilibrium in shape, size, and distribution[9]. This dynamic network enables the biogenesis, maintenance and remove of mitochondria in the cellular homeostasis [10]. Recent work suggests that mitochondria—beyond their roles in cellular homeostasis—also play a role in defense against microbes. For example, the intracellular protozoan human parasite *Toxoplasma gondii* (*Toxoplasma*) uses host nutrients to grow and

proliferate. Host mitochondria counter parasitic siphoning of nutrients by elongating and increasing their uptake of fatty acids [11]. Interestingly, host mitochondria also exhibit physical contact with the *Toxoplasma* PV (parasitophorous vacuole). We used *Toxoplasma*-infection to investigate more broadly how mitochondria respond to intracellular infection.

This chapter introduces the fundamental characteristics and diverse functions of mitochondria, and discusses the crosstalk between host mitochondria and *Toxoplasma*.

3.1 Mitochondrial function

Mitochondria are now recognized as organelles that are essential for life and that perform diverse metabolic functions including ATP production, metabolite synthesis as well as having a role in signaling pathways. The first essential role of mitochondria for the metabolic health of the cell was established in 1940, when Hans Krebs discovered the TCA (tricarboxylic acid) cycle. The TCA cycle is also known as the Krebs or citric acid cycle and enables “the oxidation of a triose equivalent involves one complete citric acid cycle and three repetitions of the Szent Gyorgyi cycle”[12]. In 1949, Kennedy and Lehninger reported that the complex enzyme systems responsible for TCA intermediates are localized in the isolated fraction which consists of morphologically intact mitochondria, “almost completely free of other formed elements” [13]. Next, Mitchell in 1961 demonstrated the transformation of chemo-osmotic energy into ATP in the mitochondrial matrix and the intermembrane space [14].

3.1.1 Mitochondrial ATP production

Mitochondrial adenosine triphosphate (ATP) is the primary energy source for the cell, accounting for 70%-90% of the ATP generated in different cells lines under normoxic conditions[15]. Mitochondrial ATP generation requires the oxidative phosphorylation (OXPHOS) system. The OXPHOS system is composed of five complexes (CI-CV) that are all embedded in the IMM and exposed to the IMM and mitochondrial matrix except CII which faces the matrix[16]. Complexes I-IV and the mobile electron carrier hydrophobic ubiquinone (CoQ) and cytochrome c (Cyt c) together form the Electron Transport Chain (ETC). This transport process of electrons is fueled by NADH and FADH₂ derived from the TCA cycle in the mitochondrial matrix and glycolysis that occurs in the cytosol (**Figure 1**). Complex V is the FoF1-ATP synthase that generates the bulk of ATP driven by the proton-motive force (PMF) generated upstream by complexes I-IV [17]. Complexes I-V are derived from a combination of nuclear DNA (nDNA) and mitochondria DNA (mDNA) encoded subunits at different ratios.

CI (also known as NADH-ubiquinone oxidoreductase) is regarded as the largest OXPHOS complex in mammalian cells, which consists of 45 subunits (7 mDNA-

encoded, 38 nDNA-encoded). CI receives electrons from NADH that is oxidized to NAD⁺, donates the electrons to CoQ, and pumps protons[18]. Despite its size, a set of 14 evolutionary conserved subunits are sufficient to carry out its enzymatic reactions, including the 7 mtDNA-encoded peptides and 7 nDNA-encoded subunits [19]. CI has an L-shaped assembly that consists of a matrix protruding hydrophilic arm and IMM embedded lipophilic arm [20]. CI contributes ~40% of the PMF required for mitochondrial ATP synthesis and plays an essential role in redox control during proliferation, regulation of longevity, and resistance to cell death [21], [22].

CII (also known as succinate dehydrogenase (SDH)) consists of four nDNA-encoded subunits (SDHA, SDHB, SDHC, and SDHD) that form a heterotetrameric complex. Structurally, the complex begins with the assembly position of SDHC. The SDHC subunits are embedded in the IMM and protrude into the matrix[23]. Functionally, CII participates in both the OXPHOS system and the TCA cycle. In the OXPHOS system, CII receives electrons from FADH₂ that is oxidized to flavin adenine dinucleotide (FAD) and donates the electrons to CoQ [24]. CoQ may also receive electrons from other potential enzymes donors including s,n-glycerophosphate dehydrogenase and the IMM-associated electron-transferring flavoprotein (ETF)-ubiquinone oxidoreductase [25]. In the TCA cycle, SDH oxidizes succinate to fumarate. To sustain OXPHOS, SDH also transfers electrons from succinate to ubiquinone (UbQ) [23]. CII deficiency gives rise to many diseases, such as the mutation of SDHD and SDHC in hereditary paraganglioma[26] and post-translational modifications of SDHA and SDHB in metabolic heart disease [27].

CIII (also known as cytochrome *bc1* oxidoreductase) is a homodimer consisting of 1 mtDNA encoding subunit and 10 nDNA encoding subunits. CIII receives electrons in the form of quinol from CoQ, transports the electrons to CIV by Cyt c, and pumps protons[28]. CIII also accepts electrons from several dehydrogenases, such as sulfide:quinone oxidoreductase, dihydroorotate dehydrogenase, glycerol 3-phosphate dehydrogenase, choline dehydrogenase, proline dehydrogenase, and electron transfer flavoprotein:ubiquinone oxidoreductase [25]. CIII deficiency results in a loss of T cell-

suppression capacity in regulatory T cells, diminished endothelial cells proliferation, and impairment in tumor angiogenesis [29], [30].

CIV (also referred to cytochrome *c* oxidase) contains 3 mtDNA encoding subunits and 11 nDNA encoding subunits. CIV receives the electrons from Cyt *c* and donates them to molecular oxygen (O_2) to produce water and pump protons. The pumping efflux of protons (H^+) that consumes the energy released by the electron transport from the matrix to IMS results in mitochondrial membrane potential ($\Delta\psi$) and pH difference (ΔpH) across the IMM[31]. CIV is the central regulator that is the rate limiting step of the respiratory chain. The regulation of CIV is achieved through the binding of various effectors, reversible phosphorylation, and the expression of subunit isoforms. Additionally, the feedback inhibition by ATP enables CIV to maintain a low and healthy $\Delta\psi$ and prevents the formation of reactive oxygen species (ROS). Under stressful conditions, the impaired feedback inhibition leads to monomerization and movement of NDUFA4 from CI to CIV, higher CIV activity and ATP synthesis, but increased ROS formation. [31].

CV or FoF1-ATP synthase consists of 2 mtDNA encoding subunits and 17 nDNA encoding subunits. CV has two mechanical rotary motors— Fo and F1—that generate ATP from ADP and inorganic phosphate (P_i) by dissipating the PMF, or that promote trans-IMM proton efflux by consuming ATP [32]. CV averages a backflow of 2.7 protons from the IMS to the matrix for each new synthesized ATP in eukaryotes. The maintenance of $\Delta\psi$ and/or ΔpH gradient is not only necessary for ATP production, but is also required for other mitochondrial pathways, including mitochondrial precursor import, mitochondrial dynamics, and metabolite/ion exchange between mitochondria and the cytosol. For example, the negative $\Delta\psi$ promotes mitochondrial Ca^{2+} uptake and malate–aspartate shuttle [33], [34].

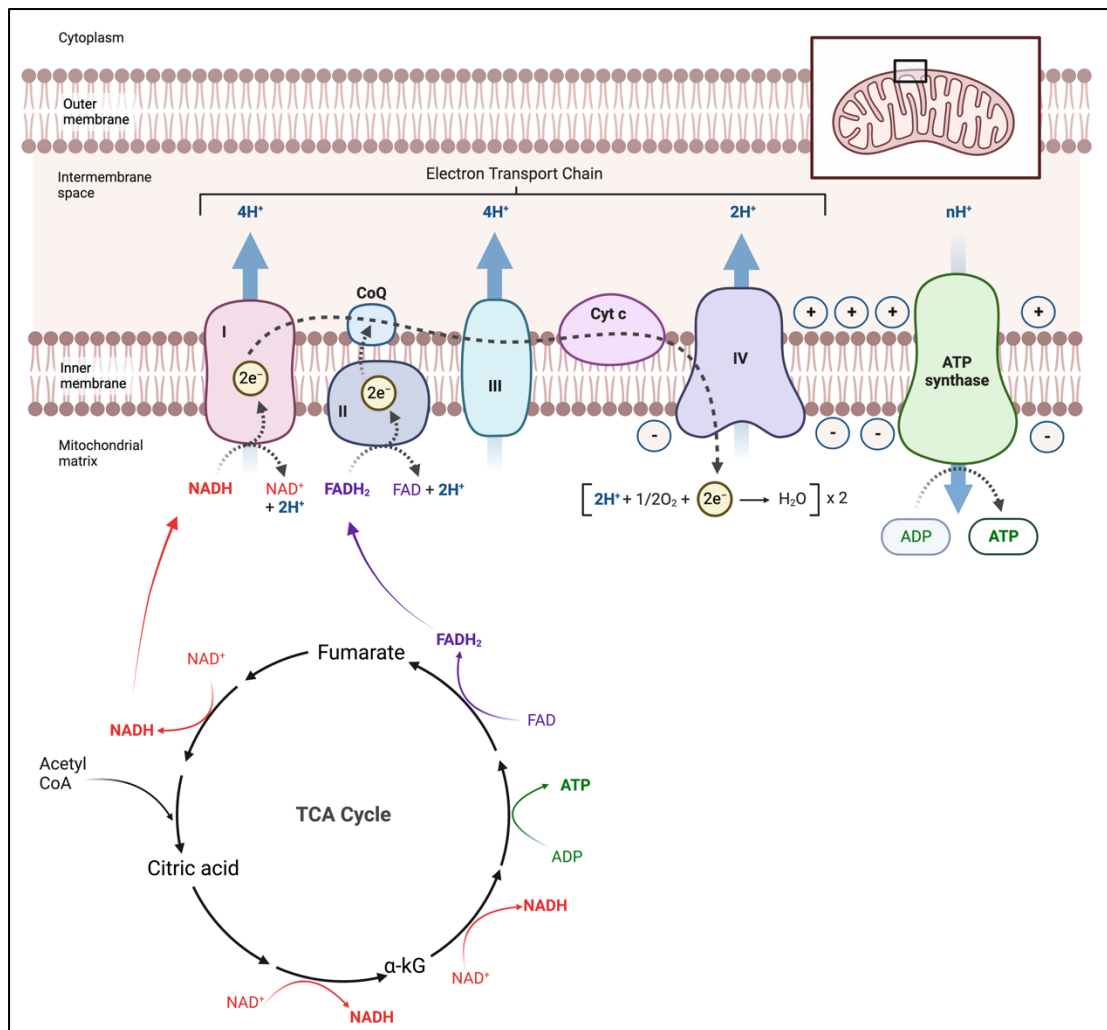


Figure 1. The schematic of mitochondrial OXPHOS system fed by TCA cycle. All figures in the introduction chapter were made with Biorender.com.

3.1.2 Mitochondrial metabolite synthesis

Another key function of mitochondria is metabolite synthesis. The TCA cycle is one of the most important pathways for the synthesis of many metabolites. It starts from the two-carbon acetyl-CoA, which can be generated from fatty acids, amino acids, or pyruvate oxidation. Acetyl-CoA reacts with a four-carbon oxaloacetate (OAA) to generate the six-carbon citrate, which is converted into its isomer isocitrate in the next step. Following up, isocitrate is converted into the five-carbon α -ketoglutarate (α -KG) and subsequently into the four-carbon succinyl-CoA through two step reactions with two oxidative decarboxylation. The two reactions release two molecules of CO₂ and generate 2x NADH. Next, succinyl-CoA converts into succinate with the generation of

GTP. Succinate is oxidized by SDH (or CII in ETC) generating the four-carbon molecule fumarate and transferring two hydrogen atoms to FAD, producing 2x FADH. Then, fumarate is converted into malate and further into OAA. OAA combines with another acetyl-CoA molecule to continue the TCA cycle[35]. The intermediates and products of the TCA cycle are used in the mitochondria or cytosol, where they fuel the synthesis of many metabolites. This section highlights the contribution of mitochondria to the biosynthesis of building blocks including fatty acids (FAs), amino acids and nucleotides [36].

Fatty Acids. Fatty acids (FAs) play essential roles in cells as structural elements of membranes, energy storage, and signaling molecules. A variety of FAs is synthesized in cells by the ligation of multiple acetyl CoA units that are derived from mitochondrial citrate. The six-carbon citrate is generated by the reaction between acetyl-CoA and four-carbon oxaloacetate (OAA) in the TCA cycle. Once it is synthesized, citrate is transported into cytosol by mitochondrial citrate transporters (CTP) and subsequently acetylated to be acetyl-CoA used for FAs synthesis and elongation. The key carbon donors for acetyl-CoA used for FAs synthesis is glucose and glutamine, which feed the TCA cycle via their derivatives pyruvate and alpha-ketoglutarate [37].

Amino acids. The synthesis of several amino acids occurs in the mitochondria. Most reactions involve a simple transamination derived from the amino donor glutamate which is converted into alpha-ketoglutarate (α -KG). For example, before its conversion into acetyl-CoA, pyruvate can be transaminated into alanine. Glutamine can be converted into proline with 2x NADH. The malate–aspartate shuttle is a series of reactions that move the amino acids glutamate and aspartate between mitochondria and cytosol, and that is functionally connected to the TCA cycle. One aspartate molecule is effluxed from mitochondria and one glutamate molecule influx into mitochondria [34]. The cytosolic aspartate can be converted into malate which is transported into mitochondria in exchange for one α -KG transported into the cytosol. Malate can be converted into OAA via the TCA cycle and subsequently into aspartate with the aspartate-aminotransferase which can be used for the synthesis of asparagine and arginine [38].

Nucleotides. Stable de novo nucleotide synthesis sufficiently fuels a wide range of biological processes in all cells. One-carbon (1C) metabolism is a fundamental metabolic process for the biosynthesis of purines and thymidine through activation and transfer of 1C units mediated by the folate cofactor tetrahydrofolate that can occur both in the mitochondria and in the cytosol (THF)[39][36]. Mitochondrial THF imported from the cytosol is converted by serine hydroxymethyltransferase (SHMT2) into 5,10 methylene-THF and glycine. The cytosolic SHMT1 enables THF to be restored via the reversed flux in the absence of SHMT2 in mitochondria [40]. 5,10 methylene-THF is converted to 10-formyl-THF by mitochondrial methylenetetrahydrofolate dehydrogenase (MTHFD2), which is critical for growth and proliferation[41]. Then, the formate is generated in mitochondria by using the 10-formyl-THF and exported into the cytosol where it is converted into 10-formyl-THF. The IMM enzyme dihydroorotate dehydrogenase (DHODH) is a rate-limiting enzyme in the de novo biosynthesis pathway of pyrimidines and is in the IMM to catalyze the oxidation of dihydro-orotate (DHO) to orotate [42]. DHODH activity is elevated in DNA damage to increase nucleotide synthesis for DNA repair [43].

3.1.3 Mitochondrial regulation of cell death

Mitochondria not only fuel life but also function as a checkpoint for several forms of programmed cell death, such as apoptosis, necroptosis, ferroptosis, and pyroptosis. Apoptosis is a major form of regulated cell death that ensures a homeostatic balance that is crucial to embryonic development and autoimmune regulation. Under the stress of DNA damage or growth factor deprivation, mitochondria initiate apoptosis by releasing the soluble protein Cyt c which is a consequence of mitochondrial outer membrane permeabilization (MOMP) and disrupted cristae structure. This permeabilization is driven by effector pro-apoptotic proteins of the B cell lymphoma 2 (BCL-2) family (prominently BAX and BAK). Cyt c binds apoptotic peptidase activating factor 1 (APAF1) to form the “apoptosome” complex that activates the initiator caspase 9 and leads to a signaling cascade through Caspase 3/7 [44]. In contrast

to the intrinsic pathway, the extrinsic apoptotic pathway is caspase 8-dependent and occurs through Caspase 3/7 directly or is activated by tBID-mediated MOMP at mitochondria[45].

Following stimulation with tumor necrosis factor (TNF), viral infection, or the activation of toll receptor signaling, necroptosis is activated through the formation of the necrosome that consists of the activated receptor interacting protein kinase 1/3(RIPK1/3). The necrosome phosphorylates mixed lineage kinase domain-like pseudokinase (MLKL), leading to its oligomerization and permeabilization of the plasma membrane [46]. Mitochondria promote the activation of RIPK1 and the formation of the necrosome through releasing reactive oxygen species (ROS) [47].

Pyroptosis is a gasdermin-mediated programmed necrotic cell death associated with innate immunity and diseases. Under oxidative stress, Cyt c is released into the cytoplasm through the MOMP via the recruitment of Bax to mitochondria and then activates inflammatory caspases that eventually causes pyroptosis [48].

Ferroptosis is an iron-dependent type of cell death reported in recent years[49], which has an essential role in the occurrence and development of many diseases, such as tumors, neurological diseases, acute kidney injury. Ferroptosis is triggered by membrane lipid peroxidation that is promoted by the Fenton reaction. The reaction can occur with mitochondria released ROS and free Fe²⁺ from iron-binding proteins ferritin and heme-containing proteins [50].

3.1.4 Innate immune signaling

Mitochondria are an essential player in the innate immune system. These organelles serve as an innate immune signaling platform and contain a reservoir of molecules that elicit immune responses, known as Damage Associated Molecular Patterns (mDAMPs), including N-formyl peptide, cardiolipin, mtDNA, and ROS [51].

The OMM houses the adaptor protein mitochondrial antiviral signaling (MAVS). MAVS is activated following the activation of the retinoic acid-inducible gene I (RIG-I) and RIG-I-like receptors (RLRs) MDA5 by viral RNA. The binding of RIG-I and

MDA5 to MAVS induces the prion-like aggregation of the MAVS CARD-domain, and the subsequent activation of TANK (TRAF family member-associated NF- κ B activator)-binding kinase 1 (TBK1) complexes and IRF3 and/or IRF7. IRF3/7 bind to IFN-stimulated response elements and induce the transcription of target genes such as type I interferons (IFNs) which promote antiviral signaling [52].

mDAMPs are important signaling molecules during infection and mitochondrial damage. N-formyl peptides are common molecular signatures of bacteria that also exist in mitochondria. During mitochondrial protein translation, the initiation factor 2 exclusively uses the N-formylated methionine (fMet), while the unformylated methionine is involved in the process of protein elongation. Usually, N-formyl peptides are retained in the matrix of healthy mitochondria, but are released into the cytoplasm from damaged mitochondria and subsequently activate the formyl peptide receptor (FPR) leading to chemotaxis, oxidative burst, and inflammation [53]. Cardiolipin is a tetra-acylated diphosphatidylglycerol lipid. It is found in prokaryotic membranes. In eukaryotic cells, it is only found in the mitochondrial IMM but is absent in the OMM. When mitochondria are damaged, cardiolipin is exposed to the cytoplasm leading to the activation of NLRP3 inflammasomes and proinflammatory cytokines [54]. mtDNA are circular double stranded DNA containing methylation patterns that differ from nuclear DNA. Under stimulations and cell death, mtDNA is released into the cytoplasm and the methylation patterns of mtDNA are sensed by several innate immune receptors, such as TLR9, NLRP3, and cGAS-STING. cGAS signals through cGAMP and STING to activate inflammatory gene transcription [55][56]. ROS are the byproducts of normal OXPHOS activity. In response to different conditions, ROS can function as positive intermediates of cellular signaling pathways under hypoxia, or as toxic agents that induce cellular damage and pathologies through the inflammation[57].

3.2 Mitochondrial dynamics

Although mitochondria vary in mass, shape, and distribution in diverse tissues and cell lines, they maintain a dynamic network through the conserved processes of fusion and fission (**Figure 2**). In this section, we discuss mitochondrial dynamic mechanism by which maintains the integrated mitochondrial network and related mitochondrial functions.

3.2.1 Mitochondrial fission

Mitochondrial fission is required for the generation of daughter mitochondrion and the removal of damaged mitochondria. Impairment of fission causes OXPHOS deficiencies, significant increases in ROS production, and has been linked to neurodegeneration, endothelial inflammation, and other related diseases [58].

In mammals, mitochondrial fission proceeds by a series of regulated steps (Figure 2). First, in a step mediated by actin, ERs mark sites of fission. The cytosolic Drp1 is recruited to ER-marked sites on the OMM and assembles into dimers and oligomers that form a spiral-shaped superstructure [59][60][61]. The recruitment of Drp1 is an essential step that is mediated by several receptors including mitochondrial fission factor (MFF), mitochondrial dynamics proteins of 49 kDa and 51 kDa (MiD49 and MiD510, and fission 1 (FIS1) [62]. Reversible phosphorylation of Drp1 plays a critical role in the process of fission via the control of Drp1 GTPase activity, and regulates GTP hydrolysis and the constriction of Drp1 helix required to complete the mitochondrial fission process[63]. Various cytosolic factors affect Drp1 fission activity via post-translational modification, for example, activation of protein kinase A and cytosolic Ca²⁺ levels which leads to DRP1 phosphorylation. Compromising these factors is associated with serious human diseases. Recent work has shown that contact sites between lysosome and mitochondria may also induce fission through RAB7 GTP hydrolysis [64]. A cellular stress that often triggers to mitochondrial fission is infection, which is discussed in the session 3.6.1.

3.2.2 Mitochondrial fusion

Mitochondria fusion is required to sustain a healthy and functional network which is indispensable for cellular homeostasis. Inhibition of mitochondrial dynamics alters ATP supply, apoptosis, immune signaling, embryonic development, and many cellular and organismal processes.

Mitochondrial fusion is mediated by machinery that resides on both the outer and inner membranes (Figure 2). Mitofusin 1 and 2 (MFN1 and MFN2) are OMM proteins that contain an N-terminal GTPase domain, a coiled-coiled heptad repeat (HR1) domain, a short transmembrane domain responsible for their OMM insertion, and a second coiled-coiled heptad repeat (HR2) domain at the C-terminus [65]. MFN1 and MFN2 molecules on different mitochondria form homo- or hetero- dimers to promote tethering and the fusion of the OMM. The main regulator of IMM fusion is OPA1. The activity of OPA1 is regulated by the IMM proteases OMA1 or YME1L, which proteolyze the OPA1 to yield l-OPA1 and s-OPA1 [66]. It remains unclear how l-OPA1 and s-OPA1 mediate IMM fusion.

The dysfunction of MFN1/2 and OPA1 causes the impaired mitochondrial fusion that imply the OXPHOS deficiencies, mtDNA loss, and mitochondrial motility defects [58]. Interestingly, although the depletion of dynamins MFN1/2 and OPA1 all abolish fusion, their loss impacts mitochondrial morphology and cellular function differently. Depletion of MFN1 leads to small and fragmented mitochondria while of MFN2 cause fragmented but swollen mitochondria. This suggests MFN1 may have a higher capacity for OMM tethering than MFN2 [67]. Importantly, studies show that these proteins each have different functions in addition to their role in fusion. For example, MFN2, but not MFN1, lead to Charcot-Marie-Tooth disease type 2A [68]. MFN2 is required for mitochondria-ER interaction which is essential for essential for the mitochondrial calcium homeostasis and energy metabolism [69]. MFN2 but not MFN1 is a prerequisite for the response of mitochondrial respiration to the infection of *Listeria*, *Mycobacterium tuberculosis* or LPS endotoxemia, as well as for the production of reactive oxygen species (ROS) in macrophages [68]. During infection of *Toxoplasma*,

mitochondrial fusion mediated by MFN1/2 is required for mitochondrial FAs uptake to restrict the growth of *Toxoplasma* [11]. Moreover, mitochondrial elongation requires OPA1 and MFN1 but not MFN2 under stressful conditions, such as nutrient and oxygen deprivation or ER impairment [70]. In early stages of spermatogenesis, the expression of MFN2 corrects the defects of germ cell development, but not MFN1. The mitochondrial fusion machinery also plays different roles during infection which is discussed in section 3.6.1.

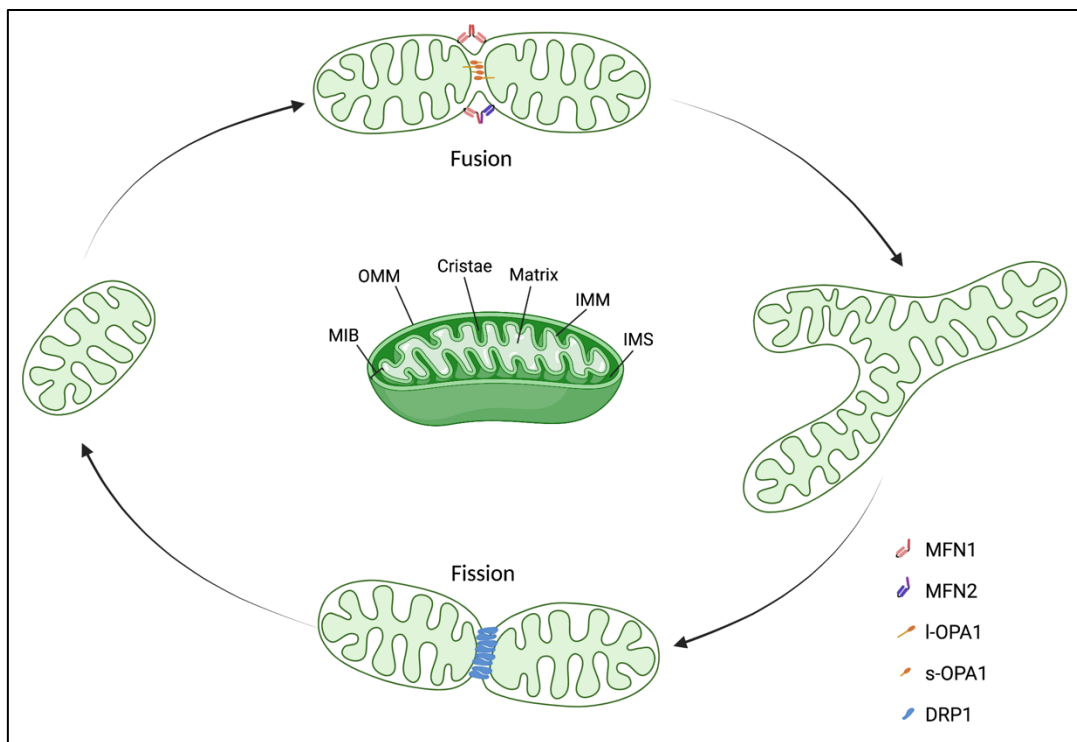


Figure 2. The schematic of mitochondrial structure and dynamics (fusion and fission).

3.3 Mitochondrial structure

Mitochondrial structure is essential for the health of these organelles and their functional flexibility. In this section, we present defining features of mitochondrial architecture (**Figure 2**).

3.3.1 Mitochondrial structure

Mitochondria are the only organelles in mammalian cells that possess two membranes, the OMM and IMM. Each membrane has different properties that confer functional flexibility to these organelles.

The OMM plays a key role as the gatekeeper that maintains an independent niche within mitochondria. For example, calcium is imported through the OMM from the cytoplasm, which requires the OMM located Voltage-dependent anion-selective channel protein (VDAC), which also forms the ER-mitochondria contact site[71]. The OMM is also in contact with several other cellular compartments, including ribosomes, peroxisomes, lipid droplets, and the nucleus [72] and even intracellular microbes [73]. Under certain stress stimuli, the OMM integrity is disrupted by the formation of BAX/BAK pores leading to the release of mDAMPs, such as mtDNA and cytochrome c, and [74].

The IMM has two substructures: the mitochondrial cristae and the inner boundary membrane (IBM). The IBM is parallel to and tightly bound to the OMM. Mitochondrial cristae are formed by invaginations of the IMM. The cristae structure hosts the respiratory chain complexes and are the site for iron-sulfur cluster biogenesis and mtDNA maintenance [75]. The transition and connection between IBM and cristae are the pore-like structures known as cristae junctions (CJs) which are narrow gaps that prevent the contents of cristae from being released into IMS.

Cristae structure is regulated by two essential players, OPA1 and ATP synthase. The two isoforms l-OPA1 and s-OPA1 form the oligomers to maintain the CJs and cristae structure. Destabilization of OPA1 oligomers impairs CJ number and tightness, the widening of cristae structure, and also enables the release of cytochrome c during tBid-induced apoptosis[76][76]. The interaction between OPA1 and MIC60 controls the

number and stability of CJs, while OPA1 achieves the control independent of MIC60 suggesting it is epistatic to MIC60[77][78]. The F1FO-ATP synthase dimers assemble into rows or other oligomeric configurations that bend the IMM into positive curvature at cristae rims[79]. A key determinant of cristae structure is the main lipid constituent cardiolipin. Cardiolipin has a conical structure and is enriched on the concave surfaces of the IMM facing the intermembrane space, which enables it to stabilize membrane curvature and permit the formation of mitochondrial cristae [80].

3.3.2 MIB—the bridge between the OMM and IMM

The mitochondrial intermembrane space bridging complex (MIB) connects the OMM and IMM, which promotes the formation of CJs and maintains the cristae (**Figure 3**). The MIB contains two complexes: the sorting and assembly machinery (SAM) on the OMM and the mitochondrial cristae organizing system (MICOS) on the IMM. Complexome profiling analysis indicates that MIB assembly starts from a core SAM complex (containing SAM50-MTX2-MTX3) and the core unit of the MICOS complex (including MIC60, MIC19, and MIC25), which is subsequently bound to other subunits to form the full-size MICOS complex. SAM50, MIC60, and MIC19 are the most important subunits for the assembly and stability of the MIB in human mitochondria [81]. The additional protein DNAJC11 binds the SAM complex with the MTX1 [82][83].

The MICOS complex is the key organizer of CJs [9], and contains at least 8 subunits in mammals, including Mic60, Mic19, Mic10, Mic25, Mic29, Mic27, Mic13, and Mic14. Mic60 is a conserved core subunit that plays a central role in the positioning of MICOS complex at the cristae junction and bending the membrane to form the cristae-like invagination [84]. The ablation of Mic60 leads to a loss of cristae junctions and the intensive membrane stacks of IMM [85]. Mic19 and Mic60 interact with the OMM protein SAM50 (the core subunit of the SAM complex) which forms MIB to bridge IMM and OMM [86]. Interestingly, in yeast, the IMM protein Mic60 is required for the biogenesis of β -barrel proteins, such as TOM40, through the interaction with SAM50

[87]. Recent studies show SAM50–MIC19–MIC60 axis links the SAM and MICOS complexes; strikingly, SAM50 is enriched at the OMM at sites of mitochondrial cristae junctions. The cleavage of MIC19 at the N-terminal by mitochondrial protease OMA1 with physiological stresses causes the disrupted binding between SAM50 and MIC60.

The integrity of the MIB is essential to maintain mitochondrial cristae and its functions, which are critical for organismal health. The cleaved MIC19 leads to the loss of the MIB complex, swollen mitochondria, loss of CJs, aberrant cristae, and impaired OXPHOS system. Only SAM50 deficiency rather than other SAM subunits MTX1/2/3 causes the cleavage of MIC19 and abnormal cristae [88], suggesting that SAM50 is probably the anchor that guides the formation of cristae junctions. Knockdown of MIC60 leads to the disorganization of cristae and the fragmentation, and further the release of cyto c from mitochondria during apoptosis [89]. The ablation of MIC60 also induces the formation of swollen mitochondria, where the mtDNA nucleoids are clustered and mtDNA transcription is attenuated [90]. Besides the core MIB subunits, the peripheral interactors of MIB are indicated in many biological processes, such as ORP5/8 link MIB/MICOS that contact sites and the transport of phosphatidylserine between ER and mitochondria [95]. Structural and functional changes in the MIB are pathological hallmarks in many human diseases, such as in Alzheimer's and Parkinson's disease, cancer, diabetes, and cardiovascular and muscle degenerative diseases [91].

3.4 Mitochondrial biogenesis: insights into protein import

Mitochondria dynamics preserves mitochondrial homeostasis through two opposing processes: the biogenesis of new mitochondria and the restoration or removal of damaged mitochondria. Biogenesis requires additional building-blocks and proteins to sustain mitochondrial structure and functions. However, only 13 proteins are encoded by mtDNA. The majority of mitochondrial proteins (above 1000 proteins) are encoded by nDNA, synthesized in the cytoplasm, and thus need to be imported into the mitochondria (**Figure 3**).

3.4.1 Presequence carrying mitochondrial precursors

The import pathway of presequence-carrying precursors is a relatively well-known mechanism that responds to the translocation of around 60% of mitochondrial proteins. The features of the N-terminal presequence vary in length, from 15 to 100 amino acid residues. The typical structure of the presequence is an amphipathic α -helix with a positively charged face and a hydrophobic face. The hydrophobic surface of the amphipathic helix is initially recognized by the mitochondrial import receptor TOM20. Next, the positively charged surface binds to the intermembrane space domain of the core receptor TOM22[92][93]. The β -barrel transmembrane channel TOM40 contains both hydrophilic and hydrophobic domains which specifically interact with precursor proteins. Presequence-carrying precursors are recognized by TIM50 with the help of TIM21 at the IMS-facing side of TOM40 and are subsequently handed over to the TIM23 complex on the IMM[94]. TIM23 is the core subunit that consists of two functional domains: the N-terminal domain that interacts with TIM50, and the C-terminal membrane-embedded domain that forms a channel through the IMM [95]. The TIM23 directs presequence-carrying precursors into the IMM and matrix. The IMM-sorted precursors are inserted into the IMM via the binding of its hydrophobic sorting signal to Mgr2, which is a small membrane translocase that functions as the lateral gatekeeper[96]. Matrix-targeted precursors are translocated into the matrix where they are driven by the presequence translocase-associated motor (PAM) that collaborates

with the ATP-dependent mitochondrial heat-shock protein 70 (mtHsp70). Subsequently, the presequences are removed by the dimeric mitochondrial processing peptidase (MPP)[3].

3.4.2 Non-presequence containing mitochondrial precursors

Certain mitochondrial precursors do not have cleavable presequences. Mitochondrial metabolite carriers are one such class that contain six α -helical transmembrane segments that become integrated into the IMM. In the cytosol, the newly synthesized carrier precursor is bound by chaperones Hsp70 and Hsp90, which can recognize the OMM import receptor TOM70 and promote the binding of carrier precursors to TOM70. Human TOM70 has 608 amino acids and anchors into the OMM by one transmembrane domain (39-59), which is flanked by N-terminal and C-terminal sequence facing the IMS and cytoplasm respectively. The N-terminal clamp-type TPR domain harbors the pocket-like structure which can recognize heat shock protein family molecular chaperones such as Hsp70/90, whereas the C-terminal TPR domain harbors the pocket-like structure which can recognize the internal mitochondrial targeting signals (iMTS) of precursors[97].

TOM22 receives the precursors from TOM70 and enables their insertion into the TOM40 channel[98][99]. Small TIM chaperones are recruited by the N-terminus of TOM40 in the IMS and translocate the carrier precursors from the TOM40 channel exit to the TIM22 complex. Notably, the small TIM chaperones TIM9-TIM10 are soluble in the IMS, and along with TIM12 interact with TIM54 and the TIM22 complex [100]. The TIM22 complex also mediates the import of other proteins with multiple transmembrane segments, but the structural TIM22 complex and insertion mechanism of substrates into the IMM are unknown.

3.4.3 Cysteine motif-containing precursors

The cysteine motif-containing precursors are translocated and folded by the TOM complex and oxidoreductase Mia40. The cysteine motifs contained precursors are translocated across the OMM through the TOM40 channel, but the import receptor is

still unknown[101]. Interestingly, when the precursor is exposed to the IMS through TOM40, Mia40 acts as a receptor and binds precursor hydrophobic residues and cysteine residues [102]. The formation of a transient disulfide bond between cysteine residues of precursors and Mia40 is mediated by the sulfhydryl oxidase Erv1 and promotes their conformational stabilization and assembly in IMS.

3.4.4 OMM protein biogenesis

The integrity and function of the outer mitochondrial membrane relies on the import and assembly of the OMM proteins. 2 types of proteins exist at the OMM, β -barrel proteins and α -helical proteins. β -barrel proteins generally possess multiple transmembrane β -strands that promote their insertion into the OMM by the TOM complex and SAM complex. TOM20 binds the targeting signal of the hydrophobic β -hairpin motif which is formed by two adjacent β -strands [103]. Then, the precursor enters the IMS through the import channel TOM40 and binds to the small TIM chaperones. The precursors are protected from aggregation by the small TIM chaperones and access the SAM complex which engages the precursor from the IMS side and releases it into OMM lipid phase.

α -helical membrane proteins contain one or more α -helical transmembrane segments that anchor into the OMM and exist in three main flavors: N-terminal signal-anchored proteins, C-terminal tail-anchored proteins, and polytopic (multi-spanning) outer-membrane proteins. In yeast, the mitochondrial import complex (MIM) promotes the import and insertion of N-terminal signal-anchored proteins and polytopic proteins. The MIM complex contains two subunits, MIM1 and MIM2, which are single-spanning OMM proteins. The MIM complex has three populations: free MIM complex, TOM-MIM complex, and the MIM-SAM complex [104]. The free MIM complex directly binds cytosolic single spanning precursors and directs them into the OMM. The TOM-MIM complex channels the single spanning precursors and polytopic precursors via the TOM70 receptor and MIM complex. The MIM-SAM complex participates in the early

steps of TOM complex assembly. Besides the MIM pathway and other individual examples[105][106][107][108], the lipid composition also appears sufficient to promote the insertion of C-terminal tail-anchored proteins. For example, the low-ergosterol content in the OMM promotes C-tail protein insertion [93], [111].

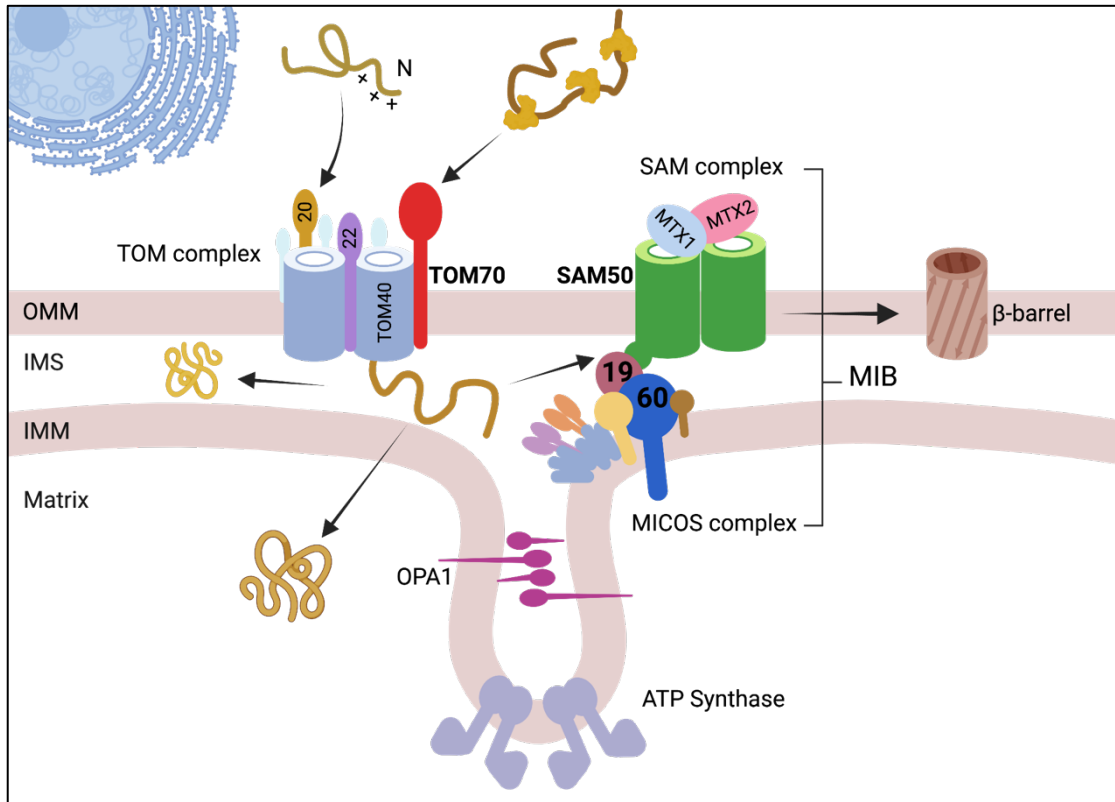


Figure 3. The schematic of the key import regulators TOM and SAM complex on the OMM, and of the MIB as the bridge of OMM-IMM.

3.5 Mitochondrial quality control

Considering the myriad of chemical reactions, metabolic processes and stresses that occur in the mitochondria, efficient quality control is consistently required to maintain mitochondrial health. The main quality control systems include: mitochondrial proteostasis, Ubiquitin-Proteasome System (UPS), mitophagy, mitochondrial-derived vesicles (MDVs), and mitochondrial dynamic.

3.5.1 Mitochondrial proteostasis

Due to the import of over 1000 mitochondria proteins and estimated 1000+ biochemical reactions occurring in mitochondria, the precise and rapid surveillance and degradation of the misfolding or dysfunctional proteins is required. Mitochondrial proteases are regarded as the first line of defense in mitochondrial quality control [109] and regulate the proteolysis of its substrates. Eighteen mitoproteases are catalytically proficient and 5 pseudomitoproteases are catalytically deficient for a total of 23 enzymes that exclusively localize to mitochondria [110]. Of the eighteen enzymes, MPP, MIP, METAP1D, XNPEP3, IMP, and ATP23 mature mitochondrial precursor proteins [111]. In the IMM/IMS, the inner membrane protease (IMP) mediates the maturation of presequence-containing translocases by removing the carboxy-terminal targeting sequence [112]. In the matrix, the mitochondrial processing peptidase (MPP) mediates the cleavage of MTSs from precursors [113]. Of the eighteen enzymes, another four well-studied ATP-dependent proteases, including LONP, CLPXP, the m-AAA protease, and the i-AAA protease, possess ring-like structures containing the internal ATP-dependent proteolytic chamber. The m-AAA for example is required for the CI activity and increased sensitivity to oxidant stress by its proteolytic activity [114]. The m-AAA protease, an IMM-embedded ATP-dependent protease facing the matrix, has proteolytic activity on the IMM and matrix proteins. Besides the quality control of OXPHOS, the main functions of the m-AAA protease are observed in calcium homeostasis and mtDNA expression. The m-AAA protease controls mitochondrial calcium by regulating the amount of the mitochondrial calcium uniporter (MCU) that

is regulated by the Essential MCU regulator (EMRE), the proteolytic substrate of m-AAA. In the matrix, mitochondrial Lon protease (LONP1) displays various functions including proteolysis, chaperone activity, and binding of mtDNA. LONP1 promotes the maturation of several proteins, such as the regulators of mtDNA replication SSBP[115], mitochondrial gene expression SLIRP and another ATP-dependent protease CLPXP [116]. LONP1 presents chaperone-like activity with mtHSP70, p53, and COX4-1 subunits in humans. Its AAA+ ATPase activity is required for the interaction with mtHSP70 that prevents it from co-aggregation with substrates[117]. LONP1 displays a unique and conserved function and binds mtDNA in a sequence specific manner, which enables it to interact with other nucleoid-related proteins to regulate mtDNA replication[118] such as the mitochondrial transcription factor A (TFAM)[119]. The caseinolytic mitochondrial matrix peptidase (CLPXP), composed of seven CLPP subunits and six CLPX subunits, participates in the maintenance of the OXPHOS system health, such as selectively degradation of the subunits of CI and CII to prevent the accumulation of dysfunctional complexes from stress condition[120]. The mitoribosome assembly is positively regulated by CLPXP via the degradation of ERAL1 (a putative 12S rRNA chaperone) from the small ribosomal subunit to promote mitochondrial translation [121].

3.5.2 The ubiquitin-proteasome system (UPS) and mitophagy

Ubiquitylation is one of the broadest and most conserved post-translational modifications that enable mechanistically diverse, quantitative, and reversible regulation. Ubiquitin is a 76 amino acids peptide that can conjugate to lysine (K) residues of target proteins in a progressive process mediated by Ub activating enzymes (E1), Ub-conjugating enzymes (E2), and Ub ligases (E3). This process is well-described: E1 uses the energy provided by ATP to actively transfer ubiquitin to E2, which subsequently cooperates with E3 to label a ubiquitylated substrate. The type of ubiquitin conjugation determines the protein outcome. Usually, monoubiquitylation changes protein-protein interactions, while protein degradation employs the polyUb

Lys48-linked and branched Lys48-Lys11 chains which signal to the proteasome[122]. The ubiquitin-proteasome system (UPS) and mitophagy are two main degradative pathways that are initially regulated by ubiquitylation and enable the cell to rapidly respond to mitochondrial insults.

In mitochondria, the OMM-localized proteins are monitored by the UPS. The mitochondrial ubiquitin ligase (MARCH 5) is a E3 with RING finger domain that enables the transfer of ubiquitin directly from E2 to the substrate to form the Lys48-linked chain to initiate proteasomal degradation[123]. Substrates of MARCH5-mediated UPS degradation include MFN1/2, Fis1, which are key factors in mitochondrial dynamics. FUNDC1, an important mitophagy receptor, is also regulated by MARCH 5, which senses hypoxic stress and fine-tuning of the mitophagy response [124]. Interestingly, the TOM40 channel can retro-translocate conformationally destabilized IMS proteins into the cytosol to enable their degradation by the proteasome, [125].

Mitophagy is another important mechanism of mitochondrial quality control. OMM proteins of depolarized mitochondria are ubiquitylated and recruit autophagosomes to recycle the whole or part of the mitochondria in a mainly PINK1/Parkin-dependent manner. PINK1 is imported through TOM complex into the matrix, cleaved into short fragments by PARL, and then is retro-translocated into the cytosol and degraded by proteasome under basal conditions. Under stressful conditions, PINK1 accumulates on the OMM of depolarized mitochondria, leading to the formation of a TOM-PINK1 complex. PINK1 initiates the phosphorylation of the primary ubiquitin of the OMM substrates and activates Parkin, a Ub E3 ligase, which unselectively ubiquitinates the substrates to form the Ub chains that PINK1 phosphorylates.

3.5.3 Mitochondrial-derived vesicles (MDVs)

Recent work has revealed that MDVs cooperate with the endosomal system to regulate mitochondrial quality control. MDVs were firstly reported to traffic to peroxisomes, or to fuse with the late-endosome/lysosome or multivesicular body

(Figure 4). MDVs have a 70-150 nm diameter under electron microscopy, in contrast to the size of normal mitochondria around 0.5-3 μm in mammalian cells. In terms of structure, MDVs contain two different sets, only OMM or OMM+IMM, and continuously bud off mitochondria under stressful conditions, such as mild mitochondrial oxidative stress due to CCCP or antimycin A treatment.

The biogenesis of MDVs is initiated by PINK1/Parkin [126] and driven by MIROs and DRP1 [127], which bud off mitochondria and carry the specific cargo proteins to late-endosome/lysosome or multivesicular body. This process is independent of autophagic regulators, such as ATG5 or LC3 [128]. A subset of PINK1/Parkin-dependent MDVs recruits Syntaxin-17 and subsequently SNAP29 and VAMP7, to assemble the soluble NSF attachment protein receptor (SNARE) machinery for fusion with late-endosome/lysosome [129]. Later, Toll-interacting protein (Tollip), an essential endosomal coordinator, is a MDVs residence and interacts with ESCRT-0 protein Tom1 to promote cargo trafficking to the late-endosome/lysosome [130].

In response to LPS stimulation or heat stress, the recruitment of the Rab9 and Sorting nexin 9 (SNX9) is required for the formation of MDVs, which contain the marker OGDH, a mitochondrial matrix protein 2-oxoglutarate dehydrogenase. Interestingly, PINK/Parkin actively impair the formation of MDVs during LPS exposure or heat stress. MDVs transport DAMP-laden cargo to lysosomes to degrade the pro-inflammatory and oxidized mitochondrial proteins in a SNX9-dependent manner, instead of the trafficking to extracellular vesicles (EVs) which cause strong immune responses [131].

Another set of MDVs buds off mitochondria in HeLa cells that are labeled by the OMM-anchored protein ligase (MAPL). MDVs with MAPL (but TOM20-) fuse with peroxisome, whereas TOM20+ / MAPL- MDVs do not [132]. Additionally, MDVs carrying Pex3/Pex14 (they called it pre-peroxisomal structures), can fuse with ER-derived vesicles enriched in Pex16 to form a hybrid vesicle with peroxisomal import competence in human patient fibroblasts lacking peroxisomes [133].

MDVs have selective cargoes. Recently, a study indicated the loading of 107 high-

confidence cargoes and the change of MDVs lipidome compared to mitochondria [127]. The TOM20+ OMM MDVs contain OMM proteins TOM40, TOM70, SAM50, MIRO1/2 and MFN1 (but not MFN2). TOM20+ OMM-IMM MDVs consist of the proteins from OXPHOS complexes III and V and the Fe-S clusters, as well as matrix proteins such as PDH, several proteins of the TCA cycle and fatty acids β -oxidation SOD2. Besides protein cargo, mtDNA is transferred into MDVs which is associated with proinflammation in Parkinson's disease [134].

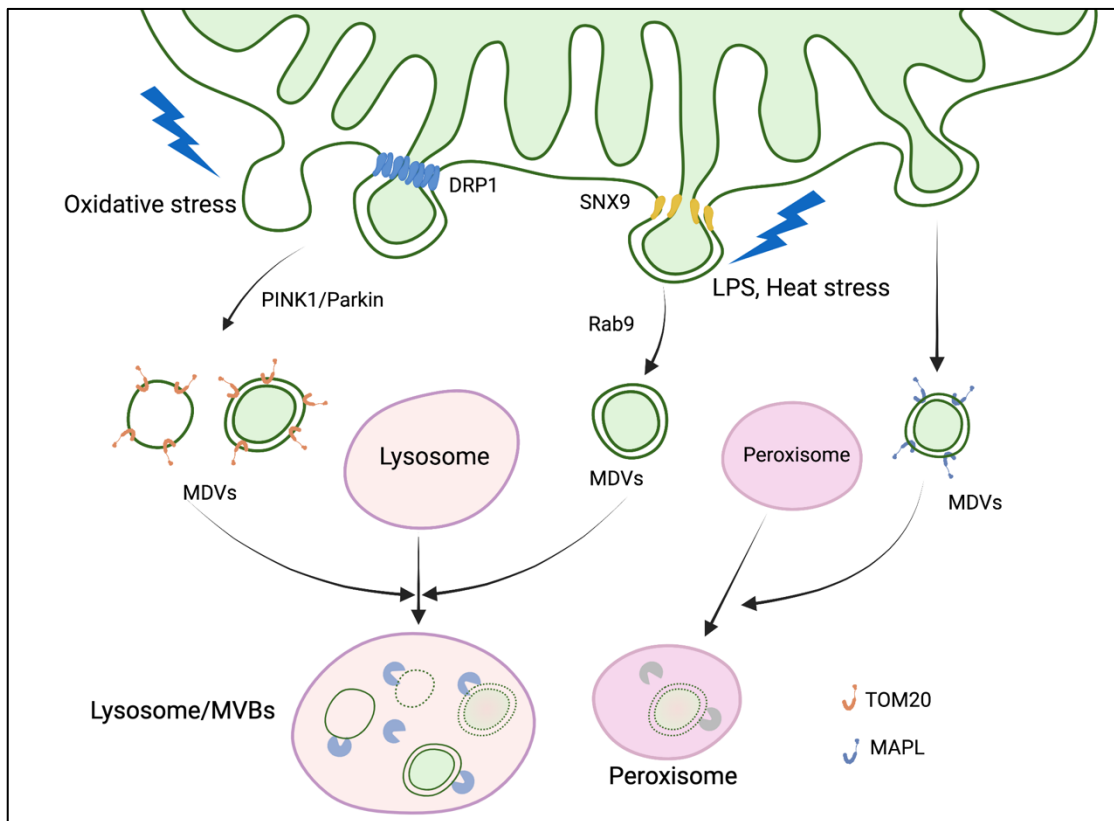


Figure 4. The schematic of the formation and fate of MDVs.

3.6 Modulation of mitochondria during microbial infection

Mitochondria are not only part of the innate immune signaling system, but can also respond to the infection through its dynamics and functions. In this section, we will discuss how mitochondria respond to and defend against different pathogens, including viruses, bacteria, and parasites.

3.6.1 Mitochondrial dynamics during infection

The most straightforward readout of mitochondria upon infection is morphological changes. From the view of pathogens, the impairment of the mitochondrial network can be beneficial to recreating a suitable microenvironment for survival and proliferation. *Listeria monocytogenes* induces mitochondrial network fragmentation by secreting pore-forming toxin listeriolysin O (LLO), which causes a rapid decrease in Mff and atypical mitochondrial fission in a DRP1-independent manner at an early infection stage. *Legionella pneumophila* establishes the Legionella-containing vacuole (LCV) that tethers with host mitochondria and induces the mitochondria fragmented network in a DNMI1L (also known as DRP1) dependent manner[135]. Host mitochondrial fission is found during infection with *Helicobacter pylori* through its vacuolating cytotoxin A (VacA) and of *Shigella flexneri* in a DRP1 dependent manner [136], [137]. Interestingly, *Chlamydia trachomatis* preserves the mitochondrial elongation network by the phosphorylation of fission-inactive serine residue 637 (S637) of DRP1. *Mitochondria* *invades* the host mitochondrial IMS and hijacks mitochondrial fusion[138].

By inhibiting the activity of DRP1, Dengue virus (DENV) nonstructural protein 4B (NS4B) promotes mitochondrial elongation and impairs the RIG-I-dependent interferon responses which are beneficial for viral proliferation[139]. Other viruses such as Influenza A, Influenza M2, SARS-CoV, and SARS-CoV-2 also promote the fusion of host mitochondria, increase ATP production, and inhibit innate immune signaling, to promote their replication [140–143]. Hepatitis C virus promotes the ubiquitylation of MFN2 leading to a fragmented mitochondria network. Hepatitis B virus facilitates the ubiquitination and degradation of MFN2 and promotes the recruitment of DRP1 by

stimulating its phosphorylation at Ser616 that results in mitochondrial fission[144], [145].

In mammalian hosts, *Trypanosoma cruzi* amastigotes exhibit a close interaction with host mitochondria via the parasite flagellum [146]. The *Plasmodium* parasite is an intracellular pathogen that causes a significant health burden in humans. Studies show that majority of the liver stage (LS)-infected hepatocytes have fragmented mitochondria. However, infected cells are also more resistant to external triggers of apoptosis. This inhibition of mitochondrial pro-apoptosis factors boosts the *Plasmodium* burden in LS-infected hepatocytes [147]. *Encephalitozoon hellem* develops in a parasitophorous vacuole (PV). The sporoplasm surface protein 1 (EhSSP1) localizes to the PVM and interacts with host mitochondrial voltage-dependent anion channels (VDACs). This contact causes the host mitochondria cluster around PVs which is a benefit for parasite proliferation[148].

3.6.2 Modulation of mitochondrial functions upon infection

Mitochondria can sense the pathogenic signals in the cytoplasm, resulting in the mitochondrial functions being mobilized to fight against pathogens. Pathogens also evolutionarily develop efficient strategies to survive and sustain their species within the long-term competition.

The virus extremely relies on the access to the nutrients from the host cell. The host mitochondrial OXPHOS system generates excessive mROS during SARS-CoV-2 infection. The high mROS activates some host cellular pathways, such as translation, to favor virus replication but also leads to an excessive innate immune response against viral infection, which leads to greater lung injury and worse clinical evolution [149]. Recently, the SARS-CoV-2 orf9b is revealed that interacts with the cytosolic segment of human TOM70 through its C-terminal pocket-like structure, leading to the inactivation of the IFN-I immune response[150].

Extracellular bacteria *Helicobacter pylori* VacA is not only essential to induce mitochondrial network fragmentation by DRP1, but also sufficient to inhibit apoptosis

by the inactivation of the proapoptotic Bcl-2-associated X (Bax) protein [137]. The intracellular *Chlamydia trachomatis* activates the mitochondria translocation of NLRX1 to enhance the levels of ROS, which can activate caspase-1 to promote its growth [151]. *Legionella pneumophila* infection triggers the rewiring of cellular bioenergetics from depressed mitochondrial respiration to elevated glycolysis, to create a permissive niche for bacteria replication by the type IV secretion system (T4SS) effector MitF (a Ran GTPase activator) [135].

Due to the specific-tissues and complex life cycle, the parasite offers a distinct view to understand the exploration of host nutrients and manipulation of the signaling pathway. *Leishmania infantum* infection switches the bioenergetic pathway of macrophages from glycolytic metabolism to OXPHOS by activating the AMPK and SIRT1, both are required for the regulation of nutrient availability from mitochondria [152]. *Plasmodium falciparum* perforin-like proteins, also known as the family of pore-forming proteins, promote the depolarization of mitochondria, leading to high mROS levels and increased intracellular calcium [153]. Cardiomyocytes infected with *Trypanosoma cruzi* also increase ROS levels following inefficient electron transport chain (ETC) activity and enhanced electron leakage at early infection stage [154]. Moreover, *Toxoplasma gondii* is one of most interesting examples that shows the fatty acid competition with host mitochondria during infection, which will be discussed in the next section.

3.7 *Toxoplasma gondii*: a competitor to host mitochondria?

Toxoplasma gondii is an obligate intracellular protozoan parasite which is the causative pathogen of toxoplasmosis in humans, other mammals, and birds. The first observation of it was in the tissues from a hamster-like rodent *Ctenodactylus gundi* in 1908. The next year, the new organism was named *Toxoplasma gondii* in term of morphology (“*Toxo*” refers to arc or bow, “*plasma*” refers to life) and the host by Nicolle and Manceaux. *Toxoplasma* has been studied over one hundred years and has a well-characterized life cycle, making it a suitable model for cell biology and crosstalk between host cells and pathogens.

In this session, we will briefly discuss *Toxoplasma*, including its biological cycle and prevalence, morphology and ultrastructure, immunology, and toxoplasmosis. Specifically, the intracellular PV niche of *Toxoplasma* where it proliferates, and which forms contact sits with host mitochondria, also known as host mitochondrial association (HMA).

3.7.1 *Toxoplasma gondii*: a very successful human parasite

Toxoplasma is approximately 4-8 μm long and 2-3 μm wide. It is a unicellular parasite which has a wide range of hosts including terrestrial and aquatic warm-blooded animals. Only cats or other species from the family *Felidae* host the sexual stages of *Toxoplasma* and are known as their definitive hosts. Other hosts, including humans, are considered intermediate hosts due to the presence of only asexual stage [155]. Although the definitive host was found since 1970, recently linoleic acid has been discovered to be the key factor regulating sexual proliferation [156]. Three predominant *Toxoplasma* lineages have been described based on genotypes referred to as type I, type II, and type III [157].

In the *Toxoplasma* life cycle, there are 3 infective stages. The *Toxoplasma* tachyzoite replicates rapidly and asexually in acute infections stage. The bradyzoite stage is found in chronic infections and is characterized by a slow asexual replication within wrapped a thick cyst wall and can be transmitted between intermediate hosts. The sporozoite is exclusively produced in the definitive host and transmits *Toxoplasma* to intermediate

hosts. Strikingly, *Toxoplasma* infects one-third of the world's population. *Toxoplasma* transmission pathways in human infection mainly include the contamination of water and food with oocysts, or undercooked contaminant meat with *Toxoplasma* cyst.

Toxoplasma is a eukaryotic cell and thus also has a nucleus, ER, Golgi complex, mitochondria and apicoplast. There is only one mitochondrion, which has a dynamic shape but lacks fusion and fission (its biogenesis following with cell cycle) and possesses the mtDNA encoding only 3 proteins. The apicoplast of *Toxoplasma* has lost the photosynthetic functionality, and now carries out the synthesis of 3 essential metabolites: haem, type II fatty acids, and isoprenoid precursors [158]. The apical complex at the anterior region is composed of the conoid and the secretory organelles (micronemes, rhoptries and dense granules). The conoid, micronemes and rhoptries coordinate to initiate the invasion process through the host plasma membrane. The dense granules which are ~0.2 µm diameter structures, contain a large set of proteins (150-200) that are translocated into the PV and/or PV membrane (PVM).

Toxoplasma can pass the intestinal epithelial barrier, and transmigrate into the muscle, liver, eyes and even brain by across the blood-brain barrier. Although the majority of the infection is asymptomatic under normal conditions, it has diverse symptoms under the condition of immunocompromise, such as retinochoroiditis and HIV infection. Recently, the major T-cell antigen for class I major histocompatibility complex (MHC I) is characterized as *Toxoplasma* dense granule 6 (GRA6) [159]. The macrophages are stimulated through the activation of TLR2, TLR4, IL-18R or IL-1R mediated by *Toxoplasma* glycosylphosphatidylinositol proteins (GPIs), to respond against *Toxoplasma* infection [160].

3.7.2 The parasitophorous vacuole (PV) of *Toxoplasma*

In the lytic cycle, The PV is formed during invasion by the invagination of the host cell plasma membrane within 25-40s. Subsequently, the cytoplasmic membrane proteins are eliminated from PVM. This is thought to render the PV nonfusogenic and invisible to the host endolysosomal system. Although the PV protects *Toxoplasma* from recognition by the innate immune system, it also is a barrier for the parasite to

effectively communicate with the host and acquire nutrients. Therefore, *Toxoplasma* explores a unique approach to redecorate the PV (**Figure 5**).

The formation of the PV is thought to occur via two-steps [161]. During the first step, at the moving junction where the invasion site is, the contents of the *Toxoplasma* rhoptries are secreted into the host cytosol resulting in the formation of discrete vesicles. Next, the ROP vesicles fuse with the requisite plasma membrane and modify its protein composition, resulting in the formation of PV. Then, the PVM is modified by rhoptry (ROP) or dense granule (GRA) proteins secreted from *Toxoplasma*, which enable the PVM to interface between *Toxoplasma* and the host. The PVM promotes communication with signaling effectors and transports the nutrients from the host, since *Toxoplasma* is auxotrophic for many nutrients [162].

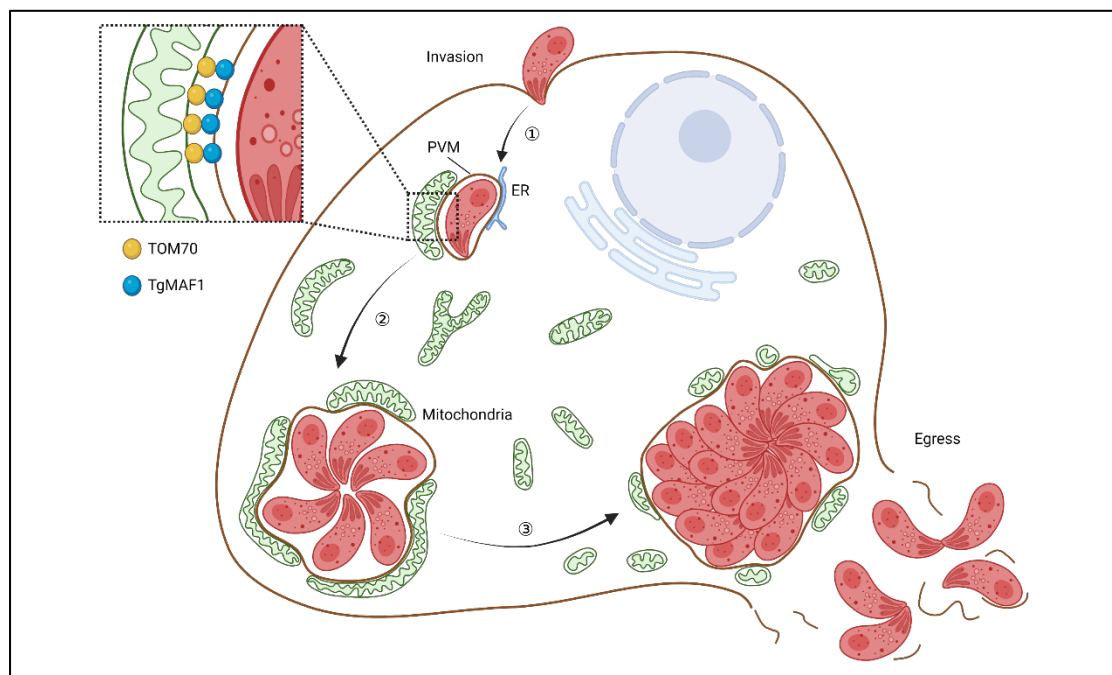


Figure 5. The schematic of *Toxoplasma* lytic cycle and the HMA during *Toxoplasma* infection.

Recently, increasing GRA effector proteins have been identified in the host cytoplasm and nucleus, such as GRA16, MYR1, GRA28, TEEGR, GRA24, IST [163]. For example, *Toxoplasma* Myc regulator 1 (MYR1) can be cleaved into 2 fragments aspartyl protease 5 (ASP5) and is subsequently transported into the host cytosol. They

are transported by the PVM resident transporters and related regulators, including MYR1, MYR2, MYR3, MYR4, ROP17, GRA44 and GRA45. Interestingly, MYR1, GRA44, and GRA45 are proteolytically cleaved in an ASP5-dependent manner, but their function as transporters is not disabled [163]. Additionally, the pore structure formed by GRA17 and GRA23 in the PVM allows the diffusion of small molecules (<1300 Da), but not larger proteins [164][165].

Toxoplasma requires many nutrients from its host cell. For example, lipoic acid is found to be synthesized in the *Toxoplasma* apicoplast but fails to reach *Toxoplasma* mitochondrion where it is required in nature. Therefore, *Toxoplasma* has to obtain it from host mitochondria where it is synthesized [166]. Other metabolites, such as purines, cholesterol, inositol, polyamines, and choline, are transferred from host to *Toxoplasma* through the PVM [167]. Although many nutrients are transported through the pore structure formed by GRA17 and GRA23, the precise mechanism and additional import machineries is little known.

3.7.3 The Host Mitochondria Association (HMA) with PVM

The PVM associates with the ER and host mitochondria, the latter which is known as [168] host mitochondria association (HMA) (**Figure 5**). It was first shown in macrophages infected with type I *Toxoplasma* strain in 1972 [169]. However, the question of which parasite factor mediates the HMA remained a mystery for four decades.

Recently, HMA was found to specifically occur during infection of *Toxoplasma* type I and III but not type II strains, which demonstrated that HMA has a genetic basis. Pernas et al revealed that the *Toxoplasma* locus mitochondria association factor 1b (MAF1b) (annotated as TGGT1_053770 in ToxoDB v7.2) is required for HMA [170]. The expression of MAF1b in Type II parasites is sufficient for HMA and the ablation of MAF1b in Type I strain leads to the loss of HMA. The exposed C-terminus of MAF1 is required to recruit host mitochondria and induces the elongation of the associated mitochondria [170]. An analysis of the multiple paralogs encoded by MAF1 revealed

that three C-terminal residues (Ser438, Thr439, and Leu441) are conserved in the HMA-competent MAF1b [171]. The expression of MAF1b with the STL residues mutated to RKK (uncharged counterparts Arg427, Lys428 and Lys430 in MAF1a) is not sufficient for HMA. Strikingly, the MAF1b with RKK mutants impairs the growth advantage *in vivo*, which provides insight into the link between pathogen proliferation and manipulation of host mitochondria. The expression of MAF1b confers a growth advantage for Type II parasites relative to wild type counterparts *in vivo* [172].

An IP-mass spectrometry analysis of host proteins bound to MAF1b revealed MIC60 and MIC19 (the subunits of MICOS in the IMM). They also hypothesized and verified that the OMM component SAM50 interacts with MAF1b, because SAM50 is another core subunit of MIB with MICOS complex. Interestingly, the interaction of MAF1b with MIC60 and SAM50 is deficient by its C-terminal HA epitope tag, but MAF1a and C-terminal mutated MAF1b keep the interaction with SAM50 [171], [173]. Another study from Blank et al performed a similar IP-mass spectrometry analysis of MAF1b-interacting proteins and identified TOM70 and the mitochondria-specific chaperone HSPA9, which both are essential for the formation of HMA. TOM70 is enriched around PVM during *Toxoplasma* infection [174]. Additionally, the loss of the PVM-localized protein ROP39 leads to a 10% reduction of HMA [175].

A consequence of HMA is the enlargement of PVM-associated mitochondria and changes to the host cell immune responses, such as the expression of chemokines and IFN-gamma-induced genes [170]. MAF1-mediated HMA preserves the growth and proliferation of parasites deficient for ACBP2, regulates cardiolipin metabolism in type II parasites through acyl-CoA-binding [176].

HMA appears to be a consequence of infection with pathogens such as SARS-CoV-2, *Listeria monocytogenes*, *Microsporidian sp.*, and so on [73]. Why does the parasite tether host mitochondria? Recently, Pernas et al found that although *Toxoplasma* triggers lipophagy to gain access to host fatty acids, host mitochondria restrict the growth of *Toxoplasma* by limiting its access to fatty acids. In cells deficient for MFN1 and MFN2 and thus mitochondrial elongation, *Toxoplasma* grew faster and took up

more FAs [11]. How FAs are transferred between OMM and PVM remains unclear. More puzzling is the fact that *Toxoplasma* has an effector protein that binds host mitochondria — their nutrient competitors.

4. Publication

We thank Nouf N. Laqtom and Monther Abu-Remaileh (Stanford University) for teaching us the mitoIP protocol; Thomas Langer (MPI-AGE) for the generous sharing of reagents; the MPI-AGE Proteomics Core, in particular Xinping Li for advice on sample preparation; the MPI-AGE FACS and Imaging Core for excellent flow cytometry, and microscopy support, and in particular Marcel Kirchner; and the CECAD imaging facility and in particular Katrin Seidel for electron microscopy support. We also thank Silvia Reato for excellent laboratory support, Patrick Krueger for manuscript feedback, and all members of the Pernas laboratory for helpful discussions.

Funding: This work was supported by the European Research Council ERC-StG-2019 852457 (to L.F.P.); Deutsche Forschungsgemeinschaft SFB 1218 Project ID: 269925409 (to L.F.P. and T.B.); Project ID: 411422114–GRK 2550 (to L.F.P.); BE 4679/2-2 Project ID 269424439 (to T.B.); BONFOR program of the University Hospital Bonn (to F.d.B.); Chinese Research Council (to X.L.); and IMPRS (to C.M.).

Author contributions: Conceptualization: Xianhe Li, Julian Straub, and Lena F. Pernas. Methodology: Xianhe Li, Julian Straub, Tânia Catarina Medeiros, Chahat Mehra, Fabian den Brave, Esra Peker, Katharina Stillger, Jan Riemer, Thomas Becker, Lena F. Pernas. Investigation: All authors. Resources: Emma Burbridge, Colin Adrain, Jonas Benjamin Michaelis, and Christian Münch. Proteomics analysis: Xianhe Li, Lena F. Pernas and Ilian Atanassov. Funding acquisition: Xianhe Li and Lena F. Pernas. Project administration: Lena F. Pernas. Writing, original draft: Xianhe Li and Lena F. Pernas. Writing, review and editing: All authors. Supervision: Lena F. Pernas. Competing interests: The authors declare that they have no competing interests.

RESEARCH ARTICLE SUMMARY

CELL BIOLOGY

Mitochondria shed their outer membrane in response to infection-induced stress

Xianhe Li, Julian Straub, Tânia Catarina Medeiros, Chahat Mehra, Fabian den Brave, Esra Peker, Ilian Atanassov, Katharina Stillger, Jonas Benjamin Michaelis, Emma Burbridge, Colin Adrain, Christian Münch, Jan Riemer, Thomas Becker, Lena F. Pernas*

INTRODUCTION: Mitochondria are dynamic organelles that coordinate many cellular functions that are essential for life, including diverse metabolic processes, cell division and differentiation, and immune signaling.

To carry out these diverse functions, mitochondria must communicate with the cytosol, a task mediated by the outer mitochondrial membrane (OMM), the gateway between mitochondria and the rest of the cell. Thus, preserving the integrity of the OMM is essential for cellular homeostasis. Although responses to stress that is artificially induced by small molecules have been described, little is known of the mechanisms by which mammalian cells respond to naturally occurring stresses of the OMM.

RATIONALE: Several intracellular microbes come in contact with the host OMM or release proteins that target the OMM. We reasoned that microbial infection would serve as a model with which to study cellular responses to natural OMM stress. To this end, we chose the human parasite *Toxoplasma gondii* because it tethers host mitochondria to its parasite vacuole; in an infected cell, areas of close membrane apposition form between the host OMM and the parasite vacuole membrane. To address how *Toxoplasma* affected the OMM, we performed live-cell imag-

ing of infected mammalian cells stably expressing OMM-targeted green fluorescent protein (GFP). We found that mitochondria in contact with the *Toxoplasma* vacuole released large structures that were positive for OMM, which we termed “SPOTs.” Analysis of SPOTs in fixed and live cells revealed that SPOTs did not contain proteins of the mitochondrial matrix and inner mitochondrial membrane (IMM).

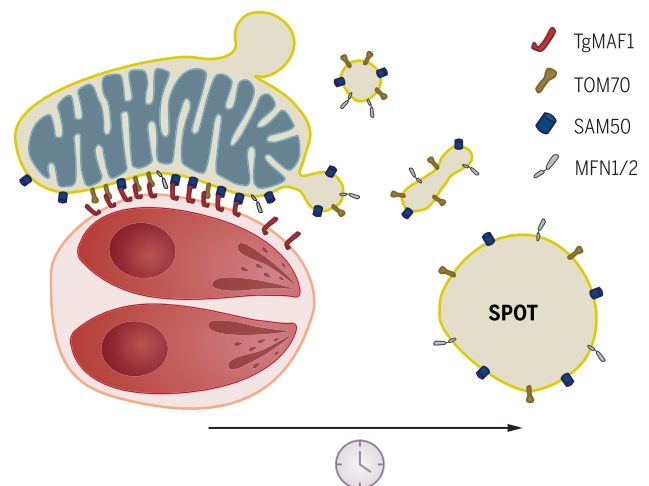
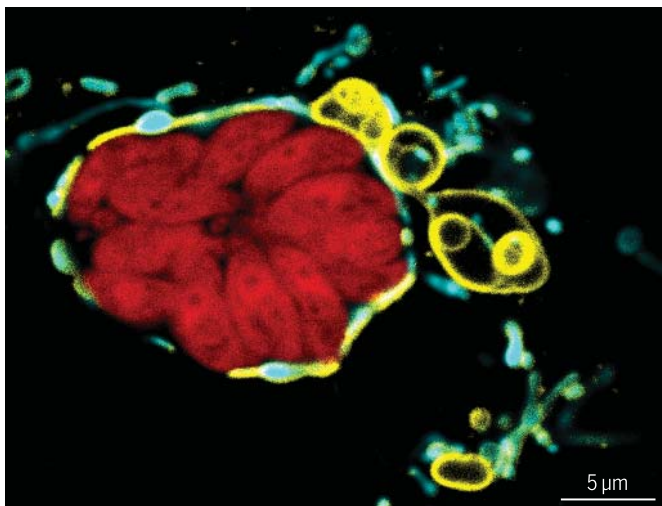
RESULTS: Having identified *Toxoplasma* infection as a natural stress that induced OMM remodeling and the shedding of SPOTs, we next dissected how these structures are formed. We found that the secreted effector protein TgMAF1 (*Toxoplasma gondii* mitochondrial association factor 1), which tethers the host OMM to the parasite vacuole membrane, was required for SPOT formation. TgMAF1 led to a decrease in the amount of mitochondrial proteins during infection. In particular, the OMM proteins mitofusin 1 and mitofusin 2 were degraded during infection. These proteins, which mediate a nutritional defense against *Toxoplasma* by promoting mitochondrial uptake of fatty acids, localized to SPOTs. The ability of TgMAF1 to induce SPOTs depended on its binding to the host OMM import receptor TOM70 (translocase of the outer membrane 70), whose import function

TgMAF1 impaired. TOM70 was required for optimal parasite growth and enabled an interaction between TgMAF1 and the OMM translocase SAM50 (sorting assembly machinery 50 kDa subunit), which is a key component of the OMM-IMM mitochondrial intermembrane space bridging (MIB) complex. The genetic ablation of SAM50 and the overexpression of an OMM-targeted protein induced the formation of SPOT-like structures independently of infection.

CONCLUSION: Because SAM50 is the only component of mitochondrial import machinery that bridges the OMM and IMM, it is in a position to translate OMM stress into the removal of compromised OMM. TgMAF1 behaves as a mitochondrial preprotein that uses the host receptor TOM70 to interact with SAM50. This enables *Toxoplasma* to hijack a cellular response to OMM stress—the formation of SPOTs—and drive the constitutive shedding of the OMM. Consequently, levels of mitochondrial proteins that restrict parasite growth are depleted, and import machinery that is required for mitochondrial biogenesis is sequestered on SPOTs. In an infection-independent context, however, we propose that SPOT-like structures could mitigate OMM stress by enabling the excision of dysfunctional OMM machinery, such as import receptors or translocases during defective import. Our finding that OMM remodeling occurs during infection and infection-independent scenarios sheds light on potential cellular mechanisms that safeguard OMM function. ■

The list of author affiliations is available in the full article online.
*Corresponding author. Email: pernas@age.mpg.de
Cite this article as X. Li et al., *Science* 375, eabi4343 (2022).
DOI: 10.1126/science.abi4343

S READ THE FULL ARTICLE AT
<https://doi.org/10.1126/science.abi4343>



Mitochondria shed SPOTs during *Toxoplasma* infection. (Left) Mitochondria surrounding the parasite *Toxoplasma* (red) shed SPOTs, large structures positive for OMM (yellow) that lack mitochondrial matrix (cyan). (Right) Cartoon depiction of image at left as infection progresses (clock). OMM proteins—including the import translocase SAM50, and MFN1 and MFN2, which are required for mitochondrial fusion—are sequestered on SPOTs.

RESEARCH ARTICLE

CELL BIOLOGY

Mitochondria shed their outer membrane in response to infection-induced stress

Xianhe Li¹, Julian Straub¹, Tânia Catarina Medeiros¹, Chahat Mehra¹, Fabian den Brave², Esra Peker³, Ilian Atanassov¹, Katharina Stillger³, Jonas Benjamin Michaelis⁴, Emma Burbridge^{5,6}, Colin Adrain^{5,6}, Christian Münch⁴, Jan Riemer^{3,7}, Thomas Becker², Lena F. Pernas^{1,7*}

The outer mitochondrial membrane (OMM) is essential for cellular homeostasis. Yet little is known of the mechanisms that remodel it during natural stresses. We found that large “SPOTs” (structures positive for OMM) emerge during *Toxoplasma gondii* infection in mammalian cells. SPOTs mediated the depletion of the OMM proteins mitofusin 1 and 2, which restrict parasite growth. The formation of SPOTs depended on the parasite effector TgMAF1 and the host mitochondrial import receptor TOM70, which is required for optimal parasite proliferation. TOM70 enabled TgMAF1 to interact with the host OMM translocase SAM50. The ablation of SAM50 or the overexpression of an OMM-targeted protein promoted OMM remodeling independently of infection. Thus, *Toxoplasma* hijacks the formation of SPOTs, a cellular response to OMM stress, to promote its growth.

Mitochondria are dynamic organelles that coordinate cellular functions essential for life, including diverse metabolic processes, cell division and differentiation, and immune signaling (1). At the interface between mitochondria and the rest of the cell, the outer mitochondrial membrane (OMM) plays a central role in all mitochondrial functions. Arguably, the most vital of these functions is to enable mitochondrial biogenesis by providing a platform for the machinery that imports almost all ~1200 nuclear-encoded mitochondrial proteins in mammals (2). Dysfunction of the mitochondrial import machinery results in systemic pathology of the organelle and organismal death (3). Because all mitochondrial functions rely on the import of proteins into the organelle, quality control pathways must regulate import processes and prevent the toxic accumulation of nonimported or mislocalized precursor proteins, several of which have been identified and studied in yeast (4). By contrast, how the OMM is protected and remodeled during import stress in mammals is largely uncharacterized.

Intracellular microbes pose a naturally occurring threat to mitochondria, which is perhaps the evolutionary consequence of the role that these organelles play in antimicrobial immune

signaling and nutritional defense (5–8). Several bacteria, for example, release effector proteins that localize to the OMM and perturb mitochondrial function (9). We used the parasite *Toxoplasma gondii*, which infects up to one-third of the human population and has an unparalleled host range, to investigate the cellular responses that remodel the OMM (10). With respect to the OMM, *Toxoplasma* is of particular interest because it is one of several pathogens to reside in vacuoles found in close physical proximity to mitochondria (11, 12).

Mitochondria shed SPOTs during *Toxoplasma* infection

To monitor the impact of *Toxoplasma* infection on the OMM, we infected mouse cells stably expressing enhanced green fluorescent protein (eGFP) fused to the OMM-targeting transmembrane (TM) domain of OMP25 (OMM-GFP) with mCherry-expressing *Toxoplasma* (13). As early as 6 hours after infection, we observed large spherical and elliptical structures enriched for OMM-GFP that were absent in uninfected cells, which we termed “SPOTs” (structures positive for outer mitochondrial membrane) (Fig. 1A). The percentage of SPOT-positive cells increased over the course of infection (Fig. 1B). At 24 hours after infection, >50% of infected cells contained between 1 and 20 SPOTs that were on average ~2.6 μm in diameter (Fig. 1, A to D). To exclude the possibility that the formation of SPOTs depended on OMM-GFP expression, we also examined infected cells using a fluorescent phosphatidylcholine conjugate (FL-HPC) that in part integrates into mitochondrial membranes. In both wild-type (WT) and OMM-BFP (blue fluorescent protein)-expressing U2OS (human) cells, FL-HPC distributed to SPOT-like structures

that were only present in infected cells (fig. S1). Thus, SPOT formation is a general consequence of *Toxoplasma* infection in mammalian cells.

Despite their large size, we suspect that SPOTs have been overlooked because although they retain OMM proteins such as TOM20 (translocase of the outer membrane 20), they are not labeled by mitotracker, a commonly used vital dye that accumulates in mitochondria in a membrane potential-dependent manner (Fig. 1, E to F, and figs. S1 and S2A). Furthermore, in live-cell imaging experiments, SPOTs also lack fluorescent markers of other mitochondrial compartments, including the matrix and inner mitochondrial membrane (IMM) (Fig. 1, G to J). We confirmed that SPOTs also lacked endogenous levels of proteins of the intermembrane space (IMS) (AIFM1), IMM (ATPF1B), and matrix (CS and mtHSP70) (fig. S2, B to E). Thus, the OMM is remodeled to release SPOTs during *Toxoplasma* infection. Hereafter, we refer to SPOTs as structures that are positive for an OMM marker but that lack markers of other mitochondrial compartments.

The large diameter and lack of mitochondrial matrix proteins in SPOTs suggested that they differed from fragmented mitochondria as well as mitochondria-derived compartments (MDCs) and mitochondria-derived vesicles (MDVs), which form in response to amino acid toxicity and oxidative stress, respectively (14–19). MDCs average 1 μm in diameter and depend on the OMM guanosine triphosphatase (GTPase) MIRO1 (mitochondrial rho GTPase 1), which mediates mitochondrial trafficking (16, 17). The smaller MDVs that transport cargo between mitochondria and peroxisomes or lysosomes—the latter of which depend on the E3 ligase parkin and the mitochondrial kinase PINK1 (PTEN-induced putative kinase protein 1)—range between 75 and 150 nm in diameter (14, 18, 20). Neither the loss of the key mitochondrial fission factor DRP1 (dynamin-related protein 1) nor of MIRO1 and its paralog MIRO2 significantly affected SPOT formation during infection (fig. S3). Moreover, SPOTs also formed during infection in HeLa cells that were deficient for PINK1 in a manner similar to that of WT HeLa cells that lacked detectable parkin expression (fig. S4) (21).

The dynamin-binding partner SNX9 (sorting nexin 9) that remodels endocytic membranes mediates the emergence of a subset of MDVs that contain the matrix proteins OGDH (oxoglutarate dehydrogenase) and mtHSP70 (22–24). We thus asked whether SNX9 also participated in SPOT formation. In infected cells, the depletion of SNX9 prevented the formation of SPOTs (fig. S5, A to E). However, *Toxoplasma*-induced SPOTs lacked both mtHSP70 and OGDH, matrix proteins that are markers of SNX9-dependent MDVs (figs. S2E and S5F). Thus, SPOTs represent an independent class of structures that bud from the OMM.

¹Max Planck Institute for Biology of Ageing, Cologne, Germany. ²Institute of Biochemistry and Molecular Biology, Medical Faculty, University of Bonn, Bonn, Germany. ³Institute of Biochemistry, University of Cologne, Cologne, Germany. ⁴Institute of Biochemistry II, Faculty of Medicine, Goethe University, Frankfurt am Main, Germany. ⁵Patrick G. Johnston Centre for Cancer Research, Queen's University Belfast, Belfast, Northern Ireland. ⁶Instituto Gulbenkian de Ciência, Oeiras, Portugal. ⁷Cologne Excellence Cluster on Cellular Stress Responses in Aging-Associated Diseases (CECAD), University of Cologne, Cologne, Germany. *Corresponding author. Email: pernas@age.mpg.de

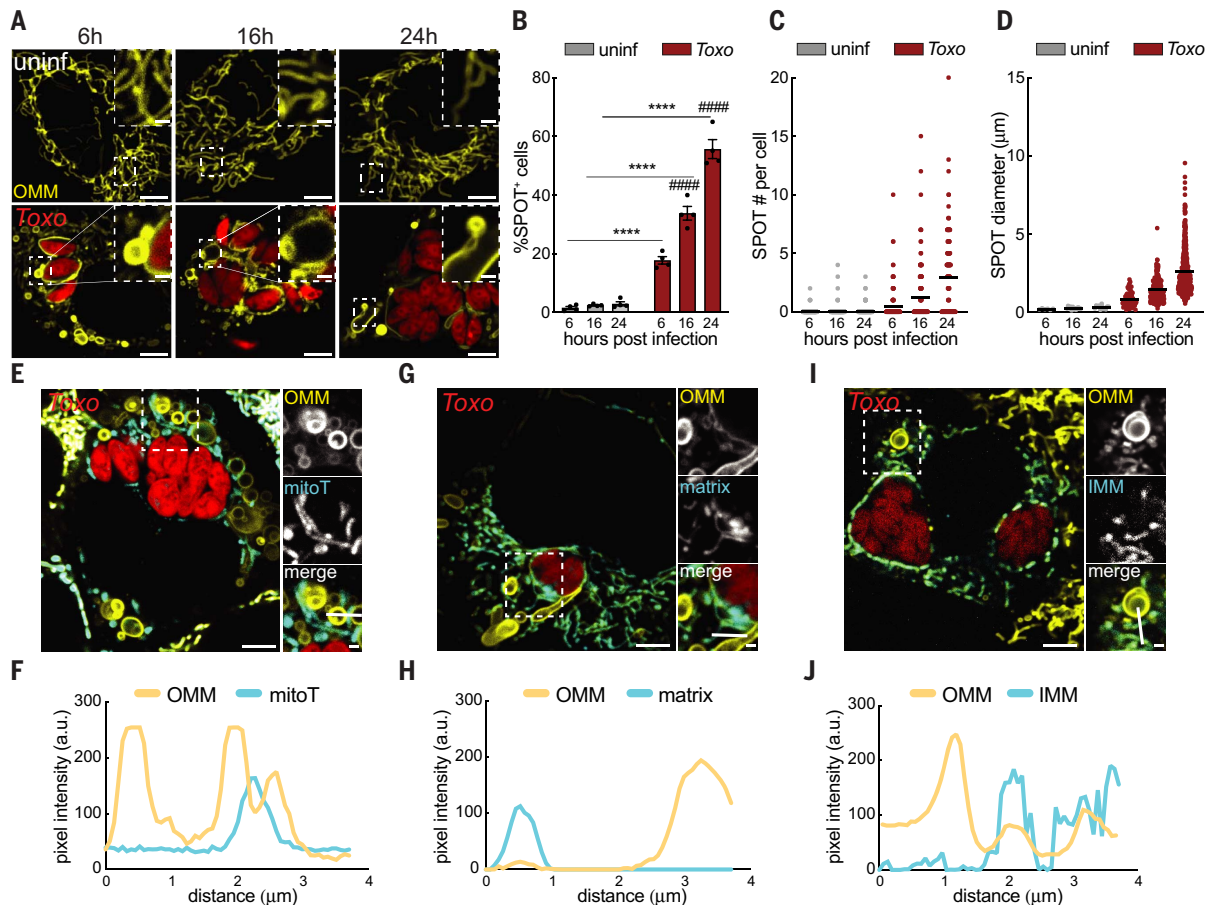


Fig. 1. The outer membrane is remodeled during *Toxoplasma* infection through the release of SPOTs. (A) Representative live-cell images of the OMM (GFP) in uninfected (uninf) and *Toxoplasma* (mCh)-infected (*Toxo*) MEFs at 6, 16, and 24 hours after infection. (B) Percentage of SPOT-positive cells in experiments as in (A); data are mean \pm SEM of more than 100 cells counted from four biological replicates; **** $P < 0.0001$ for uninfected versus infected; ##### $P < 0.0001$ for 6 hours after infection versus 16 and 24 hours after infection by means of two-way

ANOVA. (C and D) Scatterplot with mean (C) number and (D) diameter of SPOTs in experiments as in (A) from more than 30 infected cells from three biological replicates. (E, G, and I) Representative live-cell images of the OMM (GFP) in *Toxoplasma* (mCherry)-infected MEFs (E) labeled with MitoTracker Deep Red (mitoT); (G) expressing matrix-targeted BFP (matrix); or (I) expressing RFP-tagged TIM50 (IMM). (F, H, and J) Corresponding pixel intensity plots for white line in (E), (G), and (I) insets, respectively. Scale bars, 5 μ m and (insets) 1 μ m.

The parasite effector TgMAF1 is required for SPOT formation and the depletion of host mitochondrial proteins

How does *Toxoplasma* induce the formation of SPOTs? In live-cell imaging analyses of infected cells, SPOTs were readily visualized emerging from mitochondria in proximity to the parasite vacuole (PV) (Figs. 1, A, E, G, and 2A and movies S1 and S2). At the mitochondria-*Toxoplasma* interface, the OMM is tethered to the PV membrane (PVM) at a distance of 12 to 17 nm, regions that can be referred to as “contact sites,” a term that describes areas of close membrane apposition between organelles (25, 26). Mitochondria-*Toxoplasma* PV contact sites, previously termed host mitochondrial association (HMA), are completely dependent on the parasite effector protein TgMAF1 (*Toxoplasma gondii* mitochondrial association factor 1) (27). TgMAF1 is anchored in the PVM and posited to interact with host mitochondria through its cytosolically exposed

C terminus (27–29). TgMAF1 affects the host inflammatory responses during infection, but its function at mitochondria-*Toxoplasma* contact sites remains elusive (27). To test the hypothesis that TgMAF1 tethering of host mitochondria contributes to SPOT formation, we assessed the frequency of SPOTs in cells infected with WT or Δ maf1 parasites. The ablation of TgMAF1 completely prevented the formation of SPOTs (Fig. 2, B to E). Thus, TgMAF1 is required for the formation of SPOTs during infection.

The physical remodeling of the OMM during *Toxoplasma* infection prompted us to ask whether the formation of SPOTs also led to changes in its composition. To address this, we used proteomics to compare the protein abundances between whole cell extracts and mitochondria immunopurified (mitoIP) from uninfected cells and cells infected with WT or Δ maf1 parasites (13). Infection with WT parasites caused a global decrease in the whole

cell and mitoIP abundance of mitochondrial proteins that was partially prevented during infection with Δ maf1 parasites (Fig. 3, A to D; fig. S6, A to D; and data files S1 and S2). Thus, TgMAF1, beyond its tethering function, is also required for the decrease in mitochondrial proteins during infection.

A targeted analysis of changes in the OMM compartment from which SPOTs are derived revealed TgMAF1-dependent decreases in several proteins that mediate antimicrobial defense, including MIRO1, MIRO2, mitofusin 1 (MFN1), and MFN2, results we confirmed with immunoblotting (Fig. 3, E to F) (5, 30). The depletion of MFN1 and MFN2 during infection was particularly intriguing given that these OMM GTPases are essential for mitochondria to restrict parasite proliferation and raised the question of how TgMAF1 drove their decrease (5). Infection did not reduce MFN1 and MFN2 mRNA amounts (fig. S7A). Furthermore, neither the loss of PINK1, a key

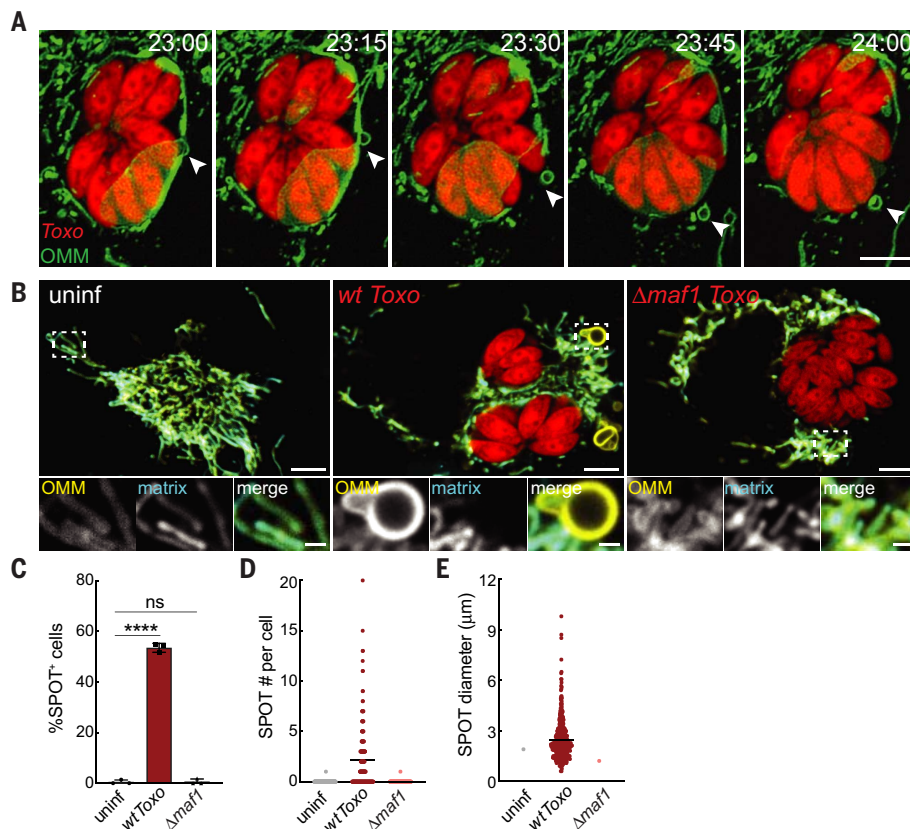


Fig. 2. TgMAF1 is required for SPOT formation. (A) Representative live-cell images of the OMM (GFP) in *Toxoplasma* (mCh)-infected HFFs. Shown is the formation of a SPOT (indicated with white arrowhead) over a 1-hour time-lapse movie starting at 23 hours after infection with frames captured every 15 min (movie S2). Scale bar, 5 μ m. (B) Representative live-cell images of the OMM (GFP) and matrix (BFP) in uninf, WT *Toxo* (mCh)-infected, or $\Delta maf1$ *Toxo* (mCh)-infected U2OS cells. Scale bars, 5 μ m and (inset) 1 μ m. (C) Percentage of SPOT-positive cells in experiments as in (B). Data are mean \pm SEM of more than 100 cells counted from three biological replicates. ns, not significant; **** $P < 0.0001$ for uninfected versus infected by means of one-way ANOVA analysis. (D and E) Scatterplots with mean (D) number and (E) diameter of SPOTs in experiments as in (B) from more than 30 infected cells from three biological replicates.

mediator of mitophagy, nor the loss of the essential autophagy gene *Atg7* prevented the *Toxoplasma*-induced reduction in MFN1 and MFN2 (fig. S7, B and C). The decrease in MFN1 and MFN2 correlated with their redistribution from mitochondria to SPOTs that were also positive for FAF2 (Fas-associated factor family member 2), a protein that recruits the proteasomal machinery required for endoplasmic reticulum (ER)-associated degradation (Fig. 3, G to J, and fig. S7, D to F) (31). Because MFN1 and MFN2 are regulated by the ubiquitin/proteasome system (UPS) and FAF2 mediates the turnover of MFN1/2 (Fzo1) in yeast, we asked whether FAF2 played such a role in our system (32, 33). In mouse embryonic fibroblasts (MEFs) in which FAF2 was ablated (FAF2 KO MEFs), the depletion of MFN1 and MFN2 in mitochondrial and whole-cell fractions that would normally be caused by infection was prevented (fig. S7G). Conversely, the expression of *Faf2* cDNA in FAF2 KO MEFs rescued their depletion during

infection (fig. S7H). To test a potential role for the UPS in mediating the degradation of MFN1 and MFN2, we turned to TAK-243, a small molecular inhibitor of the ubiquitin activation step that precedes degradation by the UPS because inhibitors of proteasomal machinery restrict parasite proliferation (fig. S7, I to J) (34). Treatment with TAK-243 did not affect parasite burden as assessed by *Toxoplasma* TgGAP45 but prevented the depletion of MFN1 and MFN2 and to a lesser extent that of MIRO1 and MIRO2, which also localized to SPOTs during infection (figs. S7, I to J, and S8). Thus, FAF2 mediates the proteolytic degradation of MFN1 and MFN2 on SPOTs, and certain OMM proteins that localize to SPOTs are targeted by the UPS for degradation.

TgMAF1 inhibits host TOM70 import function

How does TgMAF1 induce the remodeling of the OMM into SPOTs? We reasoned that identifying TgMAF1-interacting factor(s) might pro-

vide clues to host proteins involved in SPOT formation. To find these host factors, we immunopurified TgMAF1 from cells infected with $\Delta maf1$ parasites complemented with a hemagglutinin (HA)-tagged TgMAF1 ($\Delta maf1$:HA-MAF1) at a multiplicity of infection (MOI) of 1, 2.4, and 6 and identified the major interaction partners using mass spectrometry. The OMM import receptor TOM70 was the most abundant host protein found at >256-fold enrichment in TgMAF1-IPs of cells infected at all MOIs relative to control IPs (Fig. 4A and data file S3). TOM70 is required for *Toxoplasma* association with host mitochondria and is enriched on mitochondria tethered to the PV (35). To confirm that parasite TgMAF1 and host TOM70 interact during infection, we also performed an immunoblot analysis of TgMAF1-IPs. TgMAF1 coimmunoprecipitated TOM70 but not other OMM proteins, including VDAC1 (voltage-dependent anion channel 1) or VDAC2, nor its putative interacting partner HSPA9 (heat shock protein family A member 9) (Fig. 4B) (35). Furthermore, stably expressed GFP-tagged TOM70 coimmunoprecipitated TgMAF1 from lysates of infected MEFs and was enriched on the OMM of a mitochondrion tethered to the PV at 20-fold higher concentrations than those of OMM regions of the same mitochondrion not in contact with the PV (Fig. 4, C to E). This consequence of infection was completely dependent on TgMAF1 because the distribution of TOM70 did not differ between cells infected with $\Delta maf1$:HA parasites and uninfected cells (Fig. 4, D to E). To address whether TgMAF1 and TOM70 directly interact, we incubated TgMAF1 produced in a cell-free system with the purified cytosolic domain of yeast TOM70. Only full-length TgMAF1—but not a mutant lacking a predicted internal mitochondrial targeting sequence (iMITS), which mediates precursor binding to TOM70—bound to affinity-purified TOM70 (Fig. 4, F to G) (35, 36). Thus, parasite TgMAF1 and host TOM70 directly interact during infection.

TOM70 has two critical functions at the OMM. First, TOM70 recruits cytosolic chaperones such as HSP90 that mediate precursor import and thus protects against proteotoxicity owing to accumulated precursors through its N-terminal CLAMP domain (37, 38). Second, TOM70 is a major import receptor, most notably for SLC25 mitochondrial carriers that it binds through its CORE and C-tail domains (38). Thus, TgMAF1 could perturb TOM70 chaperone-binding activity or import activity to exploit a host response to import stress, leading to SPOT formation. To address these possibilities, we asked whether the abundances of HSP90 or SLC25 proteins were altered in our proteomics datasets of uninfected cells and cells infected with WT or $\Delta maf1$ parasites (Fig. 3, A to D). The levels of HSP90 were increased in mitoIPs in a

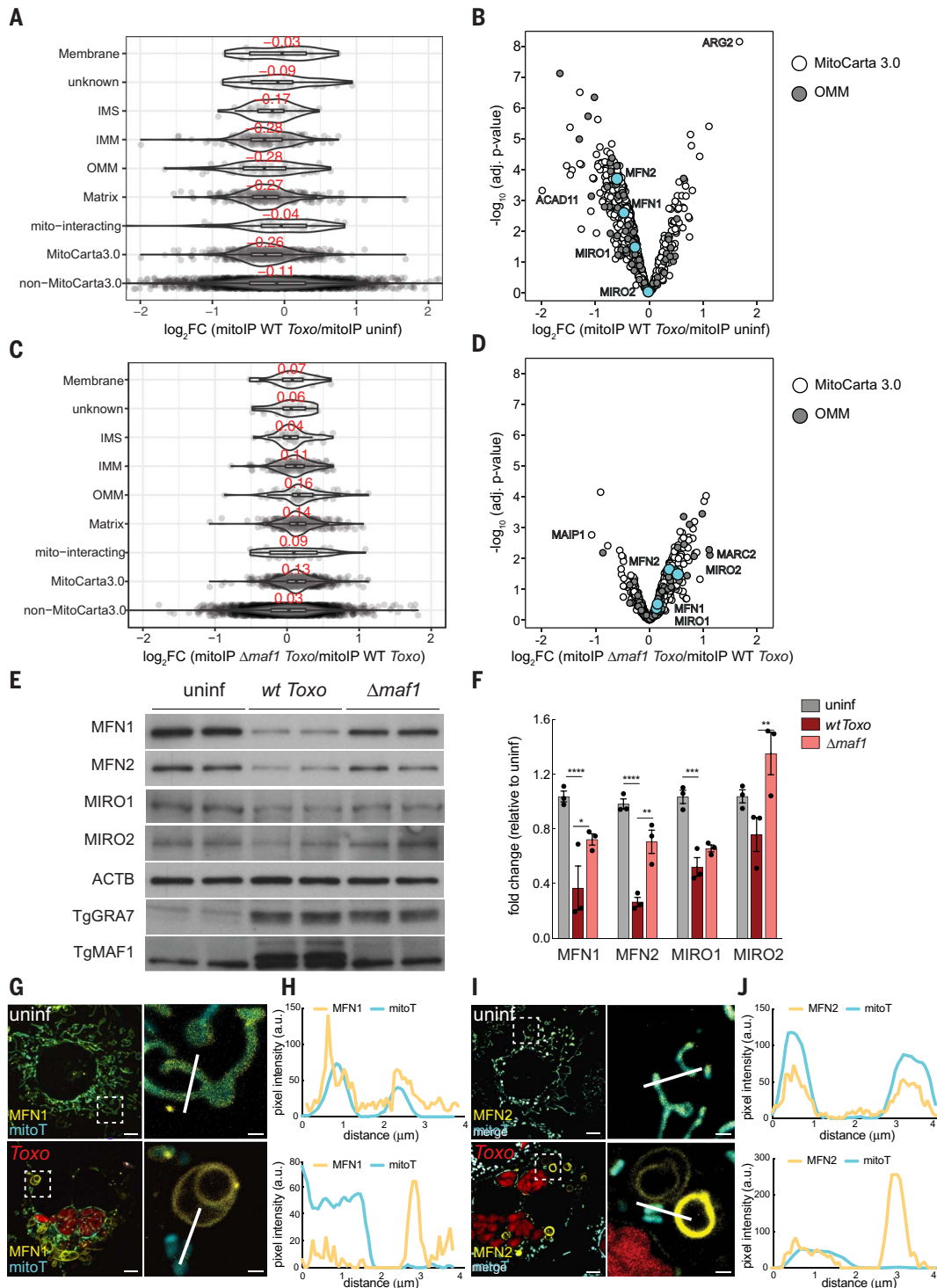


Fig. 3. TgMAF1 drives changes in the mitochondrial proteome and the depletion of certain OMM proteins that localize to SPOTS. (A and C) Mitochondria were immunopurified (mitoIP) from HeLa cells that were uninfected (uninf) ($n = 4$), WT *Toxo*-infected ($n = 4$), or $\Delta \text{maf1 Toxo}$ -infected ($n = 3$) at 24 hours after infection and analyzed by means of mass spectrometry. Shown are boxplots depicting the \log_2 -fold change (FC) of detected MitoCarta3.0 proteins between indicated treatments according to submitochondrial localization. Median values for each subcompartment are indicated in red. (B and D) Volcano plot of proteins in (A) and (C). Dark gray, OMM proteins as classified by MitoCarta3.0; white, all other MitoCarta3.0 proteins. (E) Cells were uninf,

WT *Toxo*⁻, or Δmaf1 -infected for 24 hours and analyzed by means of immunoblotting for MFN1, ~80 kDa; MFN2, ~80 kDa; MIRO1, ~75 kDa; MIRO2, ~75 kDa; ACTB, ~45 kDa; TgGRA7, ~32 kDa; and TgMAF1, ~60 kDa. (F) Fold change in density of protein bands imaged as in (E) normalized to actin and relative to mean of uninfected samples. Data are mean \pm SEM from three biological replicates; * $P < 0.05$, ** $P < 0.01$, *** $P < 0.001$, **** $P < 0.0001$ for WT *Toxo* versus uninfected or Δmaf1 -infected samples. Representative live-cell images of (G) *Mfn1*^{-/-}:GFP-*Mfn1* MEFs and (I) *Mfn2*^{-/-} MEFs expressing mCh-MFN2 at 24 hours after infection with *Toxoplasma* (BFP). (H and J) Corresponding pixel intensity plots for white line in (G) and (I) insets, respectively. Scale bars, 5 μm and (inset) 1 μm .

TgMAF1-dependent manner (fig. S9, A and B). Opposite to HSP90 however, concentrations of 11 of the 22 detected SLC25 proteins were decreased in a MAF1-dependent manner, hinting at an impact of MAF1 on TOM70-dependent import (fig. S9, A to B). To more carefully dissect how TgMAF1 affects TOM70 import function, we turned to budding yeast, a workhorse for mitochondrial import studies and a system in which TOM70 function is well characterized (36, 37). After confirming that stably expressed TgMAF1 co-immunoprecipitated yeast TOM70, we assessed its effect on TOM70 import (fig. S9C). Mitochondria isolated from TgMAF1⁺ yeast imported the TOM70-dependent precursor AAC (ADP/ATP carrier) more slowly than did mitochondria from WT yeast, whereas the Su9-DHFR (dihydrofolate reductase) fusion protein, which does not require TOM70, was imported at similar rates (fig. S9, D to G) (37, 39). Furthermore, TgMAF1 stably expressed in mammalian cells coimmunoprecipitated TOM70 and impaired the import of AAC2 in a TOM70-dependent manner (Fig. 4, H to K). Thus, TgMAF1 negatively affects TOM70-dependent import.

Host TOM70 and SAM50 are required for infection-induced SPOT formation

To further explore a potential link between TOM70 inhibition and SPOT formation, we asked whether the expression of TgMAF1 alone—which was sufficient to impair TOM70-dependent import—also induced the formation of SPOTs. However, neither TgMAF1, which localizes to host mitochondria when expressed in mammalian cells, nor an ER-anchored TgMAF1 remodeled the OMM in a manner reminiscent of *Toxoplasma*-induced SPOTs, indicating a requirement for other parasite factors in their formation (fig. S10) (27). To test the impact of a more complete loss of TOM70 function, we generated cells lacking TOM70 (Fig. 5A). Contrary to our expectation, the loss of TOM70 did not induce SPOT formation but instead prevented their formation during infection (Fig. 5, B to E), whereas HSP90 inhibition with the specific inhibitor 17-DMAG (17-dimethylaminoethylamino-17-demethoxygeldanamycin) did not affect the rate of their formation (fig. S11). We also noticed that the loss of TOM70 impaired the growth of TgMAF1⁺ but not Δ maf1 parasites (Fig. 5F). Thus, we considered an alternate scenario in which *Toxoplasma* exploits host TOM70 to mediate the import of TgMAF1 into host mitochondria through an OMM translocase. Because TgMAF1 is anchored into the PVM, its stable interaction with OMM import machinery would be sensed as a chronic stress, activating a host response that remodels the OMM through the budding of SPOTs. The constant formation of SPOTs, however, would

lead to the shedding of OMM proteins, including import machinery and MFN1 and MFN2, which restrict parasite growth (Fig. 5G) (5). To test whether a TgMAF1-TOM70 interaction was critical for SPOT formation, we generated Δ maf1 parasites expressing a TgMAF1 mutant that exhibits a diminished interaction with TOM70 because of a trio of basic residues at its C terminus (TgMAF1^{RKK}) (fig. S12, A to B) (35). Cells infected with Δ maf1:MAF1^{RKK} mutant parasites were SPOT-less, despite retaining a significant capacity to tether mitochondria to the PVM (figs. S12, C to F, and S13, A and B). Thus, a stable TgMAF1-TOM70 interaction is essential for the formation of SPOTs.

Because the loss of TOM70 did not form SPOTs, we posited that the stress required for their formation was derived from a TOM70-dependent interaction between MAF1 and another OMM host import factor (Fig. 5G). In line with this possibility, a study of TgMAF1 interactors has identified SAM50 (sorting assembly machinery 50 kDa subunit), a translocase that is essential for the OMM integration of a subset of mitochondrial proteins, and MIC19 and MIC60, proteins with which SAM50 forms the OMM-IMM mitochondrial intermembrane space bridging (MIB) complex (29, 40). We therefore asked whether TOM70 was required for a TgMAF1-SAM50 interaction. SAM50 was present in TgMAF1-IPs from infected WT cells but not cells in which TOM70 was deleted (Fig. 6A). We obtained similar results for MIC19 and MIC60 (Fig. 6A). Thus, TOM70 is required for TgMAF1 to interact with the OMM translocase SAM50 and its interacting partners MIC60 and MIC19.

SAM50 is the only component of host mitochondrial import machinery with a defined role in bridging the OMM and IMM. We thus reasoned that TgMAF1 could induce the formation of SPOTs that are OMM-positive but lack IMM by exerting an effect on SAM50. SAM50, but not its MIB-complex partner MIC60 that is tethered to the IMM, was enriched on SPOTs in infected cells (Fig. 6B and fig. S14). To directly test the possibility that SPOTs resulted from a separation of the OMM and IMM, we used cell lines in which the MIB components SAM50 and MIC60 as well as TOM70 were silenced with doxycycline-inducible short hairpin RNA (shRNA). We confirmed that TOM70 is required for SPOT formation (Fig. 6, C to F). The depletion of SAM50 was sufficient to induce smaller SPOT-like structures in >25% of uninfected cells relative to <1% of cells expressing a control shRNA (Fig. 6, C to F). Infection-induced SPOT formation in SAM50-deficient cells was blunted (Fig. 6, C to F). Furthermore, we observed minimal differences in the size and number of SPOT-like structures between uninfected and infected SAM50-depleted cells. Mitochondria-*Toxoplasma* contact sites

were unaffected by the loss of SAM50 (Fig. 6, C to F, and fig. S13). Similar results were obtained in cells depleted of MIC60 (Fig. 6, C to F, and fig. S13). To further test the possibility that SPOTs result from the separation of the OMM and IMM, we generated cells that stably express BFP fused to a tether that bridges the OMM and IMM (O-I_t) (41). Expression of the O-I_t significantly decreased the rate of formation of SPOTs. In addition, the average number of SPOTs per cell and their diameter were decreased relative to cells that express matrix-targeted BFP during infection (Fig. 6, I to J). Thus, *Toxoplasma* induces SPOTs in a SAM50-dependent manner, and the loss of SAM50 is sufficient to induce the formation of SPOT-like structures in the absence of infection.

Import-linked OMM stress induces OMM shedding independently of infection

If the remodeling of the OMM that occurs during infection represents a general response to import stress, we expected to see the formation of SPOT-like structures upon perturbation of import independently of infection, such as by the overexpression of an OMM protein. To this end, we isolated cells that express the GFP-tagged OMM-targeting α -helical TM of OMP25 at >20-fold times; greater (OMM^{hi}) than that in cells used in prior experiments (OMM^{lo}) and that slowed cell proliferation (fig. S15, A and B). We observed a substantial remodeling of the OMM in >20% of OMM^{hi} cells but not in OMM^{lo} cells, despite the overexpression of matrix-BFP in both cell lines (fig. S15, C to F). This indicated a link between stress related to the import of OMM proteins and the formation of SPOT-like structures. No remodeling of the OMM was observed after treatment with the protonophore CCCP (carbonyl cyanide m-chlorophenyl hydrazone), which dissipates mitochondrial membrane potential (MMP) and prevents the import of presequence-containing proteins, or Mitoblock6, which inhibits the IMS import pathway (fig. S16) (42). We next generated cells in which we expressed GFP fused to an artificial clogger of the TOM40 channel that forms the entry gate for almost all mitochondrial proteins other than α -helical OMM proteins (fig. S17A). The clogger contains DHFR between a cytochrome *b*₂ presequence that directs it to the IMM by way of the TOM complex and a heme binding domain that slows its import (fig. S17A) (43). The addition of methotrexate (MTX) that stabilizes the folding state of DHFR leads to its arrest at the TOM complex and further accumulation in the cytosol, as we observed (fig. S17) (43, 44). However, the expression of the clogger with vehicle or MTX did not lead to SPOT formation (fig. S17, C to F). Thus, the OMM is remodeled after stress linked to the overexpression of an α -helical OMM protein

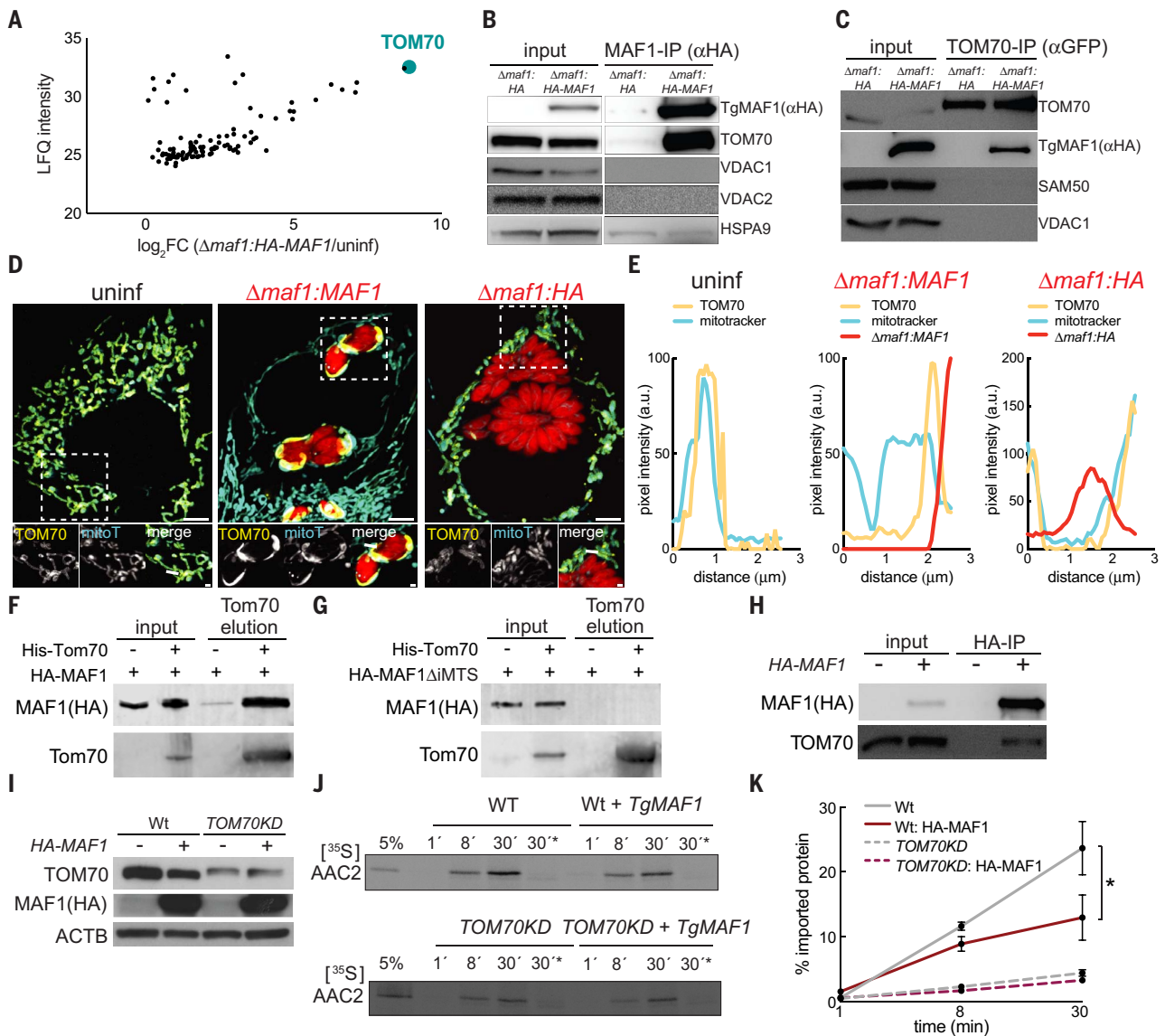


Fig. 4. TgMAF1 binds the host receptor TOM70 and inhibits its import function. (A) Anti-HA immunoprecipitates (IPs) from cells that were mock-infected (uninf) or infected with $\Delta maf1$:HA-MAF1 parasites at a MOI of 1, 2.4, and 6 and analyzed by means of mass spectrometry; data for MOI 2.4/uninf are shown for 101 human protein hits that had a positive log₂FC for the comparisons: all MOIs/uninf, MOI:6/MOI:2.4, MOI:6/MOI:1, MOI:2.4/MOI:1. LFQ, label-free quantification. (B) Anti-HA IPs from U2OS cells infected with $\Delta maf1$:HA or $\Delta maf1$:HA-MAF1 parasites and analyzed by means of immunoblotting (IB) for TgMAF1, ~60 kDa; HSPA9, ~90 kDa; VDAC1, ~34 kDa; VDAC2, ~34 kDa; TOM70, ~72 kDa. (C) Anti-GFP IPs from TOM70-GFP-expressing MEFs 24 hours after infection with $\Delta maf1$:HA or $\Delta maf1$:HA-MAF1 and analyzed by means of IB for indicated proteins: TOM70-GFP, ~105 kDa; TgMAF1, ~60 kDa; SAM50, ~55 kDa; VDAC1, ~34 kDa. (D) Representative live-cell images of mitoT-labeled TOM70-GFP MEFs at 24 hours after mock infection (uninf) or infection with $\Delta maf1$:HA-MAF1 or $\Delta maf1$:HA parasites.

Scale bars, 5 μ m and (inset) 1 μ m. (E) Corresponding pixel intensity plots for white line in (D) inset. (F) HA-MAF1 and (G) HA-MAF1 Δ iMITS were incubated with his-tagged TOM70 (cytosolic domain) and subjected to affinity purification with Ni-NTA agarose. Input and elution were analyzed by means of IB. (H) HA-IPs from MEFs expressing HA-MAF1 and analyzed by means of IB for TOM70, ~72 kDa, and HA-MAF1, ~60 kDa. (I) IB analyses of lysates from WT and TOM70-suppressed 293Ts \pm HA-MAF1 cDNA: TOM70, ~72 kDa; HA-MAF1, ~60 kDa. (J) [³⁵S]AAC2 import into mitochondria isolated from cells in (I) at indicated times was analyzed by means of SDS-polyacrylamide gel electrophoresis (SDS-PAGE) and autoradiography. Nonimported proteins were removed through proteinase K treatment; asterisk indicates CCCP treatment. (K) Signals in (J) were quantified, and the amount of imported protein relative to input (5%) was plotted. Data are mean \pm SEM from three biological replicates, **P* < 0.05 for WT versus WT:HA-MAF1 by means of two-way ANOVA analysis.

but not depolarization of the MMP, inhibition of the IMS pathway, or clogging of the TOM40 channel.

Whether mitochondria are physically remodeled during physiologically occurring stress at the OMM has been unclear. Here, we

describe the discovery of SPOTs, a mechanism of OMM remodeling during *Toxoplasma* infection. We propose that *Toxoplasma* coopts the host TOM70 receptor and SAM50 translocase to promote its insertion into the OMM (Fig. 6K). This enables *Toxoplasma* to hijack a

host response to OMM stress (Fig. 6K). During import stress independent of infection, the formation of SPOT-like structures could safeguard OMM function by sequestering defective import machinery, preventing the accumulation of precursors and misfolded proteins at

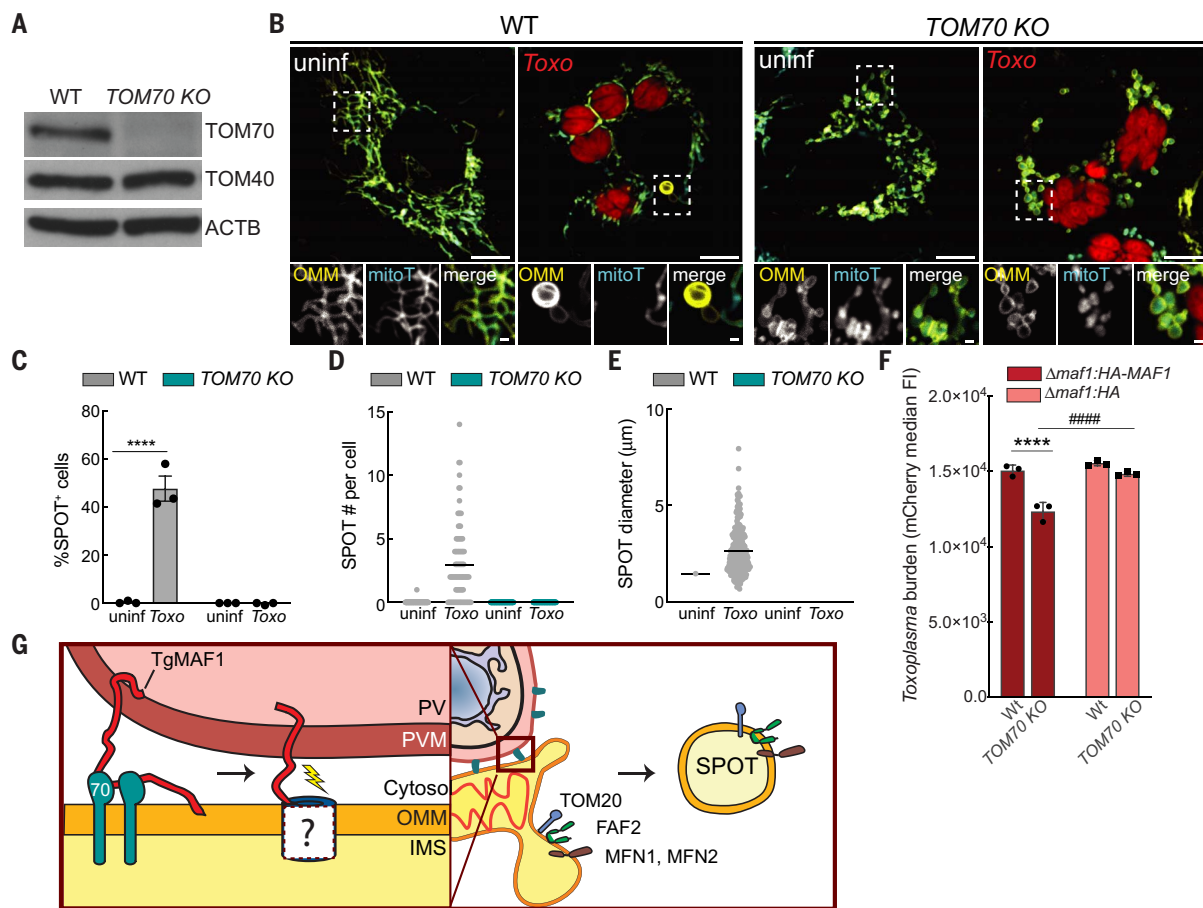


Fig. 5. TOM70 is required for SPOT formation and MAF1-dependent growth.

(A) WT and *TOM70*-deleted (*TOM70* KO) HeLas were analyzed by means of immunoblotting for TOM70, ~72 kDa; TOM40, ~40 kDa, and ACTB, ~45 kDa. (B) Representative live-cell images of the OMM (GFP) in uninfected (uninf) and *Toxoplasma* (mCh)-infected (*Toxo*) WT and *TOM70* KO HeLas labeled with mitoT. Scale bars, 5 μm and (inset) 1 μm. (C) Percentage of SPOT-positive cells in experiments as in (B). Data are mean ± SEM of more than 100 cells counted from three biological replicates; *****P* < 0.0001 for uninfected versus infected by means of two-way ANOVA analysis. (D and E) Scatterplots with mean (D) number and (E) diameter of SPOTs in experiments as in (B) from more than 30 infected cells from three biological replicates. (F) WT and *TOM70* KO HeLas

were infected with $\Delta maf1:HA-MAF1$ or $\Delta maf1:HA$ parasites, rinsed at 2 hours after infection, and analyzed 24 hours after infection by means of flow cytometry for *Toxoplasma* burden [red fluorescent protein (RFP) median FI]. Data are mean ± SEM of three biological experiments, *****P* < 0.0001 for WT versus *TOM70* KO, ####*P* < 0.0001 for $\Delta maf1:HA-MAF1$ versus $\Delta maf1:HA$ by means of two-way ANOVA analysis. (G) Cartoon model of SPOT formation. Host TOM70 mediates insertion of TgMAF1 into host mitochondria through a hypothetical OMM translocase-insertase inducing a stress that leads to SPOT formation and sequestration of import machinery (TOM20) as well as proteins such as FAF2, MFN1, and MFN2 on SPOTs. PV, parasite vacuole; PVM, PV membrane; IMS, intermembrane space.

the OMM that can have toxic consequences for the cell (fig. S18) (4, 37). In the context of infection, however, the constant formation of SPOTs mediates the removal of OMM proteins, including SAM50 and TOM20, which are key components of import machinery, and MFN1 and MFN2, which mediate mitochondrial nutrient competition (Fig. 6K) (5).

Discussion

Our data showing that stress linked to the import of OMM proteins leads to the shedding of the OMM during and independently of infection opens several questions, including whether differences in the underlying mechanism of OMM remodeling in these scenarios exist. OMM-GFP expression induced the formation of structures in a manner consistent with our

description of infection-induced SPOTs. However, the OMM was remodeled in a different manner during *SAM50* silencing/depletion. Whether the smaller *SAM50* silencing/depletion-induced structures are a consequence of defective import of OMM proteins that mediate the emergence of SPOTs or represent other classes of structures that emerge from the OMM, such as MDCs and MDVs, is unclear. Furthermore, what is the nature of the TgMAF1- or OMM-GFP-derived stress that leads to OMM remodeling? Although most known for its role in the biogenesis of β -barrel proteins, SAM50 in yeast can cooperate with the mitochondrial import (MIM) complex that inserts C-tail α -helical proteins into the OMM (45). Thus, similar machinery in mammals—so far unknown—may facilitate an interaction between the C-terminal

α -helix of TgMAF1 or the OMM-targeting α -helical TM domain of OMM-GFP with SAM50 (28). Because SAM50 is the only component of the OMM import machinery with a defined role in bridging the OMM and IMM, perhaps SAM50 can thus function as a sensor that translates stress linked to the import of OMM proteins into a removal of compromised import machinery of the OMM through the disruption of the MIB complex. Additionally, ER whorls that are morphologically similar to SPOTs and contain the ER import translocon have been observed after induction of ER stress (46).

What regulates the extent to which the OMM is shed? SNX9 is required for the emergence of a subclass of MDVs that are uniformly shaped and range between 80 and 120 nm in diameter (22–24). We found that infection induced much

Fig. 6. SAM50 loss of function mediates SPOT formation during infection.

(A) Anti-HA IPs were prepared from WT and *TOM70 KO* HeLas infected with $\Delta maf1:HA$ or $\Delta maf1:HA$ -MAF1 parasites and analyzed for TgMAF1, ~60 kDa; TOM70, ~72 kDa; SAM50, ~55 kDa; MIC60, ~88 kDa; MIC19, ~25 kDa; TOM40, ~40 kDa.

(B) Representative IF images of uninformed (uninf) and *Toxoplasma* (Toxo) HFFs at 24 hours after infection. (Inset) SPOT in *Toxo*-infected cell contains SAM50 but not MIC60 or ATP5B (IMM). Scale bars, 5 μ m and (inset) 1 μ m.

(C) Representative live-cell images of the OMM (BFP) in uninformed and *Toxoplasma*-infected CTRL, *TOM70*-, *SAM50*-, and *MIC60*-suppressed (KD) HeLas labeled with mitoT. (Insets) SPOTs are indicated with arrowheads. Scale bars, 5 μ m and (inset) 1 μ m.

(D) Percentage (%) of SPOT-positive cells in experiments as in (C); data are mean \pm SEM of more than 100 cells counted from $n = 3$ replicates; * $P < 0.05$, ** $P < 0.01$, **** $P < 0.0001$ for uninf versus inf, #### $P < 0.0001$ for CTRL KD versus *SAM50* KD, *MIC60* KD by means of two-way ANOVA analysis.

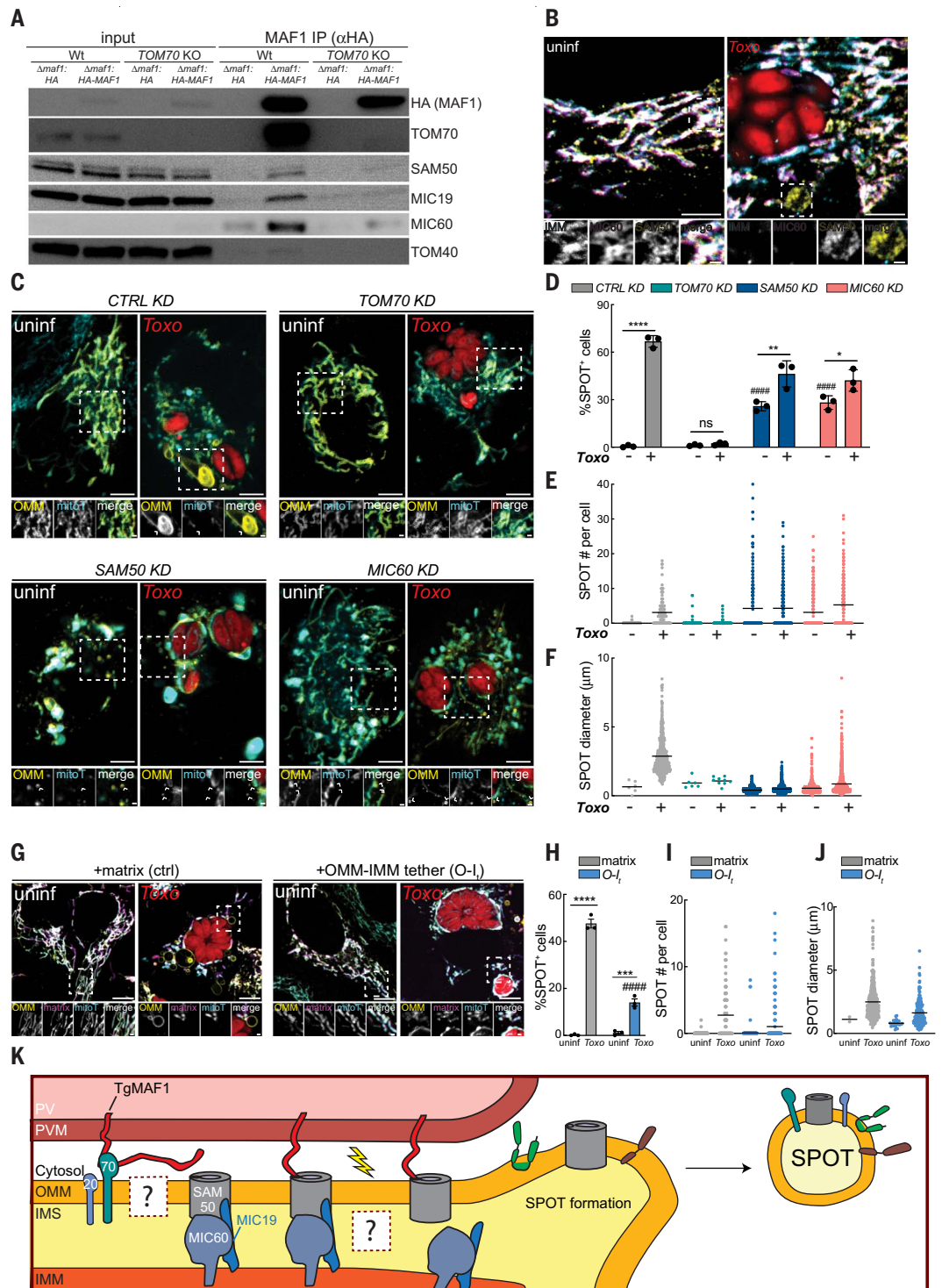
(E and F) Scatterplots with mean (E) number and (F) diameter of SPOTs in experiments as in (C) from more than 30 infected cells from three replicates. **(G)** Representative live-cell images of the OMM (GFP) in uninformed and *Toxoplasma* (mCh)-infected U2OS cells expressing matrix-BFP (matrix) or BFP fused to an OMM-IMM tether (*O-I_t*). **(H)** Percent of SPOT-positive cells in experiments as in (G). Data are mean \pm SEM of more than 100 cells counted from $n = 3$ biological replicates; *** $P < 0.001$, **** $P < 0.0001$ for uninf versus inf, #### $P < 0.0001$ for matrix versus *O-I_t* by two-way ANOVA analysis.

(I and J) Scatterplots with mean (I) number and (J) diameter of SPOTs in experiments as in (G) from more than 30 infected cells from three replicates. **(K)** Model of SPOT formation: TOM70 (70) mediates the interaction between MAF1 and SAM50 and/or a hypothetical translocase (?), which induces a disassembly of the MIB complex (SAM50, MIC60, and MIC19) and SPOT formation. The constitutive shedding of SPOTs depletes OMM proteins that restrict parasite growth (MFN1 and MFN2) and sequesters import machinery required for mitochondrial biogenesis on SPOTs.

larger SPOTs that range up to 10 μ m in diameter, are also SNX9-dependent, and vary in substructure and shape. What factors dictate their morphology and the fate of their proteins? Although MFN1 and MFN2 are targeted

for degradation, it remains possible that other SPOT-localized proteins such as SAM50, TOM70, and TOM20 are recycled into the mitochondrial network. SPOTs being oftentimes multivesicular and containing proteins required for

fusion (MFNs) and trafficking (MIROs) raises the possibility that these structures might be able to fuse with one another, or with mitochondria to reintegrate into the mitochondrial network.



Whether other pathogen effector proteins coopt host import receptors for their function, analogous to how TgMAF1 exploits host TOM70, is little explored. Pathogens such as *Toxoplasma* might target SAM50 and TOM70, key regulators of mitochondrial import, to impede the biogenesis of organelles that function as nutrient competitors or immune signaling hubs during infection (5–7). Severe acute respiratory syndrome coronavirus 2 (SARS-CoV-2) encodes for a protein of unknown function (Orf9b) that binds TOM70 to suppress antiviral interferon responses (47). Host TOM complex components also mediate contact sites between mitochondria and the vacuole in which *Chlamydia* resides, but whether this bacterium inhibits TOM receptors or induces SPOT formation is not known (48).

Our study of the interaction between the human parasite *Toxoplasma* and host mitochondria led to the discovery of a mechanism by which the OMM is remodeled: the formation of SPOTs. These findings shed light on a potentially broader mechanism of organellar response to import-related stress and reveal a strategy by which diverse pathogens may disrupt mitochondrial function.

Materials and methods

Cell culture and cell lines

All cell lines were cultured in complete DMEM (cDMEM: DMEM and 10% heat-inactivated FBS). Cells were tested every 2 weeks for *Mycoplasma* infection by means of polymerase chain reaction (PCR). Details of cell lines generated (including single-guide RNA sequences), used, and origin are in the supplementary materials.

Parasite culture and strains

Toxoplasma gondii parasites were maintained by serial passage in human foreskin fibroblast (HFF) monolayers in cDMEM. Details of parasite lines generated, used, and origin are in the supplementary materials.

Plasmid descriptions, transfections, and siRNA treatment

For transient expression, cells were transfected ~12 hours prior to infection using X-tremeGene reagent (Sigma) per manufacturer's instructions, lipofectamine RNAiMax (Invitrogen) was used per manufacturer's instructions for siRNA treatment. Details of plasmids generated, used, and origin are in the supplementary materials.

Lentiviral production generation of cells stably expressing cDNAs

For production of 293T human embryonic kidney (HEK) cells were transfected using the X-tremeGENE 9 DNA Transfection Reagent (Roche) with 1 µg pSPAX2 packaging vector (Addgene #12260), 0.3 µg pCMV-VSVG envel-

ope vector (Addgene #8454) and 1 µg of the relevant plasmid of interest. The next day, the medium was exchanged, and two days post transfection, the virus-containing supernatant was filtered with a 0.45 µm filter and supplemented with polybrene to a final concentration of 5 µg/ml. The virus-containing filtrate was added to 50,000 target cells and exchanged for cDMEM the next day. MEFs, HeLas, U2OS cells were subsequently selected with 8 to 10 µg/ml blasticidin, or 1–2 µg/ml puromycin for 3–5 days. To isolate cells positive for expression of fluorescent protein, transduced cells were sorted for low and high GFP positivity as indicated.

Live cell imaging

Cells were plated on 35mm, 6-well, or 24-well CELLview glass bottom cell culture dishes (Greiner Bio-One), treated as indicated in text (i.e., infection, transfection, 25 mM CCCP treatment for 30 min, or fixation and permeabilization while imaging), and imaged using an Olympus IXplore SpinSR 50 mm spinning disk confocal microscope. Live cell imaging was performed in cDMEM with incubation at 37°C and 5% CO₂. All images were taken with a 100X/1.35 silicon oil objective and excitation with either 405, 488, 561, or 640 laser lines, using ORCA-Flash4.0 cameras (Hamatsu), and cellSens Software. Details of mitotracker and FL-HPC labeling, immunofluorescence analysis, and antibodies used are in the supplementary materials.

Yeast strains, growth conditions, and expression plasmids

The yeast strains used in this study are based on *Saccharomyces cerevisiae* BY4741 (EUROSCARF). Yeast cells were cultured using standard protocols on SC-Leucine (0.67% [w/v] yeast nitrogen base with ammonium sulfate; 0.07% [w/v] amino acid mixture) with 2% [w/v] galactose. Cultures were grown at 30°C until early logarithmic growth phase, which was determined based on the optical density at a wavelength of 600 nm. Full details of strains used and generated, isolation of yeast and mammalian mitochondria, affinity purification of HA-MAF1 from yeast, in vitro binding to TOM70, and in vitro protein import into yeast and mammalian mitochondria in supplementary material.

Line scan analyses

Line-scan analysis of relative fluorescence intensity was performed by measuring pixel intensity across an indicated line using Fiji software.

Immunoprecipitation of mitochondria

Seven million to 8 million MEFs or 293Ts cells were plated in a 15 cm dish and the following day, cells were either mock-infected or infected with *Toxoplasma* (RH Δ ku80:mCherry⁺) at a multiplicity of infection (MOI) of 5. 24 hpi,

cells were scraped rinsed 2X in chilled 1X PBS, scraped in 1X chilled PBS supplemented with a protease and inhibitor cocktail (Thermo Scientific a32961) and Phosstop phosphatase inhibitors (Sigma 4906837001)(1XPBS+Inh). Harvested cells were centrifuged at 1000xg for 2 min at 4°C and resuspended in 1 ml 1X PBS with inhibitors. 50 µl were collected for the whole cell fraction and the rest was triturated 10X on ice using a 1 ml syringe and 27^{3/4} gauge needle. Lysed cells were centrifuged at 1000xg for 2 min at 4°C. Cleared lysate was added to 150ul anti-HA bead slurry that had previously been rinsed 3X in 1X PBS and resuspended in 100 µl 1X PBS. Subsequently, mitochondria were immunopurified as previously described and processed for immunoblot analysis or mass spectrometry analysis (13). More details on immunoblot analysis and proteomics sample preparation are provided in the supplementary materials.

Flow cytometry analysis

Monolayers of U2OS cells expressing OMM-GFP were rinsed with PBS, trypsinized and fixed in 2% paraformaldehyde in FACS buffer (3% FBS in PBS) for 10 min. After a brief spin, cells were resuspended in FACS buffer and sorted on a FACSAria Fusion Cell Sorter (BD Biosciences) GFP mean fluorescence intensity (mFI) using BD FACSDiva software. ~250,000 cells were sorted into low and high (20× greater than low) GFP bins and transferred to a cell culture dish for continued passaging.

Immunoprecipitation of HA-MAF1 or TOM70

Seven million to 8 million TOM70-expressing MEFs or U2OS cells were infected with *Toxoplasma* at an MOI of 7. 24 hpi cells were rinsed 2X in chilled 1X PBS, scraped down in chilled 1XPBS+Inh, centrifuged at 1000xg for 2 min, and resuspended in lysis buffer for 15 min at 4°C. Cleared lysates were incubated with either 80 µl magnetic anti-HA-beads (Thermo Scientific) or 25 µl magnetic anti-GFP-nanobodies (Chromotek) overnight. The beads were washed 3x times with 1XPBS+Inh. Afterwards, the samples were eluted from the magnetic beads with 2X SDS buffer by incubating them at 40°C for 10 min. Samples were processed for gel electrophoresis and probed with indicated antibodies. For more details on proteomics sample preparation, please see supplementary materials.

Statistical analyses

All statistical analyses were performed using one-way analysis of variance (ANOVA), two-way ANOVA, or an unpaired *t* test in GraphPad Prism 9 software and are indicated accordingly. Volcano plot rendering of proteomics of whole-cell and immunopurified mitochondria fractions are provided in the main and supplementary figures.

Mitochondria shed their outer membrane in response to infection-induced stress

Xianhe LiJulian StraubTânia Catarina MedeirosChahat MehraFabian den BraveEsra PekerIlian AtanassovKatharina StillgerJonas Benjamin MichaelisEmma BurbridgeColin AdrainChristian MünchJan RiemerThomas BeckerLena F. Pernas

Science, 375 (6577), eabi4343. • DOI: 10.1126/science.abi4343

Mitochondria shed their SPOTs

Outer mitochondrial membrane (OMM) function is essential for cellular health. How mitochondria respond to naturally occurring OMM stress is unknown. Li *et al.* show that, upon infection with the human parasite *Toxoplasma gondii*, mitochondria shed large structures positive for OMM (SPOTs). SPOT formation required the parasite effector TgMAF1 and its interaction with the host mitochondrial receptor TOM70 and translocase SAM50. TOM70-dependent SPOT formation mediated a depletion of mitochondrial proteins and optimal parasite growth. SPOT-like structures also formed after OMM perturbations independently of infection. Thus, membrane remodeling is a feature of cellular responses to OMM stress that *Toxoplasma* hijacks during infection. —SMH

View the article online

<https://www.science.org/doi/10.1126/science.abi4343>

Permissions

<https://www.science.org/help/reprints-and-permissions>

Use of this article is subject to the [Terms of service](#)

Science (ISSN) is published by the American Association for the Advancement of Science. 1200 New York Avenue NW, Washington, DC 20005. The title *Science* is a registered trademark of AAAS.

Copyright © 2022 The Authors, some rights reserved; exclusive licensee American Association for the Advancement of Science. No claim to original U.S. Government Works



Supplementary Materials for

Mitochondria shed their outer membrane in response to infection-induced stress

Xianhe Li et al.

Corresponding author: Lena F. Pernas, pernas@age.mpg.de

Science **375**, eabi4343 (2022)
DOI: 10.1126/science.abi4343

The PDF file includes:

Materials and Methods
Figs. S1 to S18
References

Other Supplementary Material for this manuscript includes the following:

Data Files S1 to S3
Movies S1 and S2

Materials and Methods

Cell culture and cell lines

HeLa adenocarcinoma cells, ES-2 ovary clear cell carcinoma, U2OS human osteosarcoma, and their derivatives and Wild-type (WT) as well as *Mfn1*^{-/-}, and *Mfn2*^{-/-} mouse embryonic fibroblasts (MEFs) were obtained from ATCC (CCL-2, CRL-1978, HTB-96, CRL-2991, CRL-2992, and CRL-2993, respectively); *Atg7*^{-/-} MEFs were provided by Dr. M Sandri (University of Padua); *Miro1*^{-/-}, *Miro2*^{-/-} MEFs were provided by Dr. J Kittler (U of College London)(49); *Drp1*^{-/-} MEFs were provided by Dr. K Mihara (Kyushu U)(50); TOM70-GFP MEFs were provided by Dr. J Shaw and Dr. Adam Hughes (U of Utah)(19). *CTRL KD*, *TOM70 KD*, *SAM50 KD*, *MIC60 KD* HeLa lines were provided by Dr. V Kozjak-Pavlovic (U of Würzburg)(40). Cell lines stably expressing pMXs-eGFP-OMP25 (referred to as OMM-GFP; Addgene #83356)(plasmid described in (13), OMM-BFP, matrix-BFP, FAF2-3XHA, FAF2-GFP, GFP-SAM50, GFP-MFN1, GFP-MIRO1, GFP-MIRO2, MSCV2.2 IRES-GFP/MAF1-HA, and IRES-GFP (provided by Dr. G Barton, UC Berkeley) were generated through lentiviral transduction. All cell lines were cultured in complete DMEM (cDMEM: DMEM and 10% heat-inactivated FBS). Cells were tested every 2 weeks for *Mycoplasma* infection by PCR.

Parasite culture and strains

Toxoplasma gondii parasites of the Type I (RHΔ*hxgpri*) strain (deleted for the hypoxanthine-xanthine-guanine phosphoribosyl transferase (*HXGPRT*) gene), RHΔ*ku80:mCherry*⁺, and RHΔ*ku80ΔTgMAF1:mCherry*⁺ (previously described (27)). were maintained by serial passage in human foreskin fibroblast (HFF) monolayers in cDMEM. Stable RHΔ*hxgpri* parasites expressing BFP and RHΔ*ku80:mCherry*⁺ parasites expressing HA, HA-MAF1, and HA-MAF1^{RKK} were generated via transfection.

Plasmid descriptions, transfections, and siRNA treatment

For transient expression, cells were transfected ~12 hours prior to infection using X-tremeGene reagent (Sigma) per manufacturer's instructions with mito-BFP (Addgene #49151); mCherry-Mfn2 (Plasmid #141156, Addgene); tdTomato-TOMM20-N-10 (Addgene #58137); TIM50-RFP (a gift from Dr. A. Hughes and Dr. J. Shaw, U of Utah), which is indicated as IMM in the text; pCytERM_mScarlet_N1 (Addgene #85066). For transient expression of ER-targeted MAF1, HA-MAF1 lacking the signal peptide from amino acid 1 to 23 was cloned into Addgene #85066 C-terminally to Scarlet (pCytERM_mScarlet_MAF1). For *Toxoplasma* transfection, pGra, pTgMAF1 (previously described (27)) pTgMAF1^{RKK} (generated via site-directed mutagenesis of pTgMAF1), and pCTR2T (gift from Dr. G v Dooren (Australian National U) where tandem tomato cassette was replaced with a BFP) were used. Lipofectamine RNAiMax (Invitrogen) was used for transfection siluc: CGUACGCGGAAUACUUCGA, siSNX9: GGCUCGGGUUAUGUAUGAUUU)TT according to manufacturer's instructions. For stable expression of OMM-targeted GFP, the triple hemagglutinin (3XHA-) and enhanced green fluorescent protein (eGFP) vector pMXs-3XHA-eGFP was used (Addgene #83356). For stable expression of OMM-targeted BFP, the 3XHA-eGFP in Addgene #83356 was replaced with BFP. To enable stable expression of epitope-tagged FAF2, *FAF2* cDNA was cloned into the pM6P backbone fused to the relevant epitope sequences (Dr. C Adrain, Queens U Belfast; Dr. F Randow, LMB). For stable expression of matrix-targeted BFP (pMXs-cox4-BFP), the GFP cassette of pMXspuro-GFP (Addgene #74203) was replaced with the cox4-BFP cassette from Addgene # 49151. To enable stable expression of BFP-fused to an OMM-IMM tether (pMXsBFP-O-I_t), the OMM-IMM tether cDNA (a gift from Dr. O Khalimonchuk, U of

Nebraska-Lincoln) was inserted in lieu of the *cox4* matrix-targeting signal in pMXs-matrix-BFP. For stable expression of IRES-GFP/ HA-MAF1 (lacking the signal peptide from amino acid 1 to 23), MSCV2.2 (provided by Dr. G Barton, UC Berkeley) and MSCV2.2-HA-MAF1 were used (23).

Generation of cells lacking PINK1, FAF2, and TOM70

To generate PINK1 CRISPR KO HeLa, TOM70 CRISPR KO HeLas, and TOM70 CRISPR KD 293T, the following sgRNAs were cloned into the pLenti CRISPRv2 (Addgene #5296), packaged into lentiviral particles, and used to transduce subconfluent cells HeLas or 293Ts.

Pink1 Sense: CACCGCCTCATCGAGGAAAAACAGG

Pink1 Antisense: AAACCCTGTTTTTCCTCGATGAGGC

TOM70 g1 Sense: CACCGAGCGAACGGAAGACCCCGGA

Tom70 g1: Antisense: AAACTCCGGGGTCTTCCGTTTCGCTC

Tom70 g2: Sense: CACCGAGGTCAACATTCTTCTCTGT

Tom70 g2: aaacACAGAGAAGAATGTTGACCTC

Following selection in 1-2 ug/ml puromycin, clones were isolated by limiting dilution, and validated by immunoblotting for TOM70 or PINK1. Wt and PINK1 KO HeLas stably expressing mt-mKEIMA and Parkin were generated via the Flp-In T-REX system for assessing PINK1 accumulation following treatment with small molecule inhibitors indicated in the text. To generate FAF2 CRISPR KO MEFs, the following sgRNAs were cloned into the px330 CRISPR v2 vector. Cells were transfected with a mixture of the three px330 plasmids, and following selection in puromycin, clones were isolated by limiting dilution and validated by immunoblotting for FAF2.

FAF2 g1: Sense: CACC GGAGCAGCATAACTGGAACA

FAF2 g2: Antisense: AAACCTGTTCCAGTTATGCTGCTCC

FAF2 g2: Sense: CACC GTCTCAAGACCACAACCAAG

FAF2 g2: Antisense: AAACCTTGGTTGTGGTCTTGAGAC

FAF2 g3: Sense: CACC GATGAAACAATGTCCCAACA

FAF2 g3: Antisense AAACCTGTTGGGGACATTGTTTCATC

Yeast strains, growth conditions, and expression plasmids.

For expression in yeast, a HA-tagged MAF1 lacking the signal peptide from amino acid 1 to 23 was inserted into a *p415* vector encoding for *HA-MAF1* under control of the *GAL1* promoter (51). Yeast strains used: WT BY4741 + *p415 pGAL1* and WT BY4741 + *p415 pGAL1 HA-MAF1*. Plasmids used: *p415 pGAL1*, *p415 pGAL1 HA-MAF1*, *pGEM4z-Neurospora crassa AAC*, *pGEM4z-Su9-(1-69 N. crassa)-DHFR* (mouse), plasmid for AAC2 expression was provided by Dr. J Herrmann (U of Kaiserslautern).

Isolation of yeast mitochondria

Yeast mitochondria were isolated by differential centrifugation (52). Cells were harvested (5,500 g; 8 min; 24°C) at early logarithmic growth phase, washed with distilled H₂O and incubated in DTT buffer (100 mM Tris/HCl pH 9.4; 10 mM dithiothreitol (DTT)) for 45 min at 30°C. To digest the cell wall, cells were washed in zymolyase buffer (1.2 M sorbitol; 20 mM KP_i pH 7.4) and incubated with 4 mg/g wet weight of zymolyase for 45 min at 30°C in zymolyase buffer. Subsequently, spheroblasts were resuspended in homogenization buffer (0.6 M Sorbitol; 10 mM Tris/HCl pH 7.4; 1 mM ethylenediaminetetraacetic acid (EDTA); 1 mM

phenylmethanesulfonyl fluoride (PMSF); 0.2 % [w/v] bovine serum albumin) and homogenized by 15 strokes up and down in a glass potter at 4°C. Cellular debris and nuclei were removed by centrifugation (2,500 g; 5 min; 4°C) and mitochondria were isolated from the supernatant by a second centrifugation step (17,000 g; 15 min; 4°C). To clear mitochondria, the pellet containing mitochondria was resuspended and washed with SEM buffer (250 mM sucrose; 10 mM MOPS/KOH pH7.2; 1 mM EDTA). The mitochondrial pellet was resuspended in SEM buffer in a protein concentration of 10 mg/ml, frozen in liquid nitrogen and stored until use at -80°C.

Affinity purification of HA-MAF1 from yeast

For affinity purification of HA-MAF1 expressed in yeast, isolated mitochondria were solubilized in lysis buffer (20 mM Tris pH 7.4; 0.1 mM EDTA; 50 mM NaCl; 10% [v/v] glycerol; 2 mM PMSF; 1 x protease inhibitor cocktail without EDTA) containing 1% [w/v] digitonin for 15 min at 4°C. Samples were then cleared by centrifugation (16,000 g; 10 min; 4°C) and the supernatant was subjected to affinity purification using anti-HA affinity matrix (Roche) pre-equilibrated with 0.5 M acetate. Unbound proteins were removed by washing with lysis buffer containing 0.1 % [w/v] digitonin. Bound proteins were eluted under denaturing condition by incubation with Laemmli sample buffer (2% [w/v] SDS; 10% [v/v] glycerol; 0.01% [w/v] bromophenol blue; 0.2% [v/v] β-mercaptoethanol; 60 mM Tris/HCl, pH 6.8) at 95°C for 10 min.

In vitro protein import into mitochondria

For analyzing import into yeast mitochondria, precursor proteins of AAC from *Neurospora crassa* and Su9-DHFR in pGEM4z plasmids were used for cell-free translation based on rabbit reticulocyte lysate in the presence of [³⁵S]methionine (TNT kit, Promega). The labelled precursor proteins were incubated at 16°C with isolated mitochondria for the indicated time points in import buffer (3% [w/v] BSA, 250 mM sucrose, 5 mM methionine, 80 mM KCl, 5 mM MgCl₂, 10 mM MOPS/KOH, pH 7.2, and 2 mM KH₂PO₄) containing 4 mM ATP, 4 mM NADH, 5 mM creatin phosphate and 0.1 mg/ml creatin kinase. As control, the membrane potential across the inner membrane was dissipated by adding a mixture of 8 μM (final concentration) antimycin A, 1 μM valinomycin and 20 μM oligomycin. For proteinase K treatment, samples were incubated with 50 μg/ml proteinase K for 15 min at 4°C. Reactions were stopped by addition of PMSF to a final concentration of 2 mM followed by incubation for 10 min at 4°C. Imported proteins were analyzed by blue native electrophoresis (AAC) or SDS-PAGE (Su9-DHFR). For analyzing import into mammalian mitochondria, experiments were performed as recently described (53).

In vitro binding to Tom70

The His-tagged cytosolic domain of Tom70 was recombinantly expressed and purified following published procedures (54). HA-MAF1 was translated *in vitro* using wheat germ lysate (biotech rabbit)(54). For binding studies, Tom70 was coupled to Ni-NTA agarose (Qiagen) and incubated with HA-MAF1 in binding buffer (20 mM Tris/HCl, pH 7.4, 0.1% [w/v] digitonin, 100 mM NaCl, 10% [v/v] glycerol) for 45 min at 4°C. Unbound HA-Maf1 was removed by excessive washing with excess binding buffer containing 40 mM imidazole. Bound proteins were eluted with binding buffer containing 500 mM imidazole.

Immunofluorescence Assays and Antibodies

For testing single clones of $\Delta maf1:HA$, $\Delta maf11:HA-MAF1$ and $\Delta maf1:HA-MAF1^{RKK}$ parasites, HFFs were grown to confluency on coverslips in 24-well plates. The following day, HFFs were infected with $\Delta maf1:HA$, $\Delta maf1:HA-MAF1$, and $\Delta maf1:HA-MAF1^{RKK}$ parasites. At 6 hpi, wells were once washed with ice-cold PBS and fixed for 15 min at RT in 4% paraformaldehyde, and

permeabilized for 20 min at RT with 0.2% Triton-X-100 in 3% BSA in PBS (.2% T). After 30 min blocking in 3% BSA in 1XPBS (3% B) at RT, cells were incubated in 1:500 anti-HA for 1 h at RT. After 3X 5 min washes with 1XPBS, cells were incubated in 1:2000 anti-rabbit Alexa Fluor Plus 488 Plus (Invitrogen) for 40 min to 1 h at RT. For IF analysis of SPOTs, cells were plated and infected in a 24 well glass-bottom sensoplate, fixed at 24 hpi with *Toxoplasma* in 4% paraformaldehyde (fresh) in prewarmed cDMEM for 20 min at 37C, permeabilized for 20 min at RT with .2% T, blocked in 3%B for 30 min, incubated in 1:250 of primary Ab indicated in text O/N, rinsed 3X in 1X PBS, and maintained in 1X PBS until imaging. Images were taken using an Olympus IXplore SpinSR spinning disk confocal microscope. Primary Abs: OGDH (Sigma HPA020347); mtHSP70 (abcam ab2799); SAM50 (Sigma HPA034537); MIC60 (Proteintech 10179-1-AP); ATP51B (ThermoFisher A21351); TOM20 (Sigma HPA011562, WH0009804M1); AIFM1 (abcam ab1998); CS (CST #14309); MFN1 (CST #14739); MFN2 (CST #9482S); HA (CST #3724, Roche 3F10) were used at 1:250 or 1:500 O/N. Secondary Abs: Alexa Fluor Plus 405, Alexa Fluor Plus 488, Alexa Fluor Plus 594, Alexa Fluor Plus 647 (Thermo Fisher) were used at 1:1000. All images were taken with a 100X objective and excitation with 405, 488, 561 and 640 laser lines, and processed via cellSens software.

Immunoblotting and antibodies

Whole cells were harvested in chilled lysis buffer (50mM Hepes-KOH pH 7.4, 40mM NaCl, 2mM EDTA, 1.5mM NaVO₄, 50mM NaF, 10mM NaPyrophosphate, 10mM, NaBetaGlycerophosphate (disodium salt pentahydrate), 1% Triton X-100) and lysed for 30 min on ice. Lysates were subsequently centrifuged at 10 min at 14,000 x g at 4°C and the supernatant was transferred into a fresh tube with 5X SDS added to a final of 1X SDS. Following SDS-PAGE and gel transfer, membranes were blocked with PBS-0.05% Tween 20 (PBS-T) and 5% bovine serum albumin (BSA) for overnight in primary antibodies. Following incubation, blots were washed three times in PBS-T and then incubated with horseradish peroxidase (HRP)-conjugated anti-mouse IgG (CST #7076) or anti-rabbit IgG (CST #7074) at a 1:4000 dilution for 45 minutes and developed using a chemiluminescence system (Pierce ECL substrate or Pierce ECL Plus Substrate; ThermoFisher Scientific). For WT and PINK1 KO lysate, protein samples were separated by SDS-PAGE with Bolt Bis-Tris Plus Gels, transferred to 0.45 μM nitrocellulose membranes, blocked for 1 h with Intercept® (PBS) Blocking Buffer (LI-COR Biosciences). Blots were incubated with primary antibodies overnight and detected via near-infrared secondary antibodies (LI-COR Biosciences). The following antibodies were used: MFN1/2 (abcam ab57602), MFN2 (Abnova, 157H00009927-M03J), MFN1 (CST #14739), MFN2 (CST #9482S), MIRO1 (Sigma #HPA010687), MIRO2 (CST #14061), VDAC1 (CST #4661), VDAC2 (Proteintech 11663-1-A), SAM50 (abcam 167430), CS (CST #14309), FAF2 (UBXD8)(CST #34945), CALR (CST #12238), ACTB (CST #4970), Golgin-97 (CST #13192S), TOMM40 (Sigma HPA036231), TOMM20 (HPA011562), TOMM70 (HPA048020), PISD (Proteintech 16401-1-AP), GAPDH (CST #2118), HA-HRP (Roche 12013819001). Antisera used: TgGra7 (23), TgTGMAF1 (23), TgGAP45 (Dr. D Soldati (U. of Geneva), TgHsp70 (Dr. P Bradley, UCLA). PINK1 (CST D8G3), TOMM40 (Santa Cruz sc365467), MIC60 (Proteintech 10179-1-AP); SNX9 (Sigma HPA031410); PINK1 (CST D8G3).

Generation of transgenic parasites

Transgenic parasite strains were made by electroporation of the parental Type I (RHΔ*hxgprt*) strain (for BFP-expressing parasites), or RHΔ*ku8ΔTgMAF1:mCherry*⁺ strain for Δ*maf1* mCherry⁺ parasites expressing HA (Δ*T maf1*:HA); HA-tagged MAF1 (Δ*maf1*:HA-MAF1); or

HA-tagged MAF1^{RKK} (*Δmaf1:HA-MAF1^{RKK}*). For generating RH *Δ maf1:mCherry* parasites expressing HA or HA-TgMAF1, pGra1 and pMAF1 HA encoding HA and HA-tagged TgMAF1 were used (27). To express HA-tagged TgMAF1^{RKK} the S431R, T439K, and L441K previously described mutations (28) were introduced into pMAF1 by site-directed mutagenesis using the forward and reverse primers TATAAGGCTAGCATGCTGGACTGA and CTTCCTTTCAGCCTCCTGTAAAGCCGT. All plasmids contained a chloramphenicol (CAT) resistance for drug selection. 100 μg of the corresponding plasmid was linearized using NotI and introduced into Type I RH *ΔTgMAF1:mCherry* parasites by electroporation. To isolate single parasites positive for CAT expression, parasites were treated with 20 μM chloramphenicol up to 2 weeks followed by a serial dilution. RH *ΔTgMAF1:mCherry* parasites expressing HA, HA-MAF1 and HA-MAF1^{RKK} are referred to in text as *Δmaf1:HA*, *Δmaf1:HA-MAF1*, and *Δmaf1:HA-MAF1^{RKK}*.

Proteomics sample preparation

For preparing mitoIP samples were lysed using 20 to 25 μl of 6M Guanidinium chloride or eluted from the beads and desalted as described (55) and analyzed using LC-MS/MS. For preparing samples from immunoprecipitation, on-beads digestion was performed to elute the proteins off the beads. Before adding the elution buffer, the beads were washed with detergent-free buffer (50mM Tris-HCl pH7.5) four times to remove any detergents used previously. Then 100 μl of the elution buffer (5ng/μl trypsin, 50mM Tris-HCl pH7.5, 1mM Tris(2-carboxyethyl)phosphine), 5mM chloroacetamide) was added to the beads and incubated at room temperature by vortexing from time to time, or rotating on a rotator. After 30 min, the supernatant was transferred to a 0.5 ml tube and incubated at 37°C overnight to ensure a complete tryptic digest. The digestion was stopped in the next morning by adding formic acid to the final concentration of 1%. The resulted peptides were cleaned with home-made StageTips. Alternatively, four micrograms of the eluted peptides were dried out and reconstituted in 9 μL of 0.1M TEAB and labeled with tandem mass tags (TMTpro, Thermo Fisher Scientific cat. No A44522). Labeling was carried out according to manufacturer's instruction with the following changes: 0.5 mg of TMTPro reagent was re-suspended with 33 μL of anhydrous ACN. Seven microliters of TMTPro reagent in ACN was added to 9 μL of clean peptide in 0.1M TEAB. The final ACN concentration was 43.75% and the ratio of peptides to TMTPro reagent was 1:20. After 60 min of incubation the reaction was quenched with 2 μL of 5% hydroxylamine. Labelled peptides were pooled, dried, re-suspended in 200 μL of 0.1% formic acid (FA), split into two equal parts, and desalted using home-made STAGE tips. One of the two parts was fractionated on a 1 mm x 150 mm ACQUITY column, packed with 130 Å, 1.7 μm C18 particles (Waters cat. no SKU: 186006935), using an Ultimate 3000 UHPLC (Thermo Fisher Scientific). Peptides were separated at a flow of 30 μL/min with a 88 min segmented gradient from 1% to 50% buffer B for 85 min and from 50% to 95% buffer B for 3 min; buffer A was 5% ACN, 10mM ammonium bicarbonate (ABC), buffer B was 80% ACN, 10mM ABC. Fractions were collected every three minutes, pooled in two passes (1 + 17, 2 + 18 ... etc.), and dried in a vacuum centrifuge (Eppendorf).

LC-MS/MS analysis

For label-free quantification, peptides were separated on a 75 cm, 75 μm internal diameter Acclaim™ PepMap™ analytical column (Thermo Fisher Scientific, catalogue number 164939) using an EASY-nLC 1200 (Thermo Fisher Scientific). The column was maintained at 50°C. Buffer A and B were 0.1% formic acid in water and 0.1% formic acid in 80% acetonitrile.

Peptides derived from whole cells were separated on a segmented gradient from 6% to 31% buffer B for 230 min and from 31% to 50% buffer B for 10 min at 250 nl / min. Peptides derived from enriched mitochondria were separated on a segmented gradient from 6% to 31% buffer B for 110 min and from 31% to 50% buffer B for 10 min at 250 nl / min. Eluting peptides were analyzed on a QExactive HF mass spectrometer (Thermo Fisher Scientific). Peptide precursor m/z measurements were carried out at 60000 resolution in the 300 to 1800 m/z range. The top ten most intense precursors with charge state from 2 to 7 only were selected for HCD fragmentation using 25% normalized collision energy. The m/z values of the peptide fragments were measured at 30000 resolution using a minimum AGC target of 1e4 and 55 ms maximum injection time for the whole cell samples or 15000 resolution, minimum AGS target of 1e4, and 120 ms maximum injection time for the enriched mitochondria samples. Upon fragmentation, precursors were put on a dynamic exclusion list for 45 sec. TMT labeled peptides were and separated on a 50 cm, 75 µm Acclaim PepMap column (Thermo Fisher Scientific, Product No. 164942) and analysed on a Orbitrap Lumos Tribrid mass spectrometer (Thermo Fisher Scientific) equipped with a FAIMS device (Thermo Fisher Scientific). The FAIMS device was operated in two compensation voltages, -50 V and -70 V. Synchronous precursor selection based MS3 was used for the acquisition of the TMTPro reporter ion signals. Peptide separations were performed on an EASY-nLC1200 using a 90 min linear gradient from 6% to 31% buffer; buffer A was 0.1% FA, buffer B was 0.1% FA, 80% ACN. The analytical column was operated at 50°C. Raw files were split based on the FAIMS compensation voltage using FreeStyle (Thermo Fisher Scientific).

Protein identification and quantification

Label-free quantification raw data were analyzed with MaxQuant version 1.6.0.13 (56) using the integrated Andromeda search engine (57). Peptide fragmentation spectra were searched against the canonical sequences of the human reference proteome, proteome ID UP000000589, and toxoplasma reference proteome, proteome ID UP000005641, downloaded from UniProt. Methionine oxidation and protein N-terminal acetylation were set as variable modifications; cysteine carbamidomethylation was set as fixed modification. The digestion parameters were set to “specific” and “Trypsin/P,” The minimum number of peptides and razor peptides for protein identification was 1; the minimum number of unique peptides was 0. Protein identification was performed at a peptide spectrum matches and protein false discovery rate of 0.01. The “second peptide” option was on. Successful identifications were transferred between the different raw files using the “Match between runs” option. Exploratory data analysis and visualization was done using tidyverse in R (58, 59). TMT data was analyzed using MaxQuant, version 1.6.17.0. The isotope purity correction factors, provided by the manufacturer, were included in the analysis. Differential expression analysis was performed using limma, in R (60). Volcano plots of WC and mitoIP proteins generated using Flaski (61).

Data availability

The mass spectrometry proteomics data have been deposited to the ProteomeXchange Consortium via the PRIDE (62) partner repository with the dataset identifier PXD024491; Username: reviewer_pxd024491@ebi.ac.uk, Password: OdwcqFKY.

Isolation of crude mitochondria

U2OS cells were seeded in a 4 million cells in a 10 cm dishes and infected with RH *Δhxppt:mCherry Toxoplasma* at an MOI:8. At 20 hpi, uninfected plates were treated with either 30 µM CCCP for or 0.1% DMSO (untreated control). At 24 hpi, all plates were washed 2X with

chilled 1XPBS. Cells were scraped in chilled Mannitol-Sucrose (MS) buffer (225 mM mannitol, 75 mM sucrose, 30 mM Tris-HCl pH 7.4, 12 μ M EGTA, and EDTA-free Pierce Protease inhibitor, and triturated 16 X with a 1ml syringe and 27Gx3/4 needle. Samples were centrifuged at 600 x g for 5 min and the cleared supernatant was transferred into a fresh tube. After centrifuging at 10,000 x g for 15 min, an aliquot was taken for the cytosolic fraction. The supernatant was removed and the mitochondrial pellet was twice carefully overlaid with MS buffer. The pellet was resuspended in MS buffer (mitochondrial fraction). Both fractions were then supplemented with cold lysis buffer and lysed for 30 min on ice. Lysates were centrifuged for 10 min at 14,000 x g at 4°C and the supernatant was transferred into a fresh tube.

Electron microscopy

Inducible Hela KD knockdown cell lines were grown on aclar discs, infected with different *Toxoplasma* strains in the presence of 1 μ g/ml of doxycycline, and fixed at 6 hpi in prewarmed fixative (2.0% glutaraldehyde, 2.5% sucrose, 3mM CaCl₂, 100mM HEPES, pH 7.4). Following 30 min at RT and 30 min at 4C, cells were washed 3X with 0.1M sodium cacodylate buffer and incubated with 1% osmium tetroxide and 1% potassium hexacyanoferrate for 1 h at 4C. After 3X 5 min washes with 0.1M cacodylate buffer, samples were dehydrated at 4C using ascending ethanol series for 7 min each (50%, 70% 90%, 3x100%). Infiltration was performed with a mixture of 50% epon/ethanol for 1h, 70% epon/ethanol for 2h, and with pure epon overnight at 4C. Samples were embedded into TAAB capsules and incubated at 48h at 60C. Ultrathin sections of 70nm were cut using an ultramicrotome (Leica Microsystems UC6) and a diamond knife (Diatome, Biel, Switzerland) and stained with 1.5% uranyl acetate for 15 min at 37C and Reynolds lead citrate solution for 4 min. Images were acquired using a JEM-2100 Plus Transmission Electron Microscope (JEOL) operating at 80kV equipped with a OneView 4K camera (Gatan). ImageJ was used to measure the length of the mitochondria closely associated with the parasite vacuole (<30nm) in electron micrographs in \geq 20 images per treatment.

Mitotracker and FL-HPC labeling

For staining with MitoTracker (Invitrogen), cells (24 hpi mock- or *Toxoplasma* infection) were incubated with prewarmed DMEM containing MitoTracker Deep Red at a concentration of 25 nM. After 20 min of incubation at 37°C, cells were rinsed with prewarmed 1X PBS and then incubated in prewarmed cDMEM. For visualization of phosphatidylcholine (PC), cells were incubated with 2 μ M (FL-HPC) in complete media O/N, rinsed 2X in 1X PBS, and then mock- or *Toxoplasma* infected and visualized at 24 hpi.

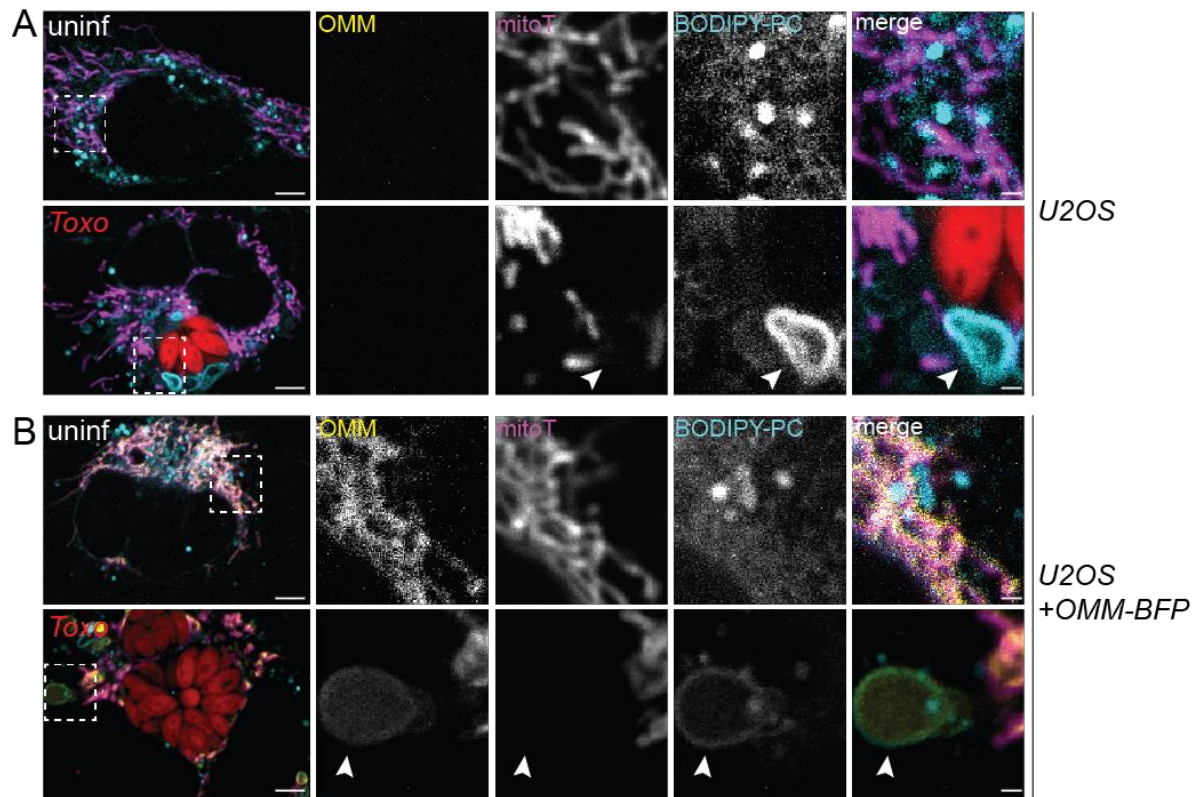


Fig. S1. SPOTs form in the absence of OMM-GFP overexpression.

Representative live-cell images of uninfected and *Toxoplasma* (mCh)-infected (A) WT U2OS cells or (B) U2OS cells expressing OMM-BFP labeled with MitoTracker Deep Red (mitoT) and the phosphatidylcholine conjugate (FL-HPC), and imaged at 24 hpi. Scale bar, 5 μm; inset 1 μm.

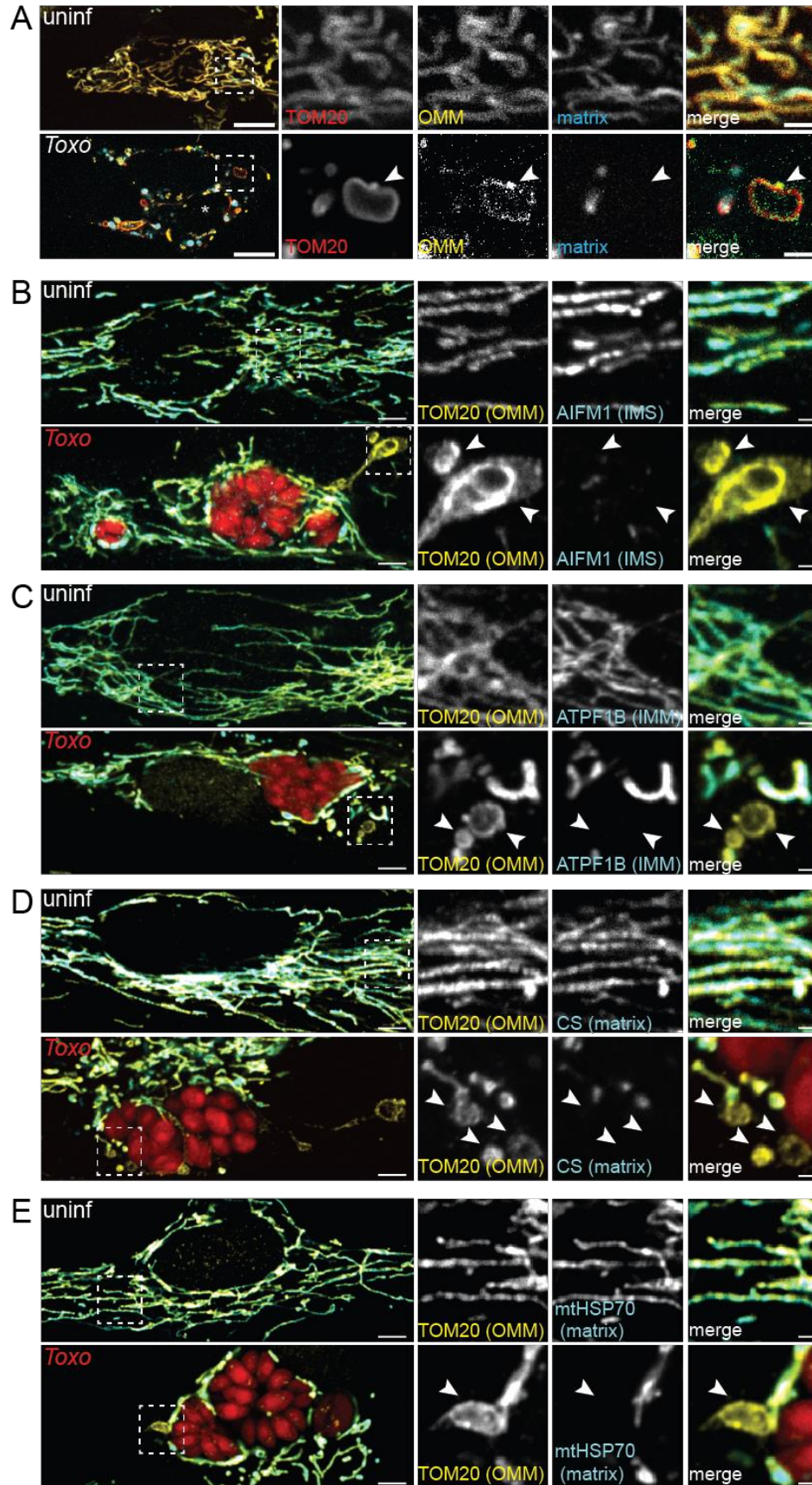


Fig. S2. Markers of the IMM, IMS, and matrix proteins do not localize to SPOTs. (A) Representative live-cell images of the OMM (GFP), matrix (BFP), and TOM20 (RFP) in uninfected and infected MEFs at 24 hpi (parasite vacuole indicated with asterisk and dotted oval). Arrowhead in inset of infected cells indicates a SPOT. Scale bar, 5 μm ; inset, 1 μm . (B to E) Representative images of *Toxoplasma* (mCh)-infected HFFs that were fixed at 24 hpi and processed for immunofluorescence (IF) analysis. SPOTs (indicated by arrowheads in the inset panels of infected cells) are positive for the OMM protein TOM20 but do not contain (B) the IMS protein AIFM1, (C) the IMM protein ATPF1B, (D) or the matrix proteins CS and (E) mtHSP70. Scale bar, 5 μm ; inset, 1 μm .

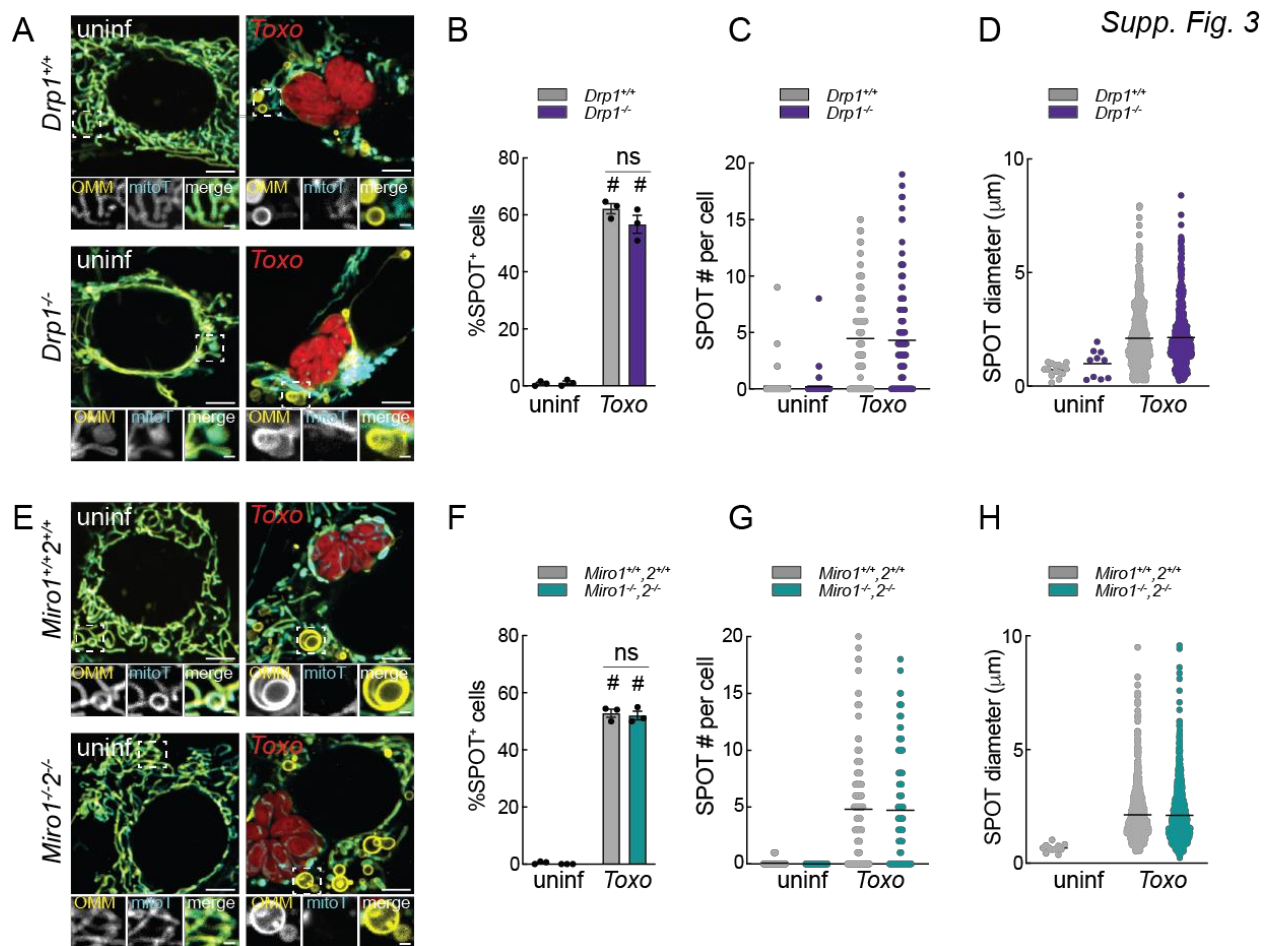


Fig. S3. SPOTs form independently of DRP1, and MIRO1 and MIRO2. (A) Representative live-cell images of the OMM (GFP) in uninfected (uninf) and *Toxoplasma* (mCh)-infected (*Toxo*) *Drp1*^{+/+} and *Drp1*^{-/-} MEFs labeled with mitoT; scale bar, 5 μm; inset 1 μm. (B) Percentage of SPOT-positive cells in experiments as in (A); data are mean ± SEM of >100 cells counted from 4 biological replicates; #p<0.0001 for uninfected versus infected by two-way ANOVA analysis. Scatterplot with mean (C) number and (D) diameter of SPOTs in experiments as in (A) from >30 infected cells from 3 biological replicates. (E) Representative live-cell images of the OMM (GFP) in uninf and *Toxoplasma* (mCh)-infected *Miro1*^{+/+2+/+} and *Miro1*^{-/-2-/-} MEFs labeled with mitoT; scale bar, 5 μm; inset 1 μm. (F) Percentage of SPOT-positive cells in experiments as in (E); data are mean ± SEM of >100 cells counted from 3 biological replicates; #p<0.0001 for uninfected versus infected by two-way ANOVA analysis. Scatterplot with mean (G) number and (H) diameter of SPOTs in experiments as in (E) from >30 infected cells from 3 biological replicates.

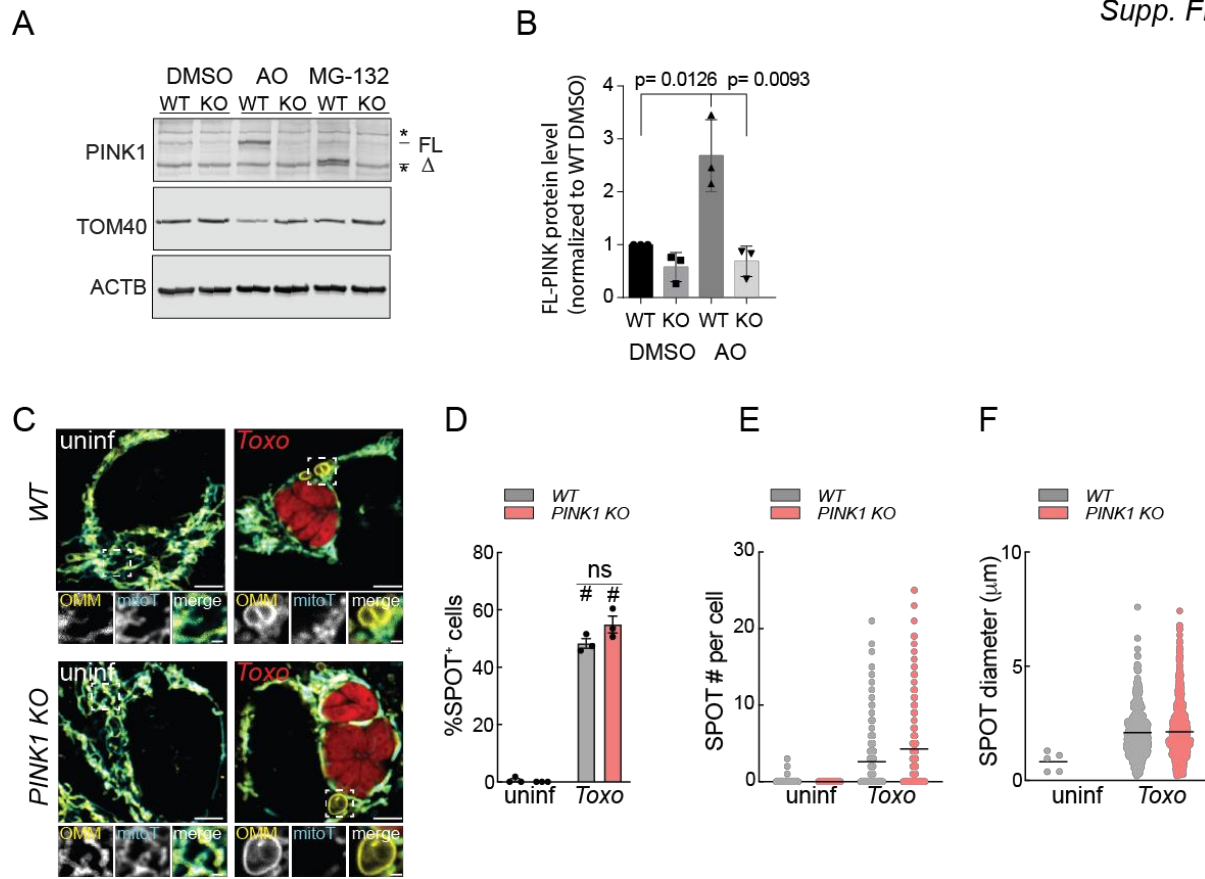


Fig. S4. SPOTs form independently of PINK1 (A) WT or PINK1 KO HeLa FlpIn TRex cells stably expressing mt-mKEIMA and Parkin were treated with 10 μ M antimycin A1 and oligomycin (AO) or 10 μ M MG-132 for 6h to accumulate PINK1 and analyzed by immunoblotting for: PINK1 ~55kDa; TOM40 ~40kDa, ACTB ~45kDa. FL: full-length; Δ : processed; * indicates non-specific bands. (B) Fold-change in density of protein bands imaged as in (A) normalized to ACTB and relative to WT DMSO. Data are mean \pm SEM from 3 biological replicates and analyzed by unpaired two-tailed t-test. (C) Representative live-cell images of the OMM (GFP) in uninfl and *Toxoplasma* (mCh)-infected WT and PINK1 KO HeLas labeled with mitoT; scale bar, 5 μ m; inset 1 μ m. (D) Percentage of SPOT-positive cells in experiments as in (C); data are mean \pm SEM of >100 cells counted from 3 biological replicates; #p<0.0001 for uninfected versus infected by two-way ANOVA analysis. Scatterplot with mean (E) number and (F) diameter of SPOTs in experiments as in (C) from >30 infected cells from 3 biological replicates.

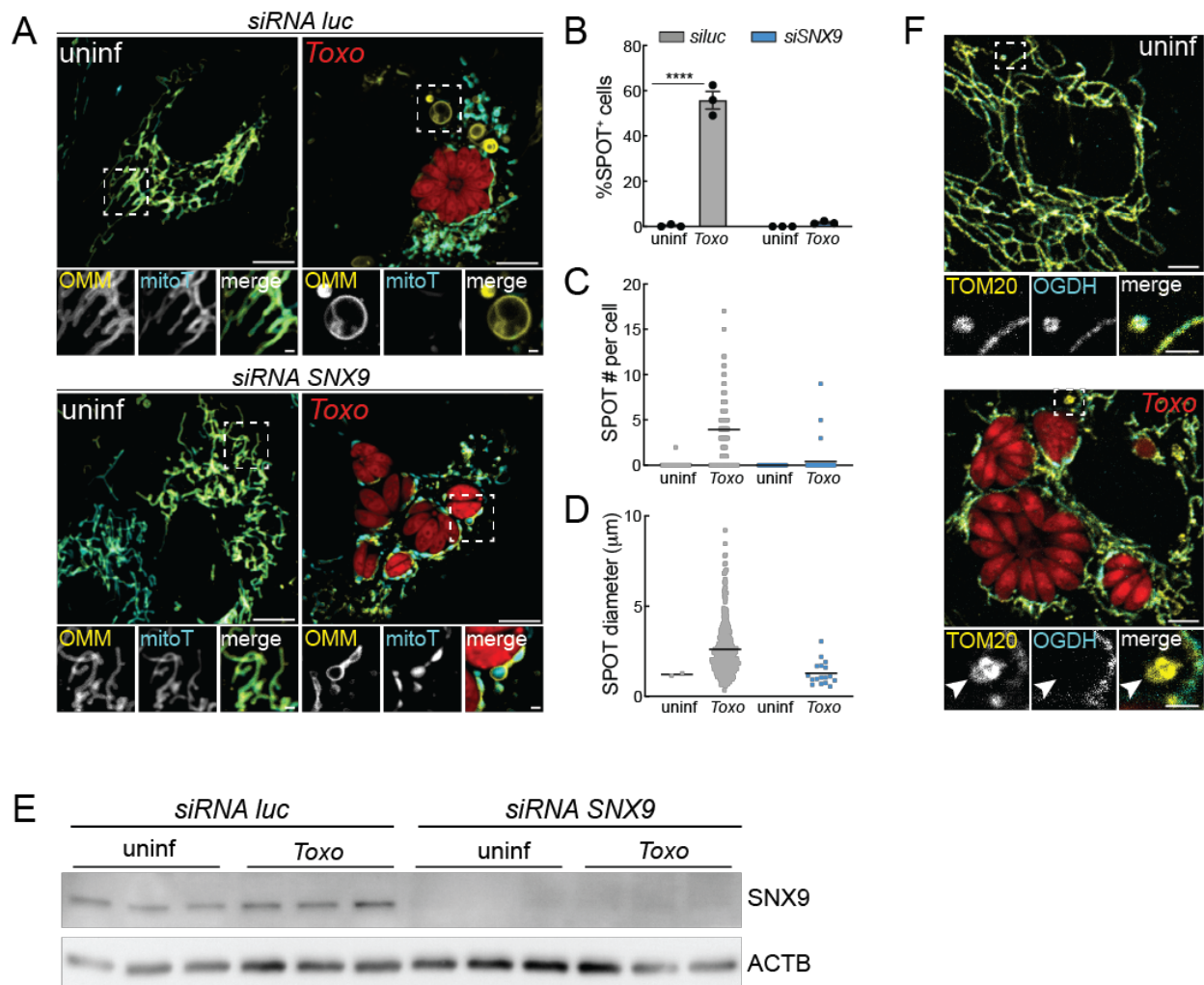


Fig. S5. Sorting nexin 9 is required for the formation of SPOTs that do not contain OGDH during *Toxoplasma* infection (A) Representative live-cell images of the OMM (GFP) in uninfected (uninf) and *Toxoplasma* (mCh)-infected (*Toxo*) *siRNA luc*- and *siRNA SNX9*-treated U2OS cells labeled with mitoT; scale bar, 5 µm; inset 1 µm. (B) Percentage of SPOT-positive cells in experiments as in (A); data are mean +/- SEM of >100 cells counted from 3 biological replicates; *****p*<0.0001 for uninfected versus infected by two-way ANOVA analysis. Scatterplot with mean (C) number and (D) diameter of SPOTs in experiments as in (A) from >30 infected cells from 3 biological replicates. *siRNA luc* and *siRNA SNX9*-treated U2OS cells. Cells treated as in (A) were analyzed by immunoblotting for: SNX9 ~70kDa; ACTB ~45kDa. (E) Representative images of *Toxoplasma* (mCh)-infected HFFs that were fixed at 24 hpi and processed for immunofluorescence microscopy. Arrowhead in inset panel of infected cell depicts a SPOT that is positive for the OMM protein TOM20 but does not contain the matrix protein OGDH. Scale bar, 5 µm; inset, 1 µm.

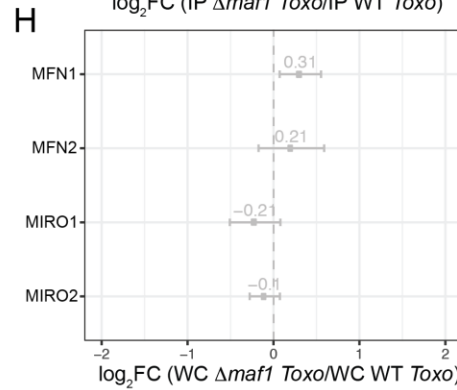
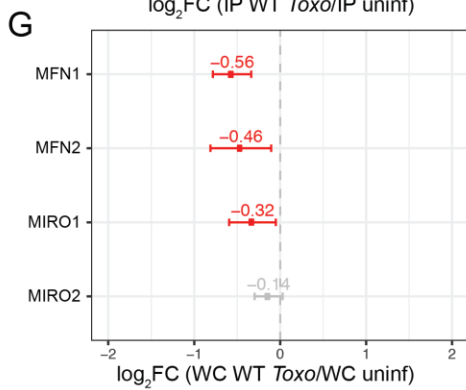
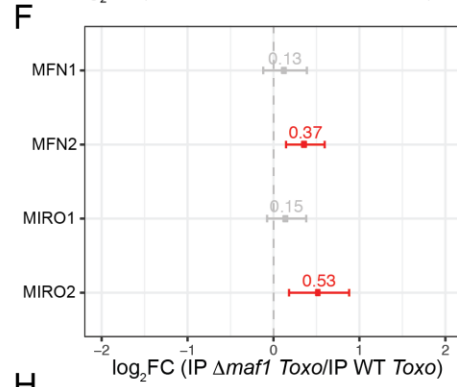
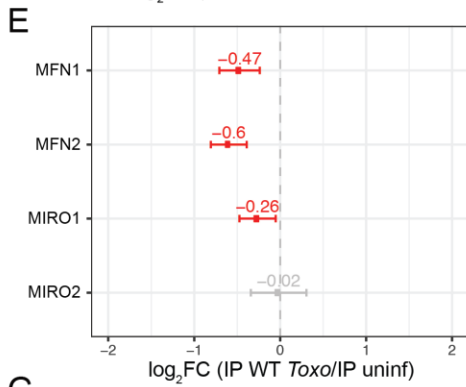
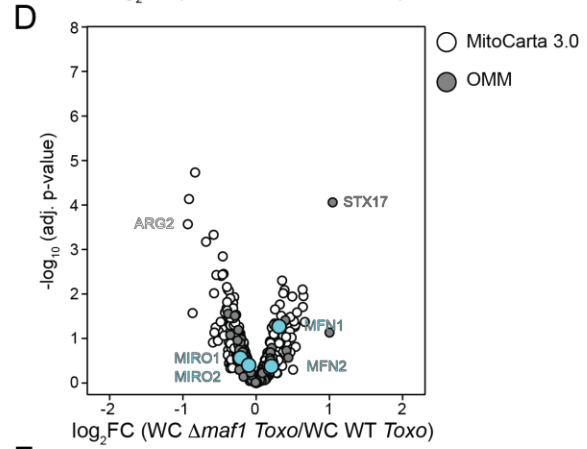
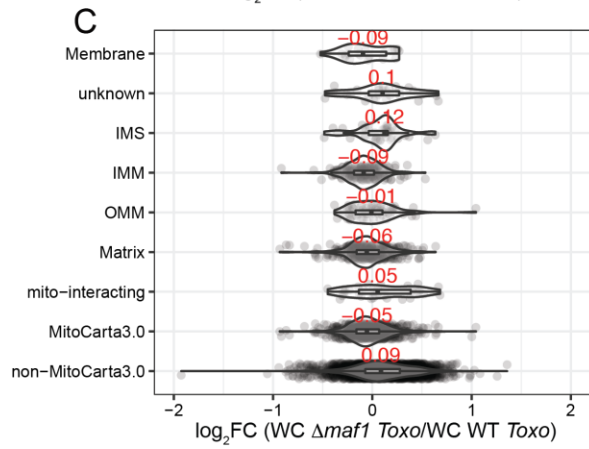
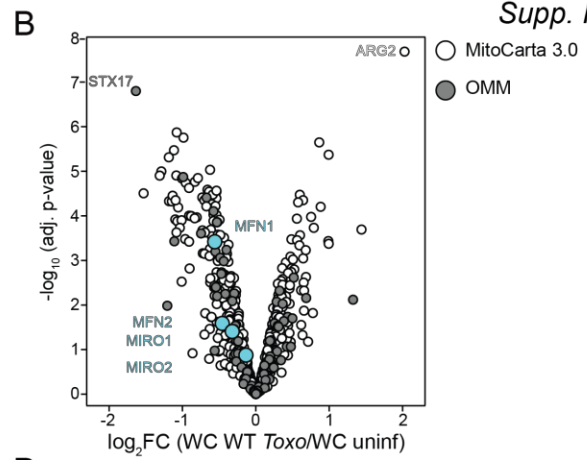
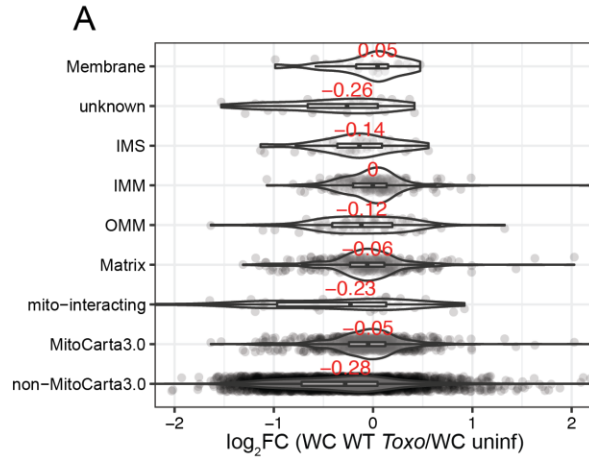


Fig. S6. Proteomic analysis of changes in mitochondria during *Toxoplasma* infection (A, C)
Whole cell (WC) fractions from HeLa cells that were uninfected (n=4), WT *Toxo*-infected (n=4), *Δmaf1* *Toxo*-infected (n=3) at 24 hpi and analyzed by mass spectrometry. Boxplot depicting the log₂-fold change (FC) of detected MitoCarta3.0 proteins between indicated treatments according to submitochondrial localization. Median values for each subcompartment are indicated in red. **(B, D)** Volcano plot of proteins in **(A, C)**; dark gray, OMM proteins as classified by MitoCarta3.0; white, all other MitoCarta3.0 proteins. **(E to H)** Mean FC with 95% confidence interval for indicated proteins and comparisons.

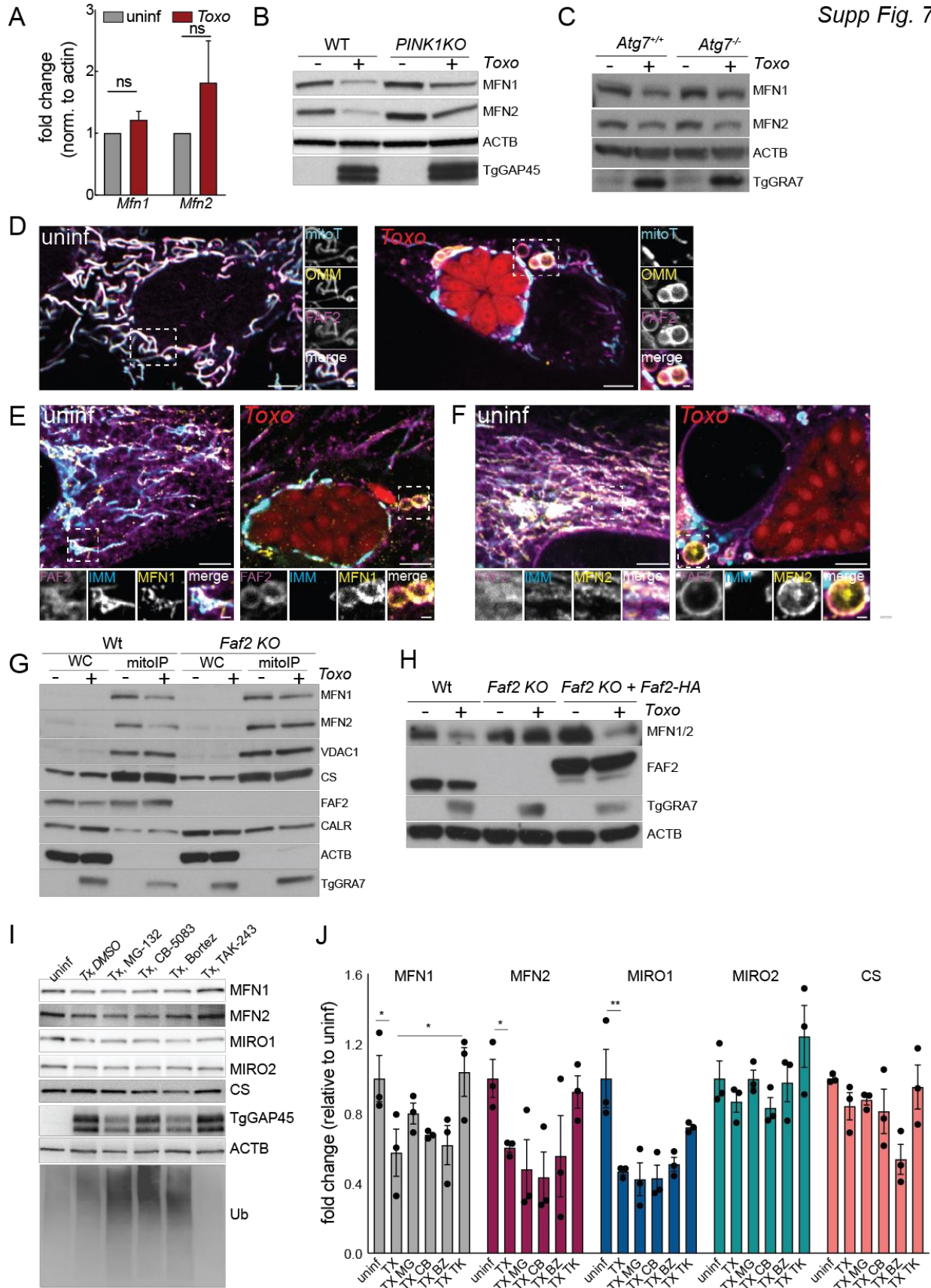


Fig. S7. FAF2 localizes to SPOTs and mediates the degradation of MFN1 and MFN2 (A) *Mfn1* and *Mfn2* mRNA levels in uninfected (uninf) and *Toxoplasma*-infected (*Toxo*) MEFs at 24hpi. mRNA expression was measured by the standard curve method and normalized to *Actb*; y-axis depicts fold-change relative to uninfected cells. Whole cell lysates from 24 h uninf and *Toxo*-infected **(B)** WT and PINK1 KO HeLas and **(C)** *Atg7^{+/+}* and *Atg7^{-/-}* MEFs were analyzed by immunoblotting for: MFN1 ~80kda; MFN2 ~80kDa; ACTB ~45kDa; TgGRA7 ~32kDa; TgGAP45 ~45kDa. **(D)** Representative live-cell images of OMM (BFP), FAF2 (GFP) in uninf and *Toxo* (mCh)-infected HFFs that were labeled with mitoT. FAF2 localizes to SPOTs (depicted in inset panels of infected cell); scale bar, 5 μ m; inset, 1 μ m. **(E to F)** Representative images of uninf and *Toxo* (mCh)-infected HFFs that were fixed at 24 hpi and processed for IF analysis. FAF2-HA, MFN1, and MFN2, but not the IMM protein ATP51B localize to SPOTs (depicted in inset panels of infected cells); scale bar, 5 μ m; inset, 1 μ m. **(G)** Whole cell (WC) fractions or mitochondria immunopurified (mitoIP) from uninf and *Toxo*-infected WT and *Faf2 KO MEFs* harvested at 24 hpi were analyzed by immunoblotting for MFN1 ~80kda; MFN2 ~80kDa; VDAC1 ~34kDa; CS ~45kDa, FAF2 ~52kDa, CALR ~55kDa, ACTB ~45kDa, TgGRA7 ~32kDa; **(H)** WT, *Faf2KO*, or *Faf2 KO* MEFs stably expressing HA-tagged FAF2 were analyzed as in **(G)**. **(I)** WT HeLas were uninf or *Toxo*-infected and at 12 hpi treated with DMSO, 1 μ M MG-132, 1 μ M CB-5083, 1 μ M Bortezomib, 1 μ M TAK-243 and analyzed by immunoblotting for: MFN1 ~80kda; MFN2 ~80kDa; MIRO1 ~75kDa; MIRO2 ~75kDa; CS ~45 kDa, ACTB ~45kDa; TgGAP45 ~45kDa; Ubiquitin (Ub). **(J)** Fold-change in density of protein bands imaged as in **(I)** normalized to ACTB and relative to WT uninf mean; data are mean +/- SEM from 3 biological replicates. *p<0.05, **p<0.01 for TX vs. uninf; TX vs. TX TAK by two-way ANOVA .

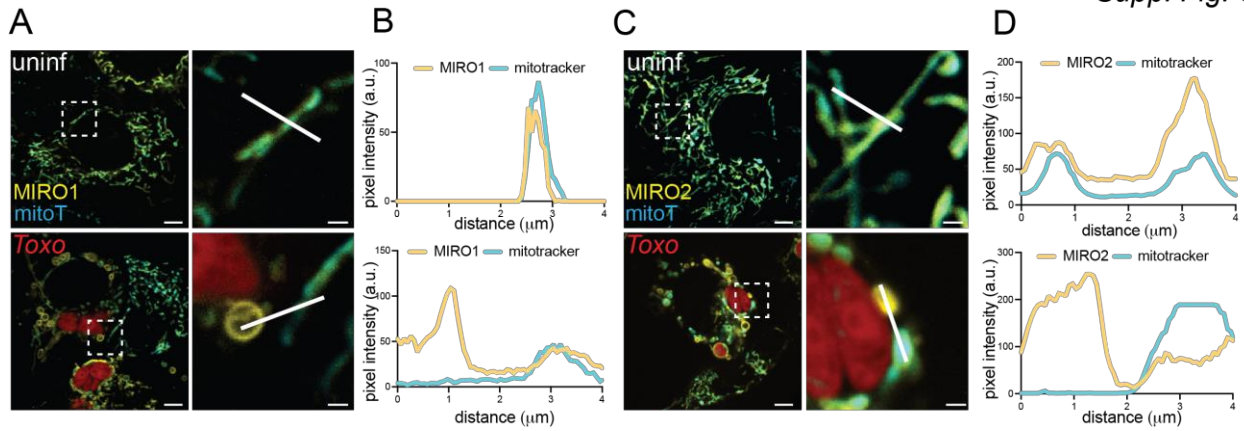


Fig. S8. MIRO1 and MIRO2 localize to SPOT-like structures during infection.

Representative live-cell imaging of (A) *Miro1*^{-/-}:GFP-Miro1 MEFs and (C) *Miro2*^{-/-}:GFP-Miro2 MEFs at 24hpi with *Toxoplasma* (mCh). (B) and (D) Corresponding pixel intensity plots for white line in inset panels in (A) and (C) respectively. Scale bars are 5 μm and 1 μm in the inset.

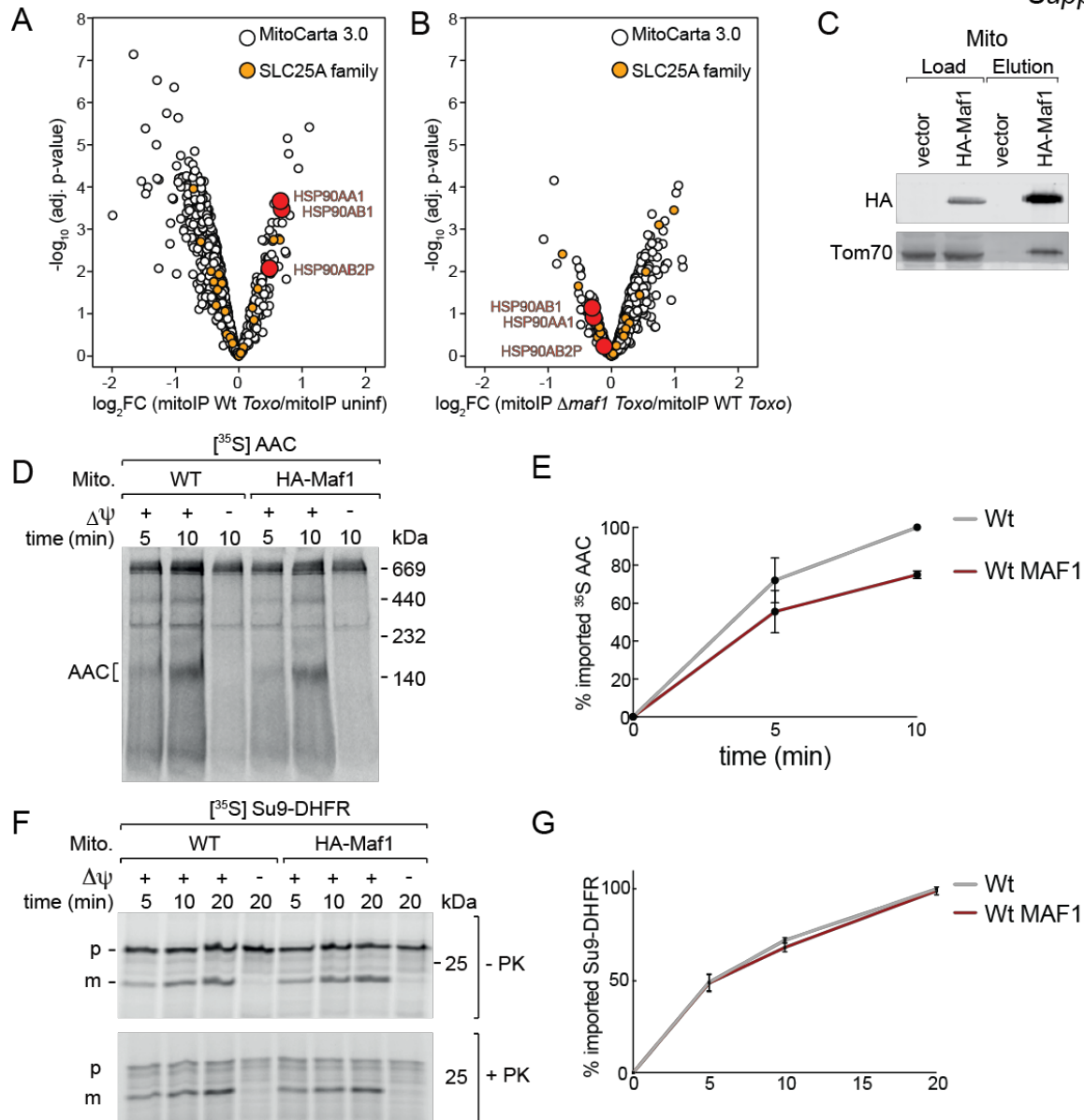


Fig. S9. MAF1 impairs TOM70-dependent import (A-B) Volcano plots as in Fig. 3B, 3D; orange, detected SLC25A family proteins, white, all other MitoCarta3.0 proteins. (C) IPs were prepared from mitochondria isolated from WT or HA-MAF1+ yeast and analyzed by immunoblotting for: TgMAF1~60kDa; TOM70~72kDa. (D) $[^{35}\text{S}]$ AAC was imported into WT and MAF1+ mitochondria and analyzed by blue native electrophoresis and autoradiography. (E) Signals in (D) were quantified and the amount of imported protein relative to WT 10 min was plotted. Data are mean \pm SEM from 4 biological replicates. (F) $[^{35}\text{S}]$ Su9-DHFR was imported into WT and MAF1+ mitochondria and analyzed by blue native electrophoresis and autoradiography; PK: proteinase K; p: precursor; m: mature. (G) Signals in (F) were quantified and the amount of imported protein relative to input WT 20 min was plotted. Data are mean \pm SEM from 3 biological replicates.

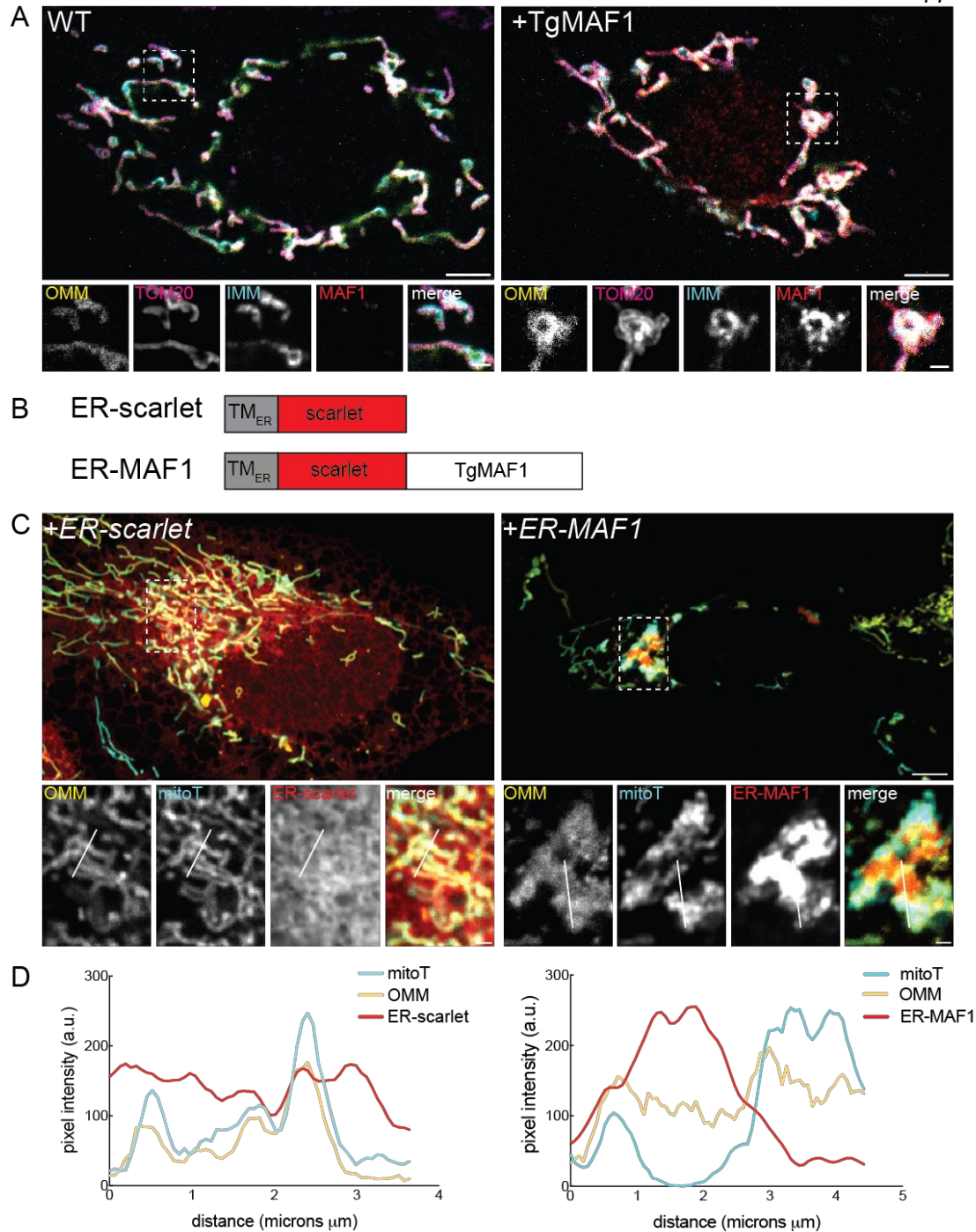


Fig. S10. MAF1 is not sufficient to induce SPOT formation independently of infection. (A) WT and HA-MAF1+ MEFs were processed for IF analysis of the OMM (BFP), TOM20, a marker of the IMM (ATP51B), and HA-MAF1 (HA); scale bar, 5 μm ; inset, 1 μm . (B) Cartoon schematic of ER-targeted scarlet fusion constructs. TM_{ER}: amino acids 1-29 of *Oryctolagus cuniculus* Cyp2C1 (C) Representative live-cell imaging of the OMM (GFP) in mitoT-labeled U2OS cells expressing constructs in (B). (D) Corresponding pixel intensity plots for white line in inset panels in (C).

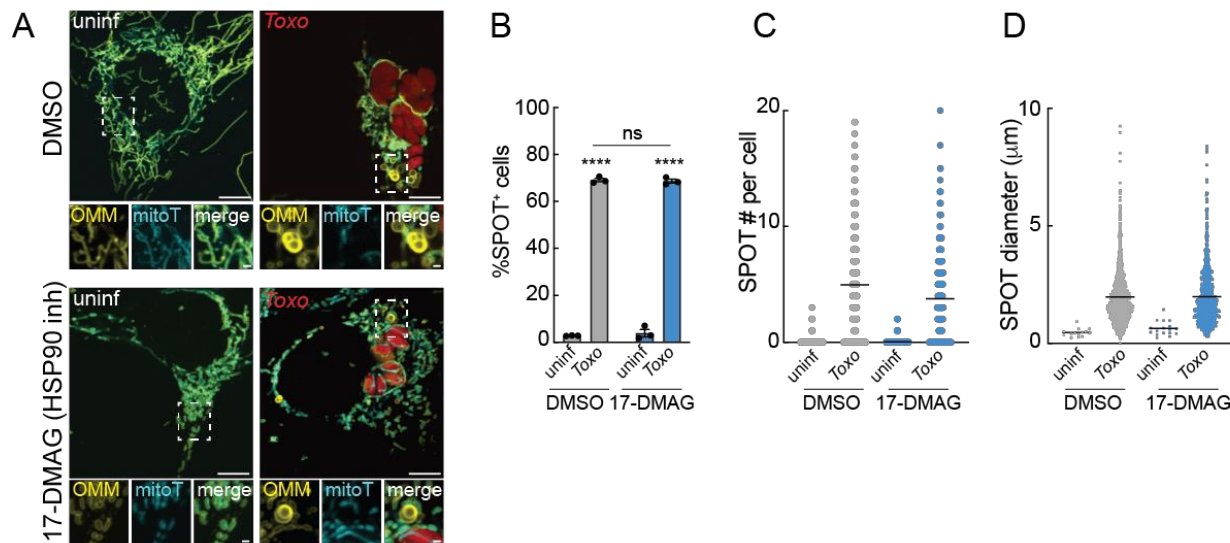


Fig. S11. An inhibitor of HSP90 does not prevent SPOT-formation during infection.

(A) Representative live-cell images of the OMM (GFP) in uninfected (uninf) and *Toxoplasma* (mCh)-infected (*Toxo*) mitoT-labeled U2OS cells at 24 h following treatment with DMSO or the HSP90-inhibitor 17-DMAG (10 μM) at 12 hpi; scale bar, 5 μm; inset 1 μm. (B) Percentage of SPOT-positive cells in experiments as in (A); data are mean +/- SEM of >100 cells counted from 3 biological replicates; ns for DMSO vs. 17-DMAG, and ****p<0.0001 for uninfected vs. infected by two-way ANOVA analysis. Scatterplot with mean (C) number and (D) diameter of SPOTs in experiments as in (A) from >30 infected cells from 3 biological replicates.

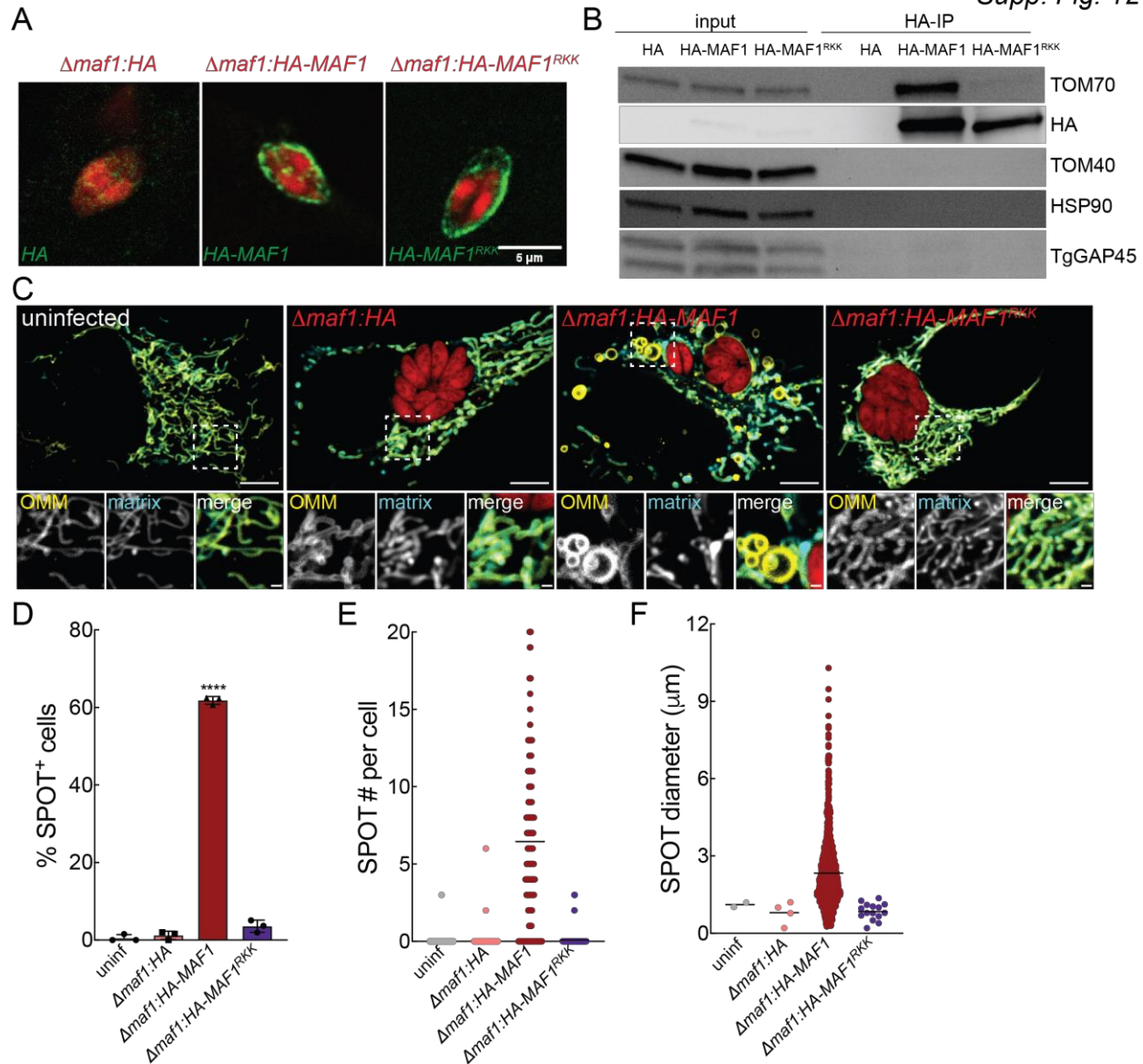


Fig. S12. A robust MAF1-TOM70 interaction is required for SPOT formation. (A) HFFs at 6 hpi with *Δmaf1* (mCh) parasites expressing HA (*Δmaf1:HA*); HA-tagged MAF1 (*Δmaf1:HA-MAF1*); or HA-tagged MAF1^{RKK} (*Δmaf1:HA-MAF1^{RKK}*) were processed for IF analysis using anti-HA antibodies; scale bar, 5 μm. (B) Anti-HA IPs were prepared from U2OS cells infected with indicated parasite strains and probed for indicated proteins. (C) Representative live-cell images of the OMM (GFP) and matrix (BFP) in U2OS cells infected with indicated strains; scale bar, 5 μm; inset 1 μm. (D) Percentage of SPOT-positive cells in experiments as in (C); data are mean +/- SEM of >100 cells counted from 3 biological replicates; ****p<0.0001 for *Δmaf1:HA-MAF1*-infected versus *Δmaf1:HA* infected by one-way ANOVA analysis. Scatterplot with mean (E) number and (F) diameter of SPOTs in experiments as in (C) from >30 infected cells from 3 biological replicates.

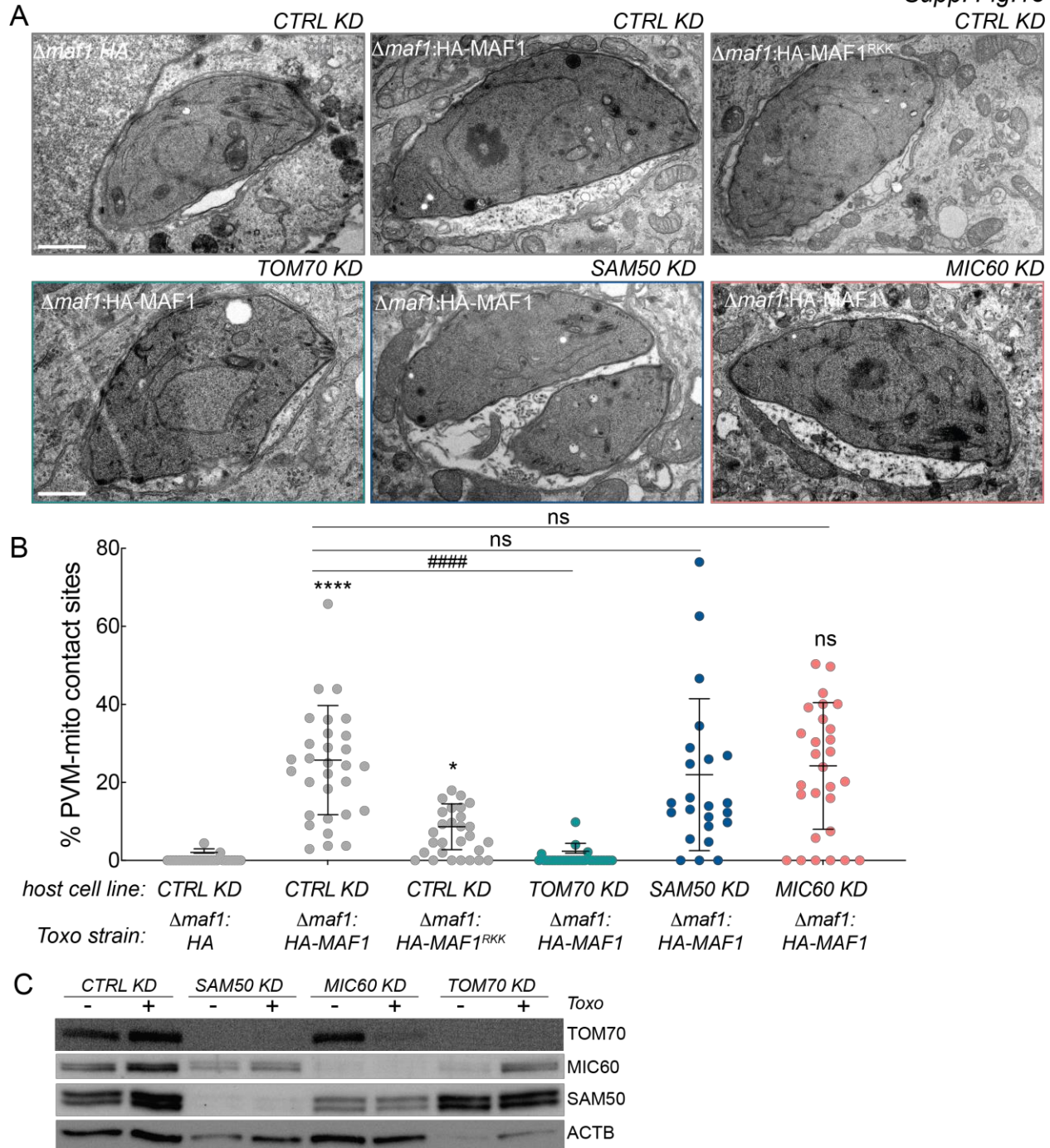


Fig. S13. SAM50 and MIC60 are not required for mitochondria-*Toxoplasma* contact sites.
(A) Representative electron microscopy images of indicated HeLa doxycycline (doxy)-inducible KD lines 7 dp doxy (1 μg/ml) treatment and 6 hpi with indicated parasite strains. Scale bar, 1 μm.
(B) Percentage of PVM associated with mitochondria in images as in **(A)** from >20 vacuoles. Data are mean +/- SD; *p<0.05, ****p<0.0001 for Δmaf1:HA vs Δmaf1:HA-MAF1 or Δmaf1:HA-MAF1^{RKK}; ##### p<0.0001 or not significant (ns) for cell line comparisons. **(C)** Lysates HeLa inducible KD lines 7 dp doxy treatment and at 24 hpi *Toxoplasma* were analyzed by immunoblotting for: TOM70 ~72kDa, MIC60 ~88kDa, SAM50 ~55kDa, ACTB ~45kDa.

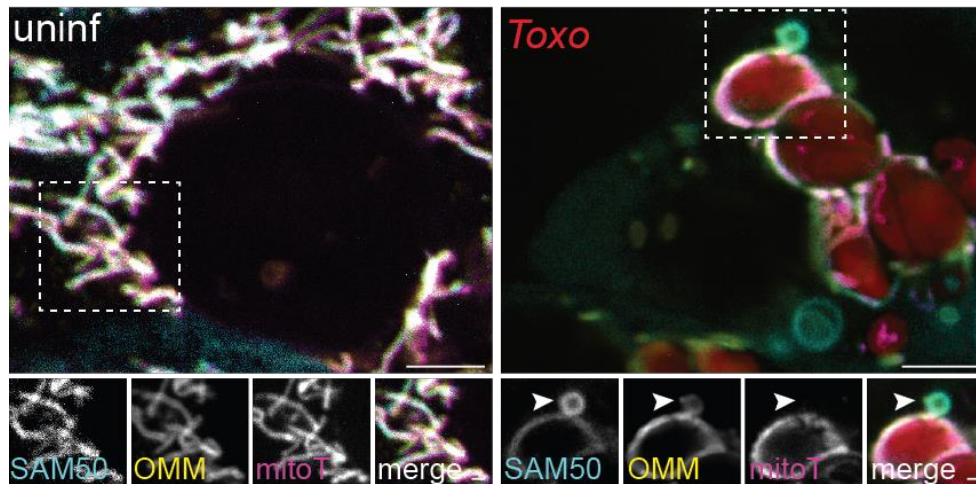


Fig. S14. SAM50 is enriched on SPOTs during infection.

Representative live-cell images of the OMM (BFP) and SAM50 (GFP) in uninfected (uninf) and *Toxoplasma* (mCh+)-infected (*Toxo*) U2OS cells labeled with mitoT at 24 hpi; scale bar, 5 μ m; inset 1 μ m. Arrowhead in inset panel of infected cell depicts a SPOT that is positive for the OMM and SAM50 but not mitoT.

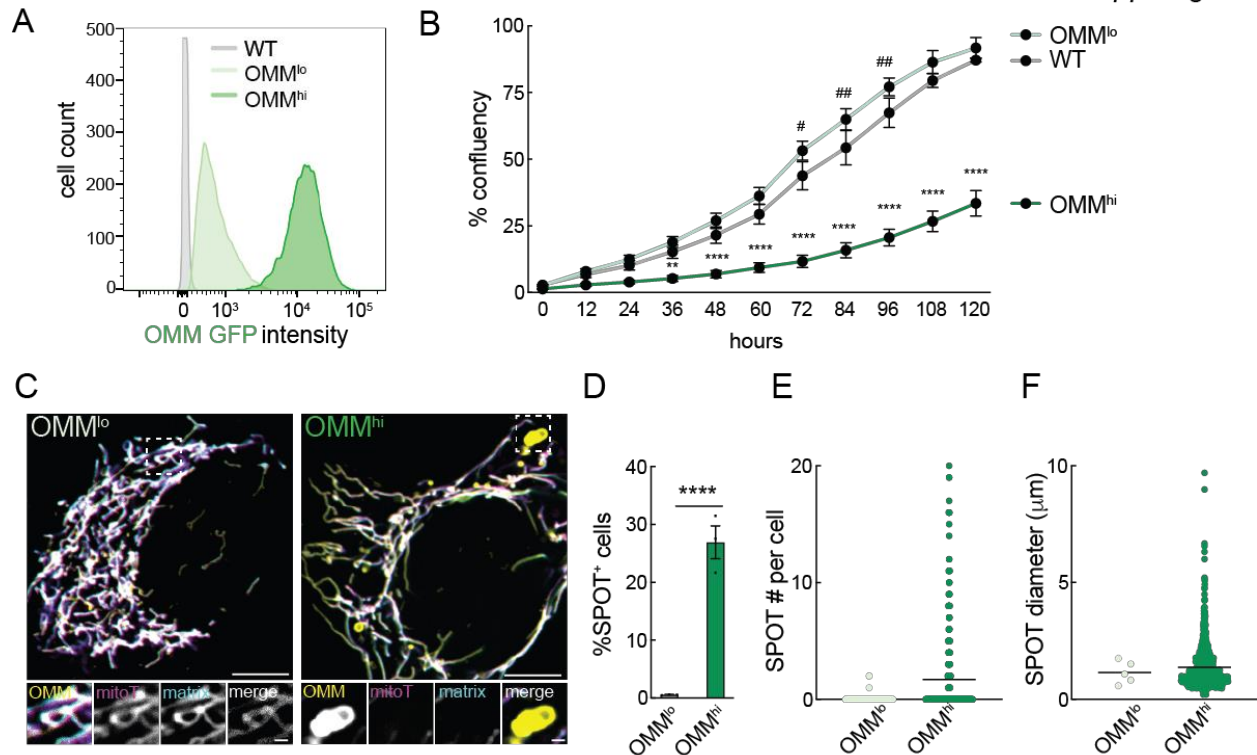


Fig. S15. The OMM is remodeled during infection-independent import stress. (A) Histograms of GFP fluorescence intensity (MFI) determined by flow cytometry analysis of U2OS cells expressing OMM-GFP and previously sorted for high (OMM^{hi}) or low (OMM^{lo}) GFP. (B) 5,000 cells of indicated line were plated and monitored for phase confluency every 12 h using the Incucyte S3 live-cell imaging system. (C) Representative live-cell images of the OMM (GFP), matrix (BFP), and indicated mitoT-labelled U2OS cell lines; scale bar, 5 μm; inset 1 μm. A SPOT is depicted in the OMM^{hi} inset panel. (D) Percentage of SPOT-positive cells in experiments as in (C); data are mean +/- SEM of >100 cells counted from 3 biological replicates; ****p<0.0001 by unpaired t-test analysis. Scatterplot with mean (E) number and (F) diameter of SPOTs in experiments as in (C) from >30 infected cells from 3 biological replicates.

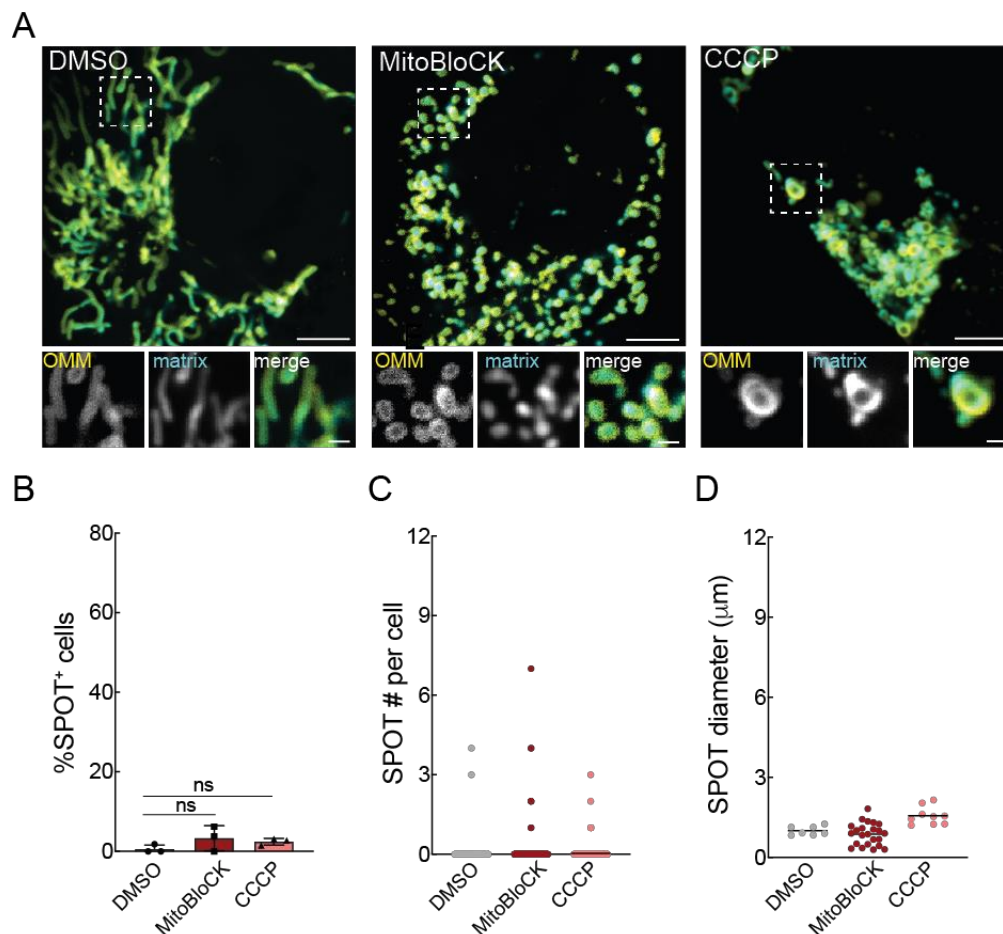


Fig. S16. MitoBloCK6 and CCCP do not induce SPOT formation.

(A) Representative live-cell images of the OMM (GFP) and matrix (BFP) in U2OS cells treated with DMSO, MitoBloCK6 (100 μ M) and CCCP (25 μ M) for 30 min; scale bar, 5 μ m; inset 1 μ m. (B) Percentage of SPOT-positive cells in experiments as in (A); data are mean \pm SEM of >100 cells counted from 3 biological replicates. Scatterplot with mean (C) number and (D) diameter of SPOTs in experiments as in (A) from >30 infected cells from 3 biological replicates.

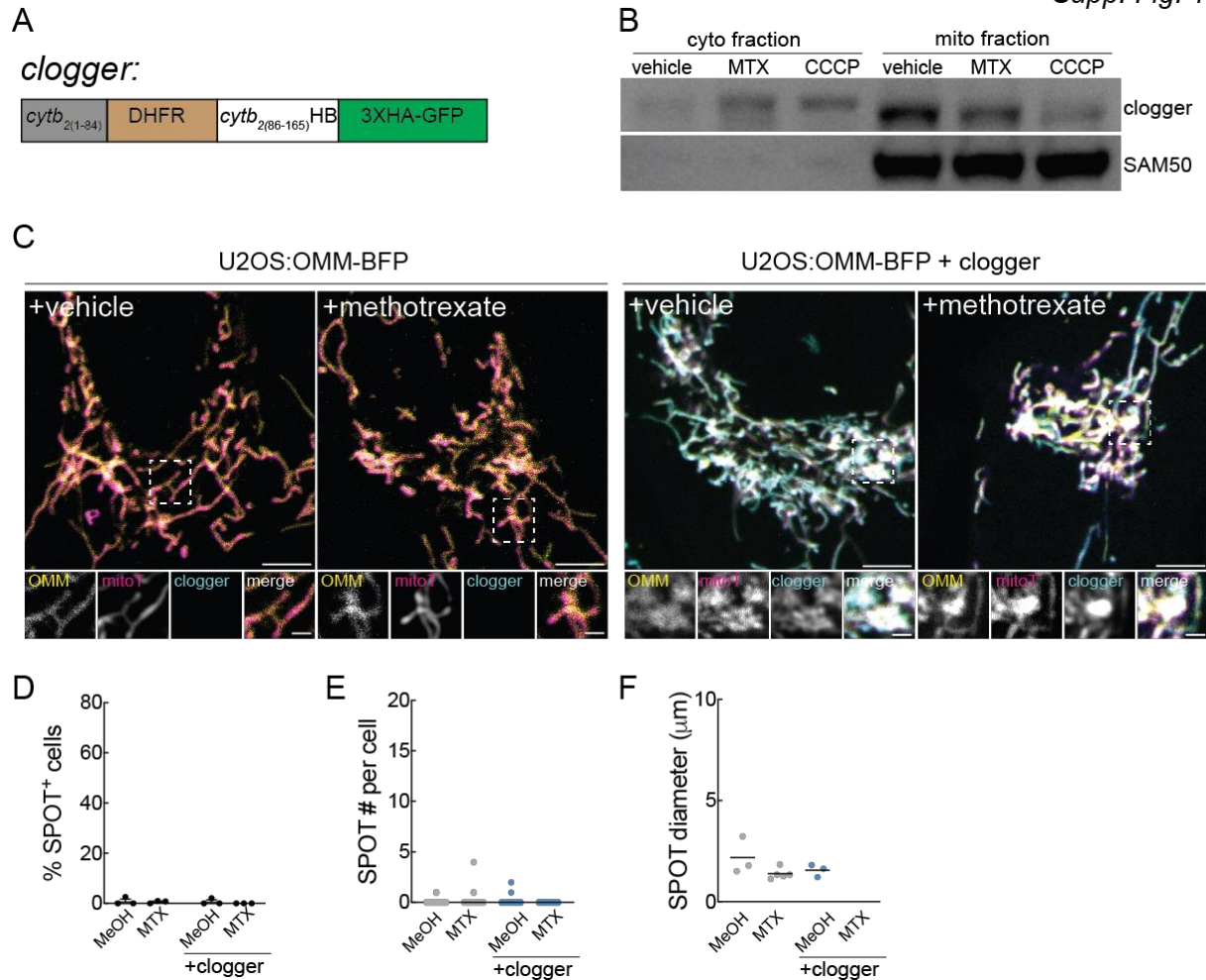


Fig. S17. Expression of an artificial clogger does not induce SPOT formation.

(A) Schematic of clogger construct: *cytb*₂₍₁₋₈₄₎; mitochondrial targeting domain, DHFR; carrier protein stabilized by methotrexate; *cytb*₂₍₈₆₋₁₆₅₎; HB; heme-binding domain. (B) Cytosolic and crude mitochondrial fractions of U2OS cells expressing the ‘clogger’ and treated for 1h as indicated (methotrexate (MTX) 20μM, CCCP 25μM), were analyzed by immunoblotting for: SAM50 ~55kDa, clogger: ~70-80 kDa (αHA) (C) Representative live-cell images of the OMM (BFP) in mitoT-treated U2OS cells +/- clogger (GFP), treated with vehicle or 20μM MTX (D) Percentage of SPOT-positive cells in experiments as in (C); data are mean +/- SEM of >100 cells counted from 3 biological replicates. Scatterplot with mean (E) number and (F) diameter of SPOTs in experiments as in (C) from >30 infected cells from 3 biological replicates.

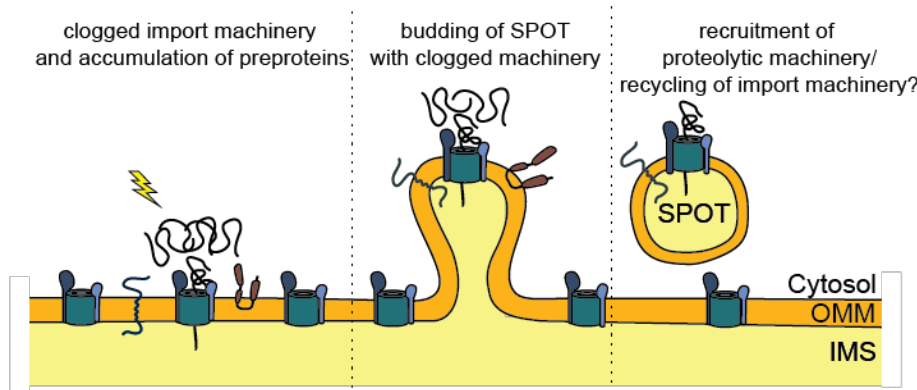


Fig. S18. Hypothetical model of SPOT formation in quality control of import machinery. Following the clogging of an OMM import machinery, misfolded precursor proteins accumulate and jeopardize the function of nearby import machinery (left panel). The formation of a SPOT, which also captures proteins in the OMM, enables the physical separation of a clogged translocase and functional import machinery (middle panel), and the subsequent targeting of SPOT localized-proteins for proteasomal degradation (or maintained on a SPOT and recycled back into the mitochondrial network at a later stage)(right panel).

References and Notes

1. L. Pernas, L. Scorrano, Mito-morphosis: Mitochondrial fusion, fission, and cristae remodeling as key mediators of cellular function. *Annu. Rev. Physiol.* **78**, 505–531 (2016).
2. S. Rath, R. Sharma, R. Gupta, T. Ast, C. Chan, T. J. Durham, R. P. Goodman, Z. Grabarek, M. E. Haas, W. H. W. Hung, P. R. Joshi, A. A. Jourdain, S. H. Kim, A. V. Kotrys, S. S. Lam, J. G. McCoy, J. D. Meisel, M. Miranda, A. Panda, A. Patgiri, R. Rogers, S. Sadre, H. Shah, O. S. Skinner, T.-L. To, M. A. Walker, H. Wang, P. S. Ward, J. Wengrod, C.-C. Yuan, S. E. Calvo, V. K. Mootha, MitoCarta3.0: An updated mitochondrial proteome now with sub-organelle localization and pathway annotations. *Nucleic Acids Res.* **49** (D1), D1541–D1547 (2021).
3. J. A. MacKenzie, R. M. Payne, Mitochondrial protein import and human health and disease. *Biochim. Biophys. Acta* **1772**, 509–523 (2007).
4. J. Song, J. M. Herrmann, T. Becker, Quality control of the mitochondrial proteome. *Nat. Rev. Mol. Cell Biol.* **22**, 54–70 (2021).
5. L. Pernas, C. Bean, J. C. Boothroyd, L. Scorrano, Mitochondria restrict growth of the intracellular parasite *Toxoplasma gondii* by limiting its uptake of fatty acids. *Cell Metab.* **27**, 886–897.e4 (2018).
6. V. Tiku, M. W. Tan, I. Dikic, Mitochondrial functions in infection and immunity. *Trends Cell Biol.* **30**, 263–275 (2020).
7. L. Pernas, Cellular metabolism in the defense against microbes. *J. Cell Sci.* **134**, jcs252023 (2021).
8. R. B. Seth, L. Sun, Z. J. Chen, Antiviral innate immunity pathways. *Cell Res.* **16**, 141–147 (2006).
9. T. Rudel, O. Kepp, V. Kozjak-Pavlovic, Interactions between bacterial pathogens and mitochondrial cell death pathways. *Nat. Rev. Microbiol.* **8**, 693–705 (2010).
10. J. G. Montoya, O. Liesenfeld, Toxoplasmosis. *Lancet* **363**, 1965–1976 (2004).
11. T. C. Medeiros, C. Mehra, L. Pernas, Contact and competition between mitochondria and microbes. *Curr. Opin. Microbiol.* **63**, 189–194 (2021).
12. M. Dumoux, R. D. Hayward, Membrane contact sites between pathogen-containing compartments and host organelles. *Biochim. Biophys. Acta* **1861** (8 Pt B), 895–899 (2016).
13. W. W. Chen, E. Freinkman, D. M. Sabatini, Rapid immunopurification of mitochondria for metabolite profiling and absolute quantification of matrix metabolites. *Nat. Protoc.* **12**, 2215–2231 (2017).
14. V. Soubannier, G.-L. McLelland, R. Zunino, E. Braschi, P. Rippstein, E. A. Fon, H. M. McBride, A vesicular transport pathway shuttles cargo from mitochondria to lysosomes. *Curr. Biol.* **22**, 135–141 (2012).
15. A. L. Hughes, C. E. Hughes, K. A. Henderson, N. Yazvenko, D. E. Gottschling, Selective sorting and destruction of mitochondrial membrane proteins in aged yeast. *eLife* **5**, e13943 (2016).

16. A. M. English, M.-H. Schuler, T. Xiao, B. Kornmann, J. M. Shaw, A. L. Hughes, ER-mitochondria contacts promote mitochondrial-derived compartment biogenesis. *J. Cell Biol.* **219**, e202002144 (2020).
17. M. H. Schuler, A. M. English, T. Xiao, T. J. Campbell, J. M. Shaw, A. L. Hughes, Mitochondrial-derived compartments facilitate cellular adaptation to amino acid stress. *Mol. Cell* **81**, 3786–3802.e13 (2021).
18. M. Neuspiel, A. C. Schauss, E. Braschi, R. Zunino, P. Rippstein, R. A. Rachubinski, M. A. Andrade-Navarro, H. M. McBride, Cargo-selected transport from the mitochondria to peroxisomes is mediated by vesicular carriers. *Curr. Biol.* **18**, 102–108 (2008).
19. M. H. Schuler, A. M. English, L. VanderMeer, J. M. Shaw, A. L. Hughes, Amino acids promote mitochondrial-derived compartment formation in mammalian cells. bioRxiv [Preprint] 23 December 2020. doi:10.1101/2020.12.23.424218.
20. G. L. McLelland, V. Soubannier, C. X. Chen, H. M. McBride, E. A. Fon, Parkin and PINK1 function in a vesicular trafficking pathway regulating mitochondrial quality control. *EMBO J.* **33**, 282–295 (2014).
21. S. R. Denison, F. Wang, N. A. Becker, B. Schüle, N. Kock, L. A. Phillips, C. Klein, D. I. Smith, Alterations in the common fragile site gene Parkin in ovarian and other cancers. *Oncogene* **22**, 8370–8378 (2003).
22. D. Matheoud, A. Sugiura, A. Bellemare-Pelletier, A. Laplante, C. Rondeau, M. Chemali, A. Fazel, J. J. Bergeron, L.-E. Trudeau, Y. Burelle, E. Gagnon, H. M. McBride, M. Desjardins, Parkinson’s disease-related proteins PINK1 and parkin repress mitochondrial antigen presentation. *Cell* **166**, 314–327 (2016).
23. R. Lundmark, S. R. Carlsson, SNX9—A prelude to vesicle release. *J. Cell Sci.* **122**, 5–11 (2009).
24. K. Todkar, L. Chikhi, V. Desjardins, F. El-Mortada, G. Pépin, M. Germain, Selective packaging of mitochondrial proteins into extracellular vesicles prevents the release of mitochondrial DAMPs. *Nat. Commun.* **12**, 1971 (2021).
25. A. P. Sinai, P. Webster, K. A. Joiner, Association of host cell endoplasmic reticulum and mitochondria with the *Toxoplasma gondii* parasitophorous vacuole membrane: A high affinity interaction. *J. Cell Sci.* **110**, 2117–2128 (1997).
26. L. Scorrano, M. A. De Matteis, S. Emr, F. Giordano, G. Hajnóczky, B. Kornmann, L. L. Lackner, T. P. Levine, L. Pellegrini, K. Reinisch, R. Rizzuto, T. Simmen, H. Stenmark, C. Ungermann, M. Schuldiner, Coming together to define membrane contact sites. *Nat. Commun.* **10**, 1287 (2019).
27. L. Pernas, Y. Adomako-Ankomah, A. J. Shastri, S. E. Ewald, M. Treeck, J. P. Boyle, J. C. Boothroyd, Toxoplasma effector MAF1 mediates recruitment of host mitochondria and impacts the host response. *PLOS Biol.* **12**, e1001845 (2014).
28. M. L. Blank, M. L. Parker, R. Ramaswamy, C. J. Powell, E. D. English, Y. Adomako-Ankomah, L. F. Pernas, S. D. Workman, J. C. Boothroyd, M. J. Boulanger, J. P. Boyle, A *Toxoplasma gondii* locus required for the direct manipulation of host mitochondria has maintained multiple ancestral functions. *Mol. Microbiol.* **108**, 519–535 (2018).

29. F. D. Kelly, B. M. Wei, A. M. Cygan, M. L. Parker, M. J. Boulanger, J. C. Boothroyd, *Toxoplasma gondii* MAF1b binds the host cell MIB complex to mediate mitochondrial association. *MSphere* **2**, e00183-17 (2017).
30. M. Suzuki, O. Danilchanka, J. J. Mekalanos, *Vibrio cholerae* T3SS effector VopE modulates mitochondrial dynamics and innate immune signaling by targeting Miro GTPases. *Cell Host Microbe* **16**, 581–591 (2014).
31. B. Mueller, E. J. Klemm, E. Spooner, J. H. Claessen, H. L. Ploegh, SEL1L nucleates a protein complex required for dislocation of misfolded glycoproteins. *Proc. Natl. Acad. Sci. U.S.A.* **105**, 12325–12330 (2008).
32. N. C. Chan, A. M. Salazar, A. H. Pham, M. J. Sweredoski, N. J. Kolawa, R. L. J. Graham, S. Hess, D. C. Chan, Broad activation of the ubiquitin-proteasome system by Parkin is critical for mitophagy. *Hum. Mol. Genet.* **20**, 1726–1737 (2011).
33. S. Nahar, A. Chowdhury, T. Ogura, M. Esaki, A AAA ATPase Cdc48 with a cofactor Ubx2 facilitates ubiquitylation of a mitochondrial fusion-promoting factor Fzo1 for proteasomal degradation. *J. Biochem.* **167**, 279–286 (2020).
34. M. K. Shaw, C. Y. He, D. S. Roos, L. G. Tilney, Proteasome inhibitors block intracellular growth and replication of *Toxoplasma gondii*. *Parasitology* **121**, 35–47 (2000).
35. M. L. Blank, J. Xia, M. M. Morcos, M. Sun, P. S. Cantrell, Y. Liu, X. Zeng, C. J. Powell, N. Yates, M. J. Boulanger, J. P. Boyle, *Toxoplasma gondii* association with host mitochondria requires key mitochondrial protein import machinery. *Proc. Natl. Acad. Sci. U.S.A.* **118**, e2013336118 (2021).
36. S. Backes, S. Hess, F. Boos, M. W. Woellhaf, S. Gödel, M. Jung, T. Mühlhaus, J. M. Herrmann, Tom70 enhances mitochondrial preprotein import efficiency by binding to internal targeting sequences. *J. Cell Biol.* **217**, 1369–1382 (2018).
37. S. Backes, Y. S. Bykov, T. Flohr, M. Räschele, J. Zhou, S. Lenhard, L. Krämer, T. Mühlhaus, C. Bibi, C. Jann, J. D. Smith, L. M. Steinmetz, D. Rapaport, Z. Storchová, M. Schuldiner, F. Boos, J. M. Herrmann, The chaperone-binding activity of the mitochondrial surface receptor Tom70 protects the cytosol against mitoprotein-induced stress. *Cell Rep.* **35**, 108936 (2021).
38. A. C. Fan, M. K. Bhangoo, J. C. Young, Hsp90 functions in the targeting and outer membrane translocation steps of Tom70-mediated mitochondrial import. *J. Biol. Chem.* **281**, 33313–33324 (2006).
39. H. Yamamoto, K. Fukui, H. Takahashi, S. Kitamura, T. Shiota, K. Terao, M. Uchida, M. Esaki, S. Nishikawa, T. Yoshihisa, K. Yamano, T. Endo, Roles of Tom70 in import of presequence-containing mitochondrial proteins. *J. Biol. Chem.* **284**, 31635–31646 (2009).
40. C. Ott, K. Ross, S. Straub, B. Thiede, M. Götz, C. Goosmann, M. Krischke, M. J. Mueller, G. Krohne, T. Rudel, V. Kozjak-Pavlovic, Sam50 functions in mitochondrial intermembrane space bridging and biogenesis of respiratory complexes. *Mol. Cell. Biol.* **32**, 1173–1188 (2012).
41. M. P. Viana, R. M. Levytskyy, R. Anand, A. S. Reichert, O. Khalimonchuk, Protease OMA1 modulates mitochondrial bioenergetics and ultrastructure through dynamic association with MICOS complex. *iScience* **24**, 102119 (2021).

42. D. V. Dabir, S. A. Hasson, K. Setoguchi, M. E. Johnson, P. Wongkongkathep, C. J. Douglas, J. Zimmerman, R. Damoiseaux, M. A. Teitell, C. M. Koehler, A small molecule inhibitor of redox-regulated protein translocation into mitochondria. *Dev. Cell* **25**, 81–92 (2013).
43. U. Bömer, M. Meijer, B. Guiard, K. Dietmeier, N. Pfanner, J. Rassow, The sorting route of cytochrome b2 branches from the general mitochondrial import pathway at the preprotein translocase of the inner membrane. *J. Biol. Chem.* **272**, 30439–30446 (1997).
44. M. Eilers, G. Schatz, Binding of a specific ligand inhibits import of a purified precursor protein into mitochondria. *Nature* **322**, 228–232 (1986).
45. K. N. Doan, A. Grevel, C. U. Mårtensson, L. Ellenrieder, N. Thornton, L.-S. Wenz, Ł. Opaliński, B. Guiard, N. Pfanner, T. Becker, The mitochondrial import complex MIM functions as main translocase for α -helical outer membrane proteins. *Cell Rep.* **31**, 107567 (2020).
46. F. Xu, W. Du, Q. Zou, Y. Wang, X. Zhang, X. Xing, Y. Li, D. Zhang, H. Wang, W. Zhang, X. Hu, X. Liu, X. Liu, S. Zhang, J. Yu, J. Fang, F. Li, Y. Zhou, T. Yue, N. Mi, H. Deng, P. Zou, X. Chen, X. Yang, L. Yu, COPII mitigates ER stress by promoting formation of ER whorls. *Cell Res.* **31**, 141–156 (2021).
47. C. U. Mårtensson, C. Priesnitz, J. Song, L. Ellenrieder, K. N. Doan, F. Boos, A. Floerchinger, N. Zufall, S. Oeljeklaus, B. Warscheid, T. Becker, Mitochondrial protein translocation-associated degradation. *Nature* **569**, 679–683 (2019).
48. I. Derré, M. Pypaert, A. Dautry-Varsat, H. Agaisse, RNAi screen in *Drosophila* cells reveals the involvement of the Tom complex in *Chlamydia* infection. *PLoS Pathog.* **3**, 1446–1458 (2007).
49. G. López-Doménech, C. Covill-Cooke, D. Ivankovic, E. F. Halff, D. F. Sheehan, R. Norkett, N. Birsa, J. T. Kittler, Miro proteins coordinate microtubule- and actin-dependent mitochondrial transport and distribution. *EMBO J.* **37**, 321–336 (2018).
50. N. Ishihara, M. Nomura, A. Jofuku, H. Kato, S. O. Suzuki, K. Masuda, H. Otera, Y. Nakanishi, I. Nonaka, Y. Goto, N. Taguchi, H. Morinaga, M. Maeda, R. Takayanagi, S. Yokota, K. Mihara, Mitochondrial fission factor Drp1 is essential for embryonic development and synapse formation in mice. *Nat. Cell Biol.* **11**, 958–966 (2009).
51. D. Mumberg, R. Müller, M. Funk, Yeast vectors for the controlled expression of heterologous proteins in different genetic backgrounds. *Gene* **156**, 119–122 (1995).
52. C. Priesnitz, N. Pfanner, T. Becker, Studying protein import into mitochondria. *Methods Cell Biol.* **155**, 45–79 (2020).
53. L. M. Murschall, E. Peker, T. MacVicar, T. Langer, J. Riemer, Protein import assay into mitochondria isolated from human cells. *Bio Protoc.* **11**, e4057 (2021).
54. T. Becker, L.-S. Wenz, V. Krüger, W. Lehmann, J. M. Müller, L. Goroncy, N. Zufall, T. Lithgow, B. Guiard, A. Chacinska, R. Wagner, C. Meisinger, N. Pfanner, The mitochondrial import protein Mim1 promotes biogenesis of multispanning outer membrane proteins. *J. Cell Biol.* **194**, 387–395 (2011).
55. X. Li, T. Franz, I. Atanassov, T. Colby, Step-by-step sample preparation of proteins for mass spectrometric analysis. *Methods Mol. Biol.* **2261**, 13–23 (2021).

56. J. Cox, M. Mann, MaxQuant enables high peptide identification rates, individualized p.p.b.-range mass accuracies and proteome-wide protein quantification. *Nat. Biotechnol.* **26**, 1367–1372 (2008).
57. J. Cox, N. Neuhauser, A. Michalski, R. A. Scheltema, J. V. Olsen, M. Mann, Andromeda: A peptide search engine integrated into the MaxQuant environment. *J. Proteome Res.* **10**, 1794–1805 (2011).
58. H. Wickham, M. Averick, J. Bryan, W. Chang, L. D. A. McGowan, R. François, G. Grolemund, A. Hayes, L. Henry, J. Hester, M. Kuhn, T. L. Pedersen, E. Miller, S. M. Bache, K. Müller, J. Ooms, D. Robinson, D. P. Seidel, V. Spinu, K. Takahashi, D. Vaughan, C. Wilke, K. Woo, H. Yutani, Welcome to the tidyverse. *J. Open Source Softw.* **4**, 1686 (2019).
59. R. C. Team, R: A language and environment for statistical computing (R Foundation for Statistical Computing, 2017).
60. M. E. Ritchie, B. Phipson, D. Wu, Y. Hu, C. W. Law, W. Shi, G. K. Smyth, limma powers differential expression analyses for RNA-sequencing and microarray studies. *Nucleic Acids Res.* **43**, e47 (2015).
61. A. Iqbal, C. Duitama, F. Metge, D. Rosskpp, J. Boucas, Flaski. Zenodo (2021) doi:10.5281/zenodo.4890981.
62. Y. Perez-Riverol, A. Csordas, J. Bai, M. Bernal-Llinares, S. Hewapathirana, D. J. Kundu, A. Inuganti, J. Griss, G. Mayer, M. Eisenacher, E. Pérez, J. Uszkoreit, J. Pfeuffer, T. Sachsenberg, S. Yilmaz, S. Tiwary, J. Cox, E. Audain, M. Walzer, A. F. Jarnuczak, T. Ternent, A. Brazma, J. A. Vizcaíno, The PRIDE database and related tools and resources in 2019: Improving support for quantification data. *Nucleic Acids Res.* **47** (D1), D442–D450 (2019).

5. Discussion

In our study, we found that infection stress linked to the OMM leads to the formation of SPOTs in a manner dependent on the interaction between the parasite effector TgMAF1 and the host mitochondrial receptor TOM70. The stable expression of TOM70 is required for SPOTs formation and confers a growth advantage of *Toxoplasma*, whereas the host mitochondria perform the defense against *Toxoplasma* by limiting its uptake of fatty acid at an early stage [11]. These different effects of host mitochondria on *Toxoplasma* growth and proliferation suggest that host mitochondria defend against intracellular microbes, but that their defenses can be counteracted by *Toxoplasma*.

Several outstanding questions remain, the first of which is how is the function of the host receptor TOM70 affected? TOM70 is significantly enrichment at the interface of PVM-OMM and decreased in mitochondria that are not associated with the PV during infection. Our proteomic analysis of mitochondria from infected cells revealed that TgMAF1 drives a loss of TOM70-dependent substrates, but does not affect chaperone association with mitochondria during infection. How does TOM70 structurally recognize TgMAF1? Does the sequestration of TOM70 only at PV-associated mitochondria impair TOM70-dependent import independent of the TgMAF1-TOM70 interaction? To address this question, a proteomic comparison of PVM-associated and unassociated mitochondria is required. Molecularly, the association of PVM and host mitochondria through TOM70 requires the three C-terminus residences of TgMAF1.

The second question regards the heterogeneity of SPOT formation — why do only some cells form SPOTs? SPOTs form in around 60-70% of infected cells. Although in SPOT-negative cells TOM70 is sequestered by TgMAF1 at the interface of OMM and PVM, why they lack SPOTs, and whether they ever form a SPOT during infection is unclear. A simple explanation could be that our analyses were limited to one z-plane, and if we had performed z-stacks for all cells analyzed, SPOTs may have been visible. Alternatively, SPOT formation could additionally depend on host factors that are differentially expressed in cells during infection. In MEFs cells expressing of TgMAF1,

the SPOTs formation is insufficiently induced, though it localizes on and trigger the mitochondria to be fragmented. A possible explanation is that the natural TgMAF1 is PVM-integral protein, while artificially expressed TgMAF1 is cytosolic and OMM-peripheral protein [173]. Moreover, infection of *N. caninum* with the expression of TgMAF1 sufficiently initiates the occurrence of host mitochondrial association with PVM [172], whether SPOTs formation is unknown. These different scenarios imply the functional OMM-targeting TgMAF1 and subsequently OMM stress are both essential for SPOTs formation.

Next, SPOTs formation is also triggered by the overexpression of an OMM-targeted protein (OMM-GFP). This poses the question of whether differences exist in the underlying mechanism of OMM remodeling during and independently of *Toxoplasma* infection? TOM70-deficient cells do not exhibit SPOTs in uninfected cells and during infection, which suggests that SPOTs formation is not caused by a loss of TOM70 function. Both TgMAF1 and OMM-GFP co-immunoprecipitate SAM50. SAM50 is a key regulator of the integrity of the MIB complex that retains OMM-IMM contact sites and cristae structure. SPOTs or SPOT-like structures form when the binding of SAM50 to the MIB components MIC60 and MIC19 is impaired by TgMAF1 during infection, or by the knockdown of SAM50 or MIC60 during infection and independent infection. These results suggest that the stability of the MIB complex are plays a key role in the SPOTs formation. However, it remains yet unclear if the molecular mechanisms triggered in the scenarios are the same.

How does the sorting nexin 9 (SNX9) promote SPOT-shedding? SNX9 is a multifunctional endocytic accessory protein involved in clathrin-mediated endocytosis, membrane trafficking, and remodeling of the cooperation with the actin-network. Recently, SNX9 was found to be required for the formation of MDVs regulated by Parkin in the oxidative stress[177]. This was consistent with our finding that SNX9 knockdown inhibited SPOT formation. However, SPOTs are different from MDVs in shape, size and motility, and SPOTs do not contain OGDH which is the marker of SNX9-mediated MDVs. Moreover, we did not observe recruitment of SNX9 on

mitochondria by immunofluorescence assay during *Toxoplasma* infection (data not shown), compared with the oxidative stress induced SNX9-enriched dots on mitochondria during the MDVs formation (reference?). Further investigation of the role of SNX9 in the SPOT-shedding will be helpful to understand the effect of SPOTs on mitochondrial health and parasite viability during infection.

SPOTs are highly dynamic in shape, size, and motility. Most SPOTs appear spherical and motile and have a diameter of around 1 μm at early stages. At late stages, SPOTs are dynamic (shape from spherical to tubular, size from 1-10 μm), have more complicated structures (from single SPOT to multi-SPOTs body), are motile, and sequester OMM-GFP and other endogenous OMM proteins. Given that MFN1/2 are highly enriched on the SPOTs, it is probable that SPOTs are able to fuse. MIRO1/2, which mediate the interaction of mitochondria with microtubules, are also on SPOTs and thus may promote SPOT motility. A question that arises is how SPOTs choose their cargo. OMM-GFP, an artificial fusion protein composed of OMM-targeting α -helical TM domain and cytosolic exposed GFP, is enriched on the SPOTs, and essentially all other OMM proteins we have detected localize to SPOTs. This suggests that SPOTs cargo is not selective. If so, an expectation is that all α -helical OMM proteins, partial or all β -barrel proteins, are translocated to SPOTs. If so, the following question is why the OMM-GFP intensity on SPOTs is dramatically higher than it on the cytosolic mitochondria? Also, is the composition of SPOT cargo the same during infection and independently of infection. An unbiased and high-resolution proteomic analysis of isolated SPOTs induced by different stresses will help address these questions.

Recently, a study indicates that high-confidence cargoes of MDVs in the COS-7 cells are delivered as fully assembled complexes to multivesicular bodies (MVBs) for mitochondrial quality control, such as the TOM complex, SAM50 (with MTX1 and DNAJC11), and all other β -barrel proteins [127]. This raises the question of whether cargo that ends up on SPOTs is also functional? For example, do SPOTs-localized MFN1/2 and MIRO1/2 mediate SPOTs dynamics and motility respectively? Can

SPOTs-localized TOM70 or TOM20 still bind to chaperones and import mitochondrial precursors? What is the fate of SPOTs cargo during infection? Considering their big size and formation dependent and independent of infection, the cell likely has a way to deal with or use SPOTs. One possibility is their extracellular export, or fusion with other organelles, such as peroxisomes or MVBs, as is known to occur with MDVs[132][178].

Another question that arises is whether the shedding of membrane is unique to mitochondria. Interestingly, membrane structures that are highly similar to SPOTs in morphology have been shown to emerge from the ER during import stress and infection and are termed ER whorls. ER whorls are highly dynamic: dynamic (shape from spherical to tubular, size up to 10 μm), complicated (from single whorls to multi-whorls body), motile (contact with other ER whorls and reticular ER), exhibit a high intensity of GFP-tagged ER-resident proteins such as Sec61B, a component of ER import translocon. The ER whorls are induced by Herpes simplex virus (HSV) infection, and the overexpression of GFP-tagged ER-resident proteins [179], [180]. What are the differences and commonalities between SPOTs and ER whorls? Do they share the same fate as both are organelle-derived structure?

Do other pathogens that induce host mitochondrial stress lead to SPOTs formation? *Toxoplasma* MAF1 coopts the host import receptor TOM70 to exploit SAM50, which leads to the import-related stress and SPOTs formation. Many pathogens have purported factors that enable pathogen binding to host mitochondrial import machinery. The SARS-CoV-2 protein Orf9b interacts with cytosolic segment of human TOM70 through its C-terminal deep “pocket” structure, leading to mitochondrial fusion and inactivation of type-I IFN immune response [150]. Host mitochondrial association with the *Chlamydia spp.* vacuole is mediated by TOM complex components and depletion of either Tom40 or Tom22 leads to the reduced *Chlamydia caviae* infection [181]. Other pathogens have unidentified factors on their vacuole membrane binding to the host mitochondria, such as *Legionella pneumophila*, *Simkania negevensis*, *Plasmodium falciparum*, and so on. Additionally, infection is known to induce import stress. For

example, *Anaplasma phagocytophilum* Ats-1 can be imported into mitochondria where it stabilizes membrane potential to prevent Bax docking on the mitochondria and apoptosis [182]. *Neisseria gonorrhoeae* PorB porin, an ATP-binding β -barrel protein, can be imported into mitochondria through the TOM complex and integrated into IMM, leading to the breakdown of the mitochondrial membrane potential and the loss of cristae structures [183]. These pathogens manipulate mitochondrial functions and trigger mitochondrial stresses, but whether SPOT formation occurs during these infections is not known.

Overall, our study of the interaction between the human parasite *Toxoplasma* and host mitochondria led to the discovery of a mechanism by which the OMM is remodeled: the formation of SPOTs. Despite many open questions about the SPOTs, these findings shed light on a potentially broader mechanism of organellar response to import-related stress and reveal a strategy by which diverse pathogens may disrupt mitochondrial function.

6. Reference

- [1] ANNESLEY, SARAH J. ; FISHER, PAUL R.: Mitochondria in Health and Disease. In: *Cells* vol. 8 (2019), Nr. 7, p. 680
- [2] PFANNER, NIKOLAUS ; WARSCHIED, BETTINA ; WIEDEMANN, NILS: Mitochondrial proteins: from biogenesis to functional networks. In: *Nature Reviews Molecular Cell Biology* vol. 20 (2019), Nr. 5, pp. 267–284
- [3] WIEDEMANN, NILS ; PFANNER, NIKOLAUS: Mitochondrial Machineries for Protein Import and Assembly. In: *Annual review of biochemistry* vol. 86 (2017), Nr. 1, pp. 685–714
- [4] SCHEFFLER, I.E.: *Mitochondria* : John Wiley & Sons, 2011
— ISBN 9781118209851
- [5] SAGAN, L: On the origin of mitosing cells. In: *Journal of theoretical biology* vol. 14 (1967), Nr. 3, pp. 255–74
- [6] MARÉCHAL, ERIC: Primary Endosymbiosis: Emergence of the Primary Chloroplast and the Chromatophore, Two Independent Events. In: *Methods in molecular biology (Clifton, N.J.)* vol. 1829 (2018), pp. 3–16
- [7] RANGARAJU, VIDHYA ; LAUTERBACH, MARCEL ; SCHUMAN, ERIN M: Spatially Stable Mitochondrial Compartments Fuel Local Translation during Plasticity. In: *Cell* vol. 176 (2019), Nr. 1–2, pp. 73-84.e15
- [8] ROCA-PORTOLES, ALBA ; TAIT, STEPHEN W G: Mitochondrial quality control: from molecule to organelle. In: *Cellular and Molecular Life Sciences* vol. 78 (2021), Nr. 8, pp. 3853–3866
- [9] PERNAS, LENA ; SCORRANO, LUCA: Mito-Morphosis: Mitochondrial Fusion, Fission, and Cristae Remodeling as Key Mediators of Cellular Function. In: *Annual review of physiology* vol. 78 (2015), Nr. 1, pp. 505–31
- [10] POPOV, LUCIA-DOINA: Mitochondrial biogenesis: An update. In: *Journal of cellular and molecular medicine* vol. 24 (2020), Nr. 9, pp. 4892–4899
- [11] PERNAS, LENA ; BEAN, CAMILLA ; BOOTHROYD, JOHN C. ; SCORRANO, LUCA: Mitochondria Restrict Growth of the Intracellular Parasite *Toxoplasma gondii* by Limiting Its Uptake of Fatty Acids. In: *Cell Metabolism* vol. 27 (2018), Nr. 4, pp. 886-897.e4

- [12] KREBS, HANS ADOLF: The citric acid cycle and the Szent-Györgyi cycle in pigeon breast muscle. In: *Biochemical Journal* vol. 34 (1940), Nr. 5, pp. 775–779
- [13] KENNEDY, E P ; LEHNINGER, A L: Oxidation of fatty acids and tricarboxylic acid cycle intermediates by isolated rat liver mitochondria. In: *The Journal of biological chemistry* vol. 179 (1949), Nr. 2, pp. 957–72
- [14] MITCHELL, PETER: Coupling of Phosphorylation to Electron and Hydrogen Transfer by a Chemi-Osmotic type of Mechanism. In: *Nature* vol. 191 (1961), Nr. 4784, pp. 144–148
- [15] FIORILLO, MARCO ; SCATENA, CRISTIAN ; NACCARATO, ANTONIO GIUSEPPE ; SOTGIA, FEDERICA ; LISANTI, MICHAEL P.: Bedaquiline, an FDA-approved drug, inhibits mitochondrial ATP production and metastasis in vivo, by targeting the gamma subunit (ATP5F1C) of the ATP synthase. In: *Cell Death and Differentiation* vol. 28 (2021), Nr. 9, pp. 2797–2817
- [16] BULTHUIS, ELIANNE P. ; ADJOBHO-HERMANS, MEREL J.W. ; WILLEMS, PETER H.G.M. ; KOOPMAN, WERNER J.H.: Mitochondrial Morphofunction in Mammalian Cells. In: *Antioxidants & Redox Signaling* vol. 30 (2019), Nr. 18, pp. 2066–2109
- [17] KOOPMAN, WERNER J H ; WILLEMS, PETER H G M ; SMEITINK, JAN A M: Monogenic mitochondrial disorders. In: *The New England journal of medicine* vol. 366 (2012), Nr. 12, pp. 1132–41
- [18] FIEDORCZUK, KAROL ; LETTS, JAMES A. ; DEGLIESPOSTI, GIANLUCA ; KASZUBA, KAROL ; SKEHEL, MARK ; SAZANOV, LEONID A.: Atomic structure of the entire mammalian mitochondrial complex I. In: *Nature* vol. 538 (2016), Nr. 7625, pp. 406–410
- [19] KAMPJUT, DOMEN ; SAZANOV, LEONID A.: Structure of respiratory complex I – An emerging blueprint for the mechanism. In: *Current Opinion in Structural Biology* vol. 74 (2022), p. 102350
- [20] CHUNG, INJAE ; WRIGHT, JOHN J. ; BRIDGES, HANNAH R. ; IVANOV, BOZHIDAR S. ; BINER, OLIVIER ; PEREIRA, CAROLINE S. ; ARANTES, GUILHERME M. ; HIRST, JUDY: Cryo-EM structures define ubiquinone-10 binding to mitochondrial complex I and conformational transitions accompanying Q-site occupancy. In: *Nature Communications* vol. 13 (2022), Nr. 1, p. 2758
- [21] STEFANATOS, RHODA ; SANZ, ALBERTO: Mitochondrial complex I: A central regulator of the aging process. In: *Cell Cycle* vol. 10 (2011), Nr. 10, pp. 1528–1532

- [22] URRA, FÉLIX A. ; MUÑOZ, FELIPE ; LOVY, ALENKA ; CÁRDENAS, CÉSAR: The Mitochondrial Complex(I)ty of Cancer. In: *Frontiers in Oncology* vol. 7 (2017), p. 118
- [23] BEZAWORK-GELETA, AYENACHEW ; ROHLENA, JAKUB ; DONG, LANFENG ; PACAK, KAREL ; NEUZIL, JIRI: Mitochondrial Complex II: At the Crossroads. In: *Trends in Biochemical Sciences* vol. 42 (2017), Nr. 4, pp. 312–325
- [24] ZHAO, RU-ZHOU ; JIANG, SHUAI ; ZHANG, LIN ; YU, ZHI-BIN: Mitochondrial electron transport chain, ROS generation and uncoupling (Review). In: *International Journal of Molecular Medicine* vol. 44 (2019), Nr. 1, pp. 3–15
- [25] VERCELLINO, IRENE ; SAZANOV, LEONID A.: The assembly, regulation and function of the mitochondrial respiratory chain. In: *Nature Reviews Molecular Cell Biology* vol. 23 (2022), Nr. 2, pp. 141–161
- [26] KLUCKOVA, KATARINA ; BEZAWORK-GELETA, AYANACHEW ; ROHLENA, JAKUB ; DONG, LANFENG ; NEUZIL, JIRI: Mitochondrial complex II, a novel target for anti-cancer agents. In: *Biochimica et Biophysica Acta (BBA) - Bioenergetics* vol. 1827 (2013), Nr. 5, pp. 552–564
- [27] SVERDLOV, AARON L. ; ELEZABY, ALY ; BEHRING, JESSICA B. ; BACHSCHMID, MARKUS M. ; LUPTAK, IVAN ; TU, VIVIAN H. ; SIWIK, DEBORAH A. ; MILLER, EDWARD J. ; ET AL.: High fat, high sucrose diet causes cardiac mitochondrial dysfunction due in part to oxidative post-translational modification of mitochondrial complex II. In: *Journal of Molecular and Cellular Cardiology* vol. 78 (2015), pp. 165–173
- [28] ORR, ADAM L. ; VARGAS, LEONARDO ; TURK, CAROLINA N. ; BAATEN, JANINE E. ; MATZEN, JASON T. ; DARDOV, VICTORIA J. ; ATTLE, STEPHEN J. ; LI, JING ; ET AL.: Suppressors of superoxide production from mitochondrial complex III. In: *Nature chemical biology* vol. 11 (2015), Nr. 11, pp. 834–836
- [29] WEINBERG, SAMUEL E. ; SINGER, BENJAMIN D. ; STEINERT, ELIZABETH M. ; MARTINEZ, CARLOS A. ; MEHTA, MANAN M. ; MARTÍNEZ-REYES, INMACULADA ; GAO, PENG ; HELMIN, KATHRYN A. ; ET AL.: Mitochondrial complex III is essential for suppressive function of regulatory T cells. In: *Nature* vol. 565 (2019), Nr. 7740, pp. 495–499
- [30] DIEBOLD, LAUREN P. ; GIL, HYE A JIN ; GAO, PENG ; MARTINEZ, CARLOS A. ; WEINBERG, SAMUEL E. ; CHANDEL, NAVDEEP S.: Mitochondrial complex III is necessary for endothelial cell proliferation during angiogenesis. In: *Nature Metabolism* vol. 1 (2019), Nr. 1, pp. 158–171

- [31] KADENBACH, BERNHARD: Complex IV – The regulatory center of mitochondrial oxidative phosphorylation. In: *Mitochondrion* vol. 58 (2021), pp. 296–302
- [32] GIORGIO, VALENTINA ; STOCKUM, SOPHIA VON ; ANTONIEL, MANUELA ; FABBRO, ASTRID ; FOGOLARI, FEDERICO ; FORTE, MICHAEL ; GLICK, GARY D. ; PETRONILLI, VALERIA ; ET AL.: Dimers of mitochondrial ATP synthase form the permeability transition pore. In: *Proceedings of the National Academy of Sciences* vol. 110 (2013), Nr. 15, pp. 5887–5892
- [33] PALLAFACCHINA, GIORGIA ; ZANIN, SOFIA ; RIZZUTO, ROSARIO: Recent advances in the molecular mechanism of mitochondrial calcium uptake. In: *F1000Research* vol. 7 (2018), p. F1000 Faculty Rev-1858
- [34] BORST, PIET: The malate–aspartate shuttle (Borst cycle): How it started and developed into a major metabolic pathway. In: *IUBMB Life* vol. 72 (2020), Nr. 11, pp. 2241–2259
- [35] MARTÍNEZ-REYES, INMACULADA ; CHANDEL, NAVDEEP S.: Mitochondrial TCA cycle metabolites control physiology and disease. In: *Nature Communications* vol. 11 (2020), Nr. 1, p. 102
- [36] SPINELLI, JESSICA B. ; HAIGIS, MARCIA C.: The multifaceted contributions of mitochondria to cellular metabolism. In: *Nature Cell Biology* vol. 20 (2018), Nr. 7, pp. 745–754
- [37] TUMANOV, SERGEY ; BULUSU, VINAY ; KAMPHORST, JURRE J.: Chapter Six Analysis of Fatty Acid Metabolism Using Stable Isotope Tracers and Mass Spectrometry. In: *Methods in Enzymology* vol. 561 (2015), pp. 197–217
- [38] GUDA, PURNIMA ; GUDA, CHITTIBABU ; SUBRAMANIAM, SHANKAR: Reconstruction of Pathways Associated with Amino Acid Metabolism in Human Mitochondria. In: *Genomics, Proteomics & Bioinformatics* vol. 5 (2007), Nr. 3–4, pp. 166–176
- [39] DUCKER, GREGORY S ; RABINOWITZ, JOSHUA D: One-Carbon Metabolism in Health and Disease. In: *Cell Metabolism* vol. 25 (2017), Nr. 1, pp. 27–42
- [40] MONTI, MICHELE ; GUIDUCCI, GIULIA ; PAONE, ALESSIO ; RINALDO, SERENA ; GIARDINA, GIORGIO ; LIBERATI, FRANCESCA ROMANA ; CUTRUZZOLÁ, FRANCESCA ; TARTAGLIA, GIAN GAETANO: Modelling of SHMT1 riboregulation predicts dynamic changes of serine and glycine levels across cellular compartments. In: *Computational and structural biotechnology journal* vol. 19 (2021), pp. 3034–3041

- [41] BEN-SAHRA, ISSAM ; HOXHAJ, GERTA ; RICOULT, STÉPHANE J. H. ; ASARA, JOHN M. ; MANNING, BRENDAN D.: mTORC1 induces purine synthesis through control of the mitochondrial tetrahydrofolate cycle. In: *Science* vol. 351 (2016), Nr. 6274, pp. 728–733
- [42] MEI-JIAO, GONG ; SHI-FANG, LI ; YAN-YAN, CHANG ; JUN-JUN, SHAO ; YUE-FENG, SUN ; TING-TING, REN ; YONG-GUANG, ZHANG ; HUI-YUN, CHANG: Antiviral effects of selected IMPDH and DHODH inhibitors against foot and mouth disease virus. In: *Biomedicine & pharmacotherapy = Biomedecine & pharmacotherapie* vol. 118 (2019), p. 109305
- [43] BROWN, KRISTIN K. ; SPINELLI, JESSICA B. ; ASARA, JOHN M. ; TOKER, ALEX: Adaptive Reprogramming of De Novo Pyrimidine Synthesis Is a Metabolic Vulnerability in Triple-Negative Breast Cancer. In: *Cancer Discovery* vol. 7 (2017), Nr. 4, pp. 391–399
- [44] CHENG, XIANRUI ; FERRELL, JAMES E: Apoptosis propagates through the cytoplasm as trigger waves. In: *Science* vol. 361 (2018), Nr. 6402, pp. 607–612
- [45] RADUCKA-JASZUL, OLGA ; BOGUSŁAWSKA, DŻAMILA M ; JĘDRUCHNIEWICZ, NATALIA ; SIKORSKI, ALEKSANDER F: Role of Extrinsic Apoptotic Signaling Pathway during Definitive Erythropoiesis in Normal Patients and in Patients with β -Thalassemia. In: *International Journal of Molecular Sciences* vol. 21 (2020), Nr. 9, p. 3325
- [46] LI, LU ; TONG, AN ; ZHANG, QIANGSHENG ; WEI, YUQUAN ; WEI, XIAWEI: The molecular mechanisms of MLKL-dependent and MLKL-independent necrosis. In: *Journal of Molecular Cell Biology* vol. 13 (2020), Nr. 1, pp. 3–14
- [47] ZHANG, YINGYING ; SU, SHENG SEAN ; ZHAO, SHUBO ; YANG, ZHENTAO ; ZHONG, CHUAN-QI ; CHEN, XIN ; CAI, QIXU ; YANG, ZHANG-HUA ; ET AL.: RIP1 autophosphorylation is promoted by mitochondrial ROS and is essential for RIP3 recruitment into necrosome. In: *Nature Communications* vol. 8 (2017), Nr. 1, p. 14329
- [48] YU, PIAN ; ZHANG, XU ; LIU, NIAN ; TANG, LING ; PENG, CONG ; CHEN, XIANG: Pyroptosis: mechanisms and diseases. In: *Signal Transduction and Targeted Therapy* vol. 6 (2021), Nr. 1, p. 128
- [49] DIXON, SCOTT J ; LEMBERG, KATHRYN M ; LAMPRECHT, MICHAEL R ; SKOUTA, RACHID ; ZAITSEV, ELEINA M ; GLEASON, CAROLINE E ; PATEL, DARPAN N ; BAUER, ANDRAS J ; ET AL.: Ferroptosis: An Iron-Dependent Form of Nonapoptotic Cell Death. In: *Cell* vol. 149 (2012), Nr. 5, pp. 1060–1072

- [50] HU, PING ; WU, TONG ; FAN, WENPEI ; CHEN, LEI ; LIU, YANYAN ; NI, DALONG ; BU, WENBO ; SHI, JIANLIN: Near infrared-assisted Fenton reaction for tumor-specific and mitochondrial DNA-targeted photochemotherapy. In: *Biomaterials* vol. 141 (2017), pp. 86–95
- [51] MEDZHITOV, RUSLAN: Innate immunity: quo vadis? In: *Nature Immunology* vol. 11 (2010), Nr. 7, pp. 551–553
- [52] REN, ZHIHUA ; DING, TING ; ZUO, ZHICAI ; XU, ZHIWEN ; DENG, JUNLIANG ; WEI, ZHANYONG: Regulation of MAVS Expression and Signaling Function in the Antiviral Innate Immune Response. In: *Frontiers in Immunology* vol. 11 (2020), p. 1030
- [53] WENCESLAU, CAMILLA F ; MCCARTHY, CAMERON G ; WEBB, R CLINTON: Formyl Peptide Receptor Activation Elicits Endothelial Cell Contraction and Vascular Leakage. In: *Frontiers in Immunology* vol. 7 (2016), p. 297
- [54] IYER, SHANKAR S. ; HE, QIONG ; JANCZY, JOHN R. ; ELLIOTT, ERIC I. ; ZHONG, ZHENYU ; OLIVIER, ALICIA K. ; SADLER, JEFFREY J. ; KNEPPER-ADRIAN, VICKIE ; ET AL.: Mitochondrial Cardiolipin Is Required for Nlrp3 Inflammasome Activation. In: *Immunity* vol. 39 (2013), Nr. 2, pp. 311–323
- [55] SHIMADA, KENICHI ; CROTHER, TIMOTHY R. ; KARLIN, JUSTIN ; DAGVADORJ, JARGALSAIKHAN ; CHIBA, NORIKA ; CHEN, SHUANG ; RAMANUJAN, V. KRISHNAN ; WOLF, ANDREA J. ; ET AL.: Oxidized Mitochondrial DNA Activates the NLRP3 Inflammasome during Apoptosis. In: *Immunity* vol. 36 (2012), Nr. 3, pp. 401–414
- [56] COLLINS, L. VINCENT ; HAJIZADEH, SHAHIN ; HOLME, ELISABETH ; JONSSON, ING-MARIE ; TARKOWSKI, ANDREJ: Endogenously oxidized mitochondrial DNA induces in vivo and in vitro inflammatory responses. In: *Journal of Leukocyte Biology* vol. 75 (2004), Nr. 6, pp. 995–1000
- [57] HAMANAKA, ROBERT B. ; CHANDEL, NAVDEEP S.: Mitochondrial reactive oxygen species regulate cellular signaling and dictate biological outcomes. In: *Trends in Biochemical Sciences* vol. 35 (2010), Nr. 9, pp. 505–513
- [58] NUNNARI, JODI ; SUOMALAINEN, ANU: Mitochondria: In Sickness and in Health. In: *Cell* vol. 148 (2012), Nr. 6, pp. 1145–1159
- [59] YOON, YISANG ; PITTS, KELLY R ; MCNIVEN, MARK A: Mammalian Dynamin-like Protein DLP1 Tubulates Membranes. In: *Molecular Biology of the Cell* vol. 12 (2001), Nr. 9, pp. 2894–2905

- [60] FRIEDMAN, JONATHAN R ; LACKNER, LAURA L ; WEST, MATTHEW ;
DIBENEDETTO, JARED R ; NUNNARI, JODI ; VOELTZ, GIA K: ER Tubules Mark Sites
of Mitochondrial Division. In: *Science* vol. 334 (2011), Nr. 6054, pp. 358–362
- [61] PRUDENT, JULIEN ; MCBRIDE, HEIDI M: Mitochondrial Dynamics: ER Actin
Tightens the Drp1 Noose. In: *Current Biology* vol. 26 (2016), Nr. 5, pp. R207–
R209
- [62] YU, RONG ; LIU, TONG ; NING, CHENFEI ; TAN, FEI ; JIN, SHAO-BO ; LENDAHL,
URBAN ; ZHAO, JIAN ; NISTÉR, MONICA: The phosphorylation status of Ser-637 in
dynamamin-related protein 1 (Drp1) does not determine Drp1 recruitment to
mitochondria. In: *Journal of Biological Chemistry* vol. 294 (2019), Nr. 46,
pp. 17262–17277
- [63] CHANG, CHUANG-RUNG ; BLACKSTONE, CRAIG: Cyclic AMP-dependent Protein
Kinase Phosphorylation of Drp1 Regulates Its GTPase Activity and Mitochondrial
Morphology. In: *Journal of Biological Chemistry* vol. 282 (2007), Nr. 30,
pp. 21583–21587
- [64] WONG, YVETTE C. ; YSSELSTEIN, DANIEL ; KRAINIC, DIMITRI: Mitochondria–
lysosome contacts regulate mitochondrial fission via RAB7 GTP hydrolysis. In:
Nature vol. 554 (2018), Nr. 7692, pp. 382–386
- [65] CAO, YU-LU ; MENG, SHUXIA ; CHEN, YANG ; FENG, JIAN-XIONG ; GU, DONG-
DONG ; YU, BING ; LI, YU-JIE ; YANG, JIN-YU ; ET AL.: Mfn1 structures reveal
nucleotide-triggered dimerization critical for mitochondrial fusion. In: *Nature* vol.
542 (2017), Nr. 7641, pp. 372–376
- [66] EHSES, SARAH ; RASCHKE, INES ; MANCUSO, GIUSEPPE ; BERNACCHIA, ANDREA ;
GEIMER, STEFAN ; TONDERA, DANIEL ; MARTINOU, JEAN-CLAUDE ; WESTERMANN,
BENEDIKT ; ET AL.: Regulation of OPA1 processing and mitochondrial fusion by
m-AAA protease isoenzymes and OMA1. In: *Journal of Cell Biology* vol. 187
(2009), Nr. 7, pp. 1023–1036
- [67] ISHIHARA, NAOTADA ; EURA, YUKA ; MIHARA, KATSUYOSHI: Mitofusin 1 and 2
play distinct roles in mitochondrial fusion reactions via GTPase activity. In:
Journal of Cell Science vol. 117 (2004), Nr. 26, pp. 6535–6546
- [68] ROCHA, AGOSTINHO G. ; FRANCO, ANTONIETTA ; KREZEL, ANDRZEJ M. ; RUMSEY,
JEANNE M. ; ALBERTI, JUSTIN M. ; KNIGHT, WILLIAM C. ; BIRIS, NIKOLAOS ;
ZACHARIOUDAKIS, EMMANOUIL ; ET AL.: MFN2 agonists reverse mitochondrial
defects in preclinical models of Charcot-Marie-Tooth disease type 2A. In: *Science*
vol. 360 (2018), Nr. 6386, pp. 336–341

- [69] BASSO, VALENTINA ; MARCHESAN, ELENA ; PEGGION, CATERINA ; CHAKRABORTY, JOY ; STOCKUM, SOPHIA VON ; GIACOMELLO, MARTA ; OTTOLINI, DENIS ; DEBATTISTI, VALENTINA ; ET AL.: Regulation of ER-mitochondria contacts by Parkin via Mfn2. In: *Pharmacological Research* vol. 138 (2018), pp. 43–56
- [70] WAI, TIMOTHY ; SAITA, SHOTARO ; NOLTE, HENDRIK ; MÜLLER, SEBASTIAN ; KÖNIG, TIM ; RICHTER-DENNERLEIN, RICARDA ; SPRENGER, HANS-GEORG ; MADRENAS, JOAQUIN ; ET AL.: The membrane scaffold SLP2 anchors a proteolytic hub in mitochondria containing PARL and the i-AAA protease YME1L. In: *EMBO reports* vol. 17 (2016), Nr. 12, pp. 1844–1856
- [71] COMBOT, YOANN ; SALO, VEIJO T. ; CHADEUF, GILLIANE ; HÖLTTÄ, MAARIT ; VEN, KATHARINA ; PULLI, ILARI ; DUCHEIX, SIMON ; PECQUEUR, CLAIRE ; ET AL.: Seipin localizes at endoplasmic-reticulum-mitochondria contact sites to control mitochondrial calcium import and metabolism in adipocytes. In: *Cell Reports* vol. 38 (2022), Nr. 2, p. 110213
- [72] GORDALIZA-ALAGUERO, ISABEL ; CANTÓ, CARLOS ; ZORZANO, ANTONIO: Metabolic implications of organelle–mitochondria communication. In: *EMBO reports* vol. 20 (2019), Nr. 9, p. e47928
- [73] MEDEIROS, TÂNIA C ; MEHRA, CHAHAT ; PERNAS, LENA: Contact and competition between mitochondria and microbes. In: *Current Opinion in Microbiology* vol. 63 (2021), pp. 189–194
- [74] FLORES-ROMERO, HECTOR ; ROS, URIS ; GARCIA-SAEZ, ANA J: Pore formation in regulated cell death. In: *The EMBO journal* vol. 39 (2020), Nr. 23, p. e105753
- [75] GIACOMELLO, MARTA ; PYAKUREL, ASWIN ; GLYTSOU, CHRISTINA ; SCORRANO, LUCA: The cell biology of mitochondrial membrane dynamics. In: *Nature Reviews Molecular Cell Biology* vol. 21 (2020), Nr. 4, pp. 204–224
- [76] FREZZA, CHRISTIAN ; CIPOLAT, SARA ; BRITO, OLGA MARTINS DE ; MICARONI, MASSIMO ; BEZNOUSSENKO, GALINA V ; RUDKA, TOMASZ ; BARTOLI, DAVIDE ; POLISHUCK, ROMAN S ; ET AL.: OPA1 Controls Apoptotic Cristae Remodeling Independently from Mitochondrial Fusion. In: *Cell* vol. 126 (2006), Nr. 1, pp. 177–189
- [77] GLYTSOU, CHRISTINA ; CALVO, ENRIQUE ; COGLIATI, SARA ; MEHROTRA, ARPIT ; ANASTASIA, IRENE ; RIGONI, GIOVANNI ; RAIMONDI, ANDREA ; SHINTANI, NORIHITO ; ET AL.: Optic Atrophy 1 Is Epistatic to the Core MICOS Component MIC60 in Mitochondrial Cristae Shape Control. In: *Cell reports* vol. 17 (2016), Nr. 11, pp. 3024–3034

- [78] ZAMBERLAN, MARGHERITA ; BOECKX, AMANDINE ; MULLER, FLORIAN ; VINELLI, FEDERICA ; EK, OLIVIER ; VIANELLO, CATERINA ; COART, EMELINE ; SHIBATA, KEITARO ; ET AL.: Inhibition of the mitochondrial protein Opa1 curtails breast cancer growth. In: *Journal of Experimental & Clinical Cancer Research* vol. 41 (2022), Nr. 1, p. 95
- [79] DAVIES, KAREN M ; ANSELMINI, CLAUDIO ; WITTIG, ILKA ; FARALDO-GÓMEZ, JOSÉ D ; KÜHLBRANDT, WERNER: Structure of the yeast F₁F_o-ATP synthase dimer and its role in shaping the mitochondrial cristae. In: *Proceedings of the National Academy of Sciences* vol. 109 (2012), Nr. 34, pp. 13602–13607
- [80] PIZZUTO, MALVINA ; PELEGRIN, PABLO: Cardiolipin in Immune Signaling and Cell Death. In: *Trends in cell biology* vol. 30 (2020), Nr. 11, pp. 892–903
- [81] OTT, CHRISTINE ; DORSCH, EVA ; FRAUNHOLZ, MARTIN ; STRAUB, SEBASTIAN ; KOZJAK-PAVLOVIC, VERA: Detailed Analysis of the Human Mitochondrial Contact Site Complex Indicate a Hierarchy of Subunits. In: *PLoS ONE* vol. 10 (2015), Nr. 3, p. e0120213
- [82] GUARANI, VIRGINIA ; MCNEILL, ELIZABETH M ; PAULO, JOAO A ; HUTTLIN, EDWARD L ; FRÖHLICH, FLORIAN ; GYGI, STEVEN P ; VACTOR, DAVID VAN ; HARPER, J WADE: QIL1 is a novel mitochondrial protein required for MICOS complex stability and cristae morphology. In: *eLife* vol. 4 (2015), p. e06265
- [83] HUYNEN, MARTIJN A. ; MÜHLMEISTER, MAREIKE ; GOTTHARDT, KATHERINA ; GUERRERO-CASTILLO, SERGIO ; BRANDT, ULRICH: Evolution and structural organization of the mitochondrial contact site (MICOS) complex and the mitochondrial intermembrane space bridging (MIB) complex. In: *Biochimica et Biophysica Acta (BBA) - Molecular Cell Research* vol. 1863 (2016), Nr. 1, pp. 91–101
- [84] TARASENKO, DARYNA ; BARBOT, MARIAM ; JANS, DANIEL C. ; KROPPEN, BENJAMIN ; SADOWSKI, BOGUSLAWA ; HEIM, GUDRUN ; MÖBIUS, WIEBKE ; JAKOBS, STEFAN ; ET AL.: The MICOS component Mic60 displays a conserved membrane-bending activity that is necessary for normal cristae morphology. In: *Journal of Cell Biology* vol. 216 (2017), Nr. 4, pp. 889–899
- [85] JOHN, GEORGE B ; SHANG, YONGLEI ; LI, LI ; RENKEN, CHRISTIAN ; MANNELLA, CARMEN A ; SELKER, JEANNE M L ; RANGELL, LINDA ; BENNETT, MICHAEL J ; ET AL.: The mitochondrial inner membrane protein mitofilin controls cristae morphology. In: *Molecular biology of the cell* vol. 16 (2005), Nr. 3, pp. 1543–54
- [86] DARSHI, MANJULA ; MENDIOLA, VINCENT L ; MACKAY, MASON R ; MURPHY, ANNE N ; KOLLER, ANTONIUS ; PERKINS, GUY A ; ELLISMAN, MARK H ; TAYLOR, SUSAN S: ChChd3, an Inner Mitochondrial Membrane Protein, Is Essential for

Maintaining Crista Integrity and Mitochondrial Function. In: *Journal of Biological Chemistry* vol. 286 (2011), Nr. 4, pp. 2918–2932

- [87] BOHNERT, MARIA ; WENZ, LENA-SOPHIE ; ZERBES, RALF M. ; HORVATH, SUSANNE E. ; STROUD, DAVID A. ; MALSBURG, KARINA VON DER ; MÜLLER, JUDITH M. ; OELJEKLAUS, SILKE ; ET AL.: Role of mitochondrial inner membrane organizing system in protein biogenesis of the mitochondrial outer membrane. In: *Molecular Biology of the Cell* vol. 23 (2012), Nr. 20, pp. 3948–3956
- [88] TANG, JUNHUI ; ZHANG, KUAN ; DONG, JUN ; YAN, CHAOJUN ; HU, CHAO ; JI, HONGCHAO ; CHEN, LIANGYI ; CHEN, SHI ; ET AL.: Sam50–Mic19–Mic60 axis determines mitochondrial cristae architecture by mediating mitochondrial outer and inner membrane contact. In: *Cell Death & Differentiation* vol. 27 (2020), Nr. 1, pp. 146–160
- [89] YANG, RUI-FENG ; ZHAO, GUO-WEI ; LIANG, SHU-TING ; ZHANG, YUAN ; SUN, LI-HONG ; CHEN, HOU-ZAO ; LIU, DE-PEI: Mitofilin regulates cytochrome c release during apoptosis by controlling mitochondrial cristae remodeling. In: *Biochemical and Biophysical Research Communications* vol. 428 (2012), Nr. 1, pp. 93–98
- [90] LI, H ; RUAN, Y ; ZHANG, K ; JIAN, F ; HU, C ; MIAO, L ; GONG, L ; SUN, L ; ET AL.: Mic60/Mitofilin determines MICOS assembly essential for mitochondrial dynamics and mtDNA nucleoid organization. In: *Cell Death & Differentiation* vol. 23 (2016), Nr. 3, pp. 380–392
- [91] ERAMO, MATTHEW ; LISNYAK, VALERIE ; FORMOSA, LUKE E ; RYAN, MICHAEL T: The “mitochondrial contact site and cristae organising system” (MICOS) in health and human disease. In: *The Journal of Biochemistry* vol. 167 (2019), Nr. 3, pp. 243–255
- [92] YAMANO, KOJI ; YATSUKAWA, YOH-ICHI ; ESAKI, MASATOSHI ; HOBBS, ALYSON E AIKEN ; JENSEN, ROBERT E ; ENDO, TOSHIYA: Tom20 and Tom22 Share the Common Signal Recognition Pathway in Mitochondrial Protein Import. In: *Journal of Biological Chemistry* vol. 283 (2008), Nr. 7, pp. 3799–3807
- [93] ABE, YOSHITO ; SHODAI, TOSHIHIRO ; MUTO, TAKANORI ; MIHARA, KATSUYOSHI ; TORII, HISAYOSHI ; NISHIKAWA, SHUH-ICHI ; ENDO, TOSHIYA ; KOHDA, DAISUKE: Structural Basis of Presequence Recognition by the Mitochondrial Protein Import Receptor Tom20. In: *Cell* vol. 100 (2000), Nr. 5, pp. 551–560
- [94] MOCZKO, M ; BÖMER, U ; KÜBRICH, M ; ZUFALL, N ; HÖNLINGER, A ; PFANNER, N: The intermembrane space domain of mitochondrial Tom22 functions as a trans binding site for preproteins with N-terminal targeting sequences. In: *Molecular and cellular biology* vol. 17 (1997), Nr. 11, pp. 6574–84

- [95] TRUSCOTT, K N ; KOVERMANN, P ; GEISSLER, A ; MERLIN, A ; MEIJER, M ; DRIESSEN, A J ; RASSOW, J ; PFANNER, N ; ET AL.: A presequence- and voltage-sensitive channel of the mitochondrial preprotein translocase formed by Tim23. In: *Nature structural biology* vol. 8 (2001), Nr. 12, pp. 1074–82
- [96] IEVA, RAFFAELE ; SCHREMPP, SANDRA G ; OPALIŃSKI, ŁUKASZ ; WOLLWEBER, FLORIAN ; HÖB, PHILIPP ; HEIßWOLF, ANNA K ; GEBERT, MICHAEL ; ZHANG, YING ; ET AL.: Mgr2 Functions as Lateral Gatekeeper for Preprotein Sorting in the Mitochondrial Inner Membrane. In: *Molecular Cell* vol. 56 (2014), Nr. 5, pp. 641–652
- [97] LIU, XIN-YI ; WEI, BO ; SHI, HE-XIN ; SHAN, YU-FEI ; WANG, CHEN: Tom70 mediates activation of interferon regulatory factor 3 on mitochondria. In: *Cell Research* vol. 20 (2010), Nr. 9, pp. 994–1011
- [98] YOUNG, JASON C ; HOOGENRAAD, NICHOLAS J ; HARTL, F ULRICH: Molecular chaperones Hsp90 and Hsp70 deliver preproteins to the mitochondrial import receptor Tom70. In: *Cell* vol. 112 (2003), Nr. 1, pp. 41–50
- [99] CHACINSKA, AGNIESZKA ; KOEHLER, CARLA M ; MILENKOVIC, DUSANKA ; LITHGOW, TREVOR ; PFANNER, NIKOLAUS: Importing Mitochondrial Proteins: Machineries and Mechanisms. In: *Cell* vol. 138 (2009), Nr. 4, pp. 628–644
- [100] WEBB, CHAILLE T ; GORMAN, MICHAEL A ; LAZAROU, MICHAEL ; RYAN, MICHAEL T ; GULBIS, JACQUELINE M: Crystal Structure of the Mitochondrial Chaperone TIM9•10 Reveals a Six-Bladed α -Propeller. In: *Molecular Cell* vol. 21 (2006), Nr. 1, pp. 123–133
- [101] GORNICKA, AGNIESZKA ; BRAGOSZEWSKI, PIOTR ; CHROSCICKI, PIOTR ; WENZ, LENA-SOPHIE ; SCHULZ, CHRISTIAN ; REHLING, PETER ; CHACINSKA, AGNIESZKA: A discrete pathway for the transfer of intermembrane space proteins across the outer membrane of mitochondria. In: *Molecular Biology of the Cell* vol. 25 (2014), Nr. 25, pp. 3999–4009
- [102] PELEH, VALENTINA ; CORDAT, EMMANUELLE ; HERRMANN, JOHANNES M: Mia40 is a trans-site receptor that drives protein import into the mitochondrial intermembrane space by hydrophobic substrate binding. In: *eLife* vol. 5 (2016), p. e16177
- [103] JORES, TOBIAS ; KLINGER, ANNA ; GROß, LUCIA E ; KAWANO, SHIN ; FLINNER, NADINE ; DUCHARDT-FERNER, ELKE ; WÖHNERT, JENS ; KALBACHER, HUBERT ; ET AL.: Characterization of the targeting signal in mitochondrial β -barrel proteins. In: *Nature Communications* vol. 7 (2016), Nr. 1, p. 12036

- [104] DOAN, KIM NGUYEN ; GREVEL, ALEXANDER ; MÅRTENSSON, CHRISTOPH U. ; ELLENRIEDER, LARS ; THORNTON, NICOLAS ; WENZ, LENA-SOPHIE ; OPALIŃSKI, ŁUKASZ ; GUIARD, BERNARD ; ET AL.: The Mitochondrial Import Complex MIM Functions as Main Translocase for α -Helical Outer Membrane Proteins. In: *Cell Reports* vol. 31 (2020), Nr. 4, p. 107567
- [105] PAPIĆ, DRAŽEN ; ELBAZ-ALON, YAEL ; KOERDT, SOPHIA NINA ; LEOPOLD, KAROLINE ; WORM, DENNIS ; JUNG, MARTIN ; SCHULDINER, MAYA ; RAPAPORT, DORON: The Role of Djpl in Import of the Mitochondrial Protein Mim1 Demonstrates Specificity between a Cochaperone and Its Substrate Protein. In: *Molecular and Cellular Biology* vol. 33 (2013), Nr. 20, pp. 4083–4094
- [106] BHANGOO, MELANIE K. ; TZANKOV, STEFAN ; FAN, ANNA C.Y. ; DEJGAARD, KURT ; THOMAS, DAVID Y. ; YOUNG, JASON C.: Multiple 40-kDa Heat-Shock Protein Chaperones Function in Tom70-dependent Mitochondrial Import. In: *Molecular Biology of the Cell* vol. 18 (2007), Nr. 9, pp. 3414–3428
- [107] SINZEL, MONIKA ; TAN, TAO ; WENDLING, PHILIPP ; KALBACHER, HUBERT ; ÖZBALCI, CAGAKAN ; CHELIUS, XENIA ; WESTERMANN, BENEDIKT ; BRÜGGER, BRITTA ; ET AL.: Mcp3 is a novel mitochondrial outer membrane protein that follows a unique IMP-dependent biogenesis pathway. In: *EMBO reports* vol. 17 (2016), Nr. 7, pp. 965–981
- [108] HARNER, MAX ; NEUPERT, WALTER ; DEPONTE, MARCEL: Lateral release of proteins from the TOM complex into the outer membrane of mitochondria. In: *The EMBO Journal* vol. 30 (2011), Nr. 16, pp. 3232–3241
- [109] LEONHARD, KLAUS ; STIEGLER, ALEXANDRA ; NEUPERT, WALTER ; LANGER, THOMAS: Chaperone-like activity of the AAA domain of the yeast Yme1 AAA protease. In: *Nature* vol. 398 (1999), Nr. 6725, pp. 348–351
- [110] DESHWAL, SONI ; FIEDLER, KAI UWE ; LANGER, THOMAS: Mitochondrial Proteases: Multifaceted Regulators of Mitochondrial Plasticity. In: *Annual Review of Biochemistry* vol. 89 (2020), Nr. 1, pp. 1–28
- [111] TEIXEIRA, PEDRO FILIPE ; GLASER, ELZBIETA: Processing peptidases in mitochondria and chloroplasts. In: *Biochimica et Biophysica Acta (BBA) - Molecular Cell Research* vol. 1833 (2013), Nr. 2, pp. 360–370
- [112] IEVA, RAFFAELE ; HEIßWOLF, ANNA K. ; GEBERT, MICHAEL ; VÖGTLE, F.-NORA ; WOLLWEBER, FLORIAN ; MEHNERT, CAROLA S. ; OELJEKLAUS, SILKE ; WARSCHIED, BETTINA ; ET AL.: Mitochondrial inner membrane protease promotes assembly of presequence translocase by removing a carboxy-terminal targeting sequence. In: *Nature Communications* vol. 4 (2013), Nr. 1, p. 2853

- [113] GAKH, OLEKSANDR ; CAVADINI, PATRIZIA ; ISAYA, GRAZIA: Mitochondrial processing peptidases. In: *Biochimica et Biophysica Acta (BBA) - Molecular Cell Research* vol. 1592 (2002), Nr. 1, pp. 63–77
- [114] ATORINO, LUIGIA ; SILVESTRI, LAURA ; KOPPEN, MIRKO ; CASSINA, LAURA ; BALLABIO, ANDREA ; MARCONI, ROBERTO ; LANGER, THOMAS ; CASARI, GIORGIO: Loss of m-AAA protease in mitochondria causes complex I deficiency and increased sensitivity to oxidative stress in hereditary spastic paraplegia. In: *The Journal of Cell Biology* vol. 163 (2003), Nr. 4, pp. 777–787
- [115] YANG, QIYUAN ; LIU, PENG PENG ; ANDERSON, NADINE S. ; SHPILKA, TOMER ; DU, YUNGUANG ; NARESH, NANDHITHA UMA ; LI, RUI ; ZHU, LIHUA JULIE ; ET AL.: LONP-1 and ATFS-1 sustain deleterious heteroplasmy by promoting mtDNA replication in dysfunctional mitochondria. In: *Nature Cell Biology* vol. 24 (2022), Nr. 2, pp. 181–193
- [116] RENDÓN, OLGA ZURITA ; SHOUBRIDGE, ERIC A: LONP1 Is Required for Maturation of a Subset of Mitochondrial Proteins, and Its Loss Elicits an Integrated Stress Response. In: *Molecular and Cellular Biology* vol. 38 (2018), Nr. 20
- [117] SHIN, CHUN-SHIK ; MENG, SHUXIA ; GARBIS, SPIROS D. ; MORADIAN, ANNIE ; TAYLOR, ROBERT W. ; SWEREDOSKI, MICHAEL J. ; LOMENICK, BRETT ; CHAN, DAVID C.: LONP1 and mtHSP70 cooperate to promote mitochondrial protein folding. In: *Nature Communications* vol. 12 (2021), Nr. 1, p. 265
- [118] GIBELLINI, LARA ; GAETANO, ANNA DE ; MANDRIOLI, MAURO ; TONGEREN, ELIA VAN ; BORTOLOTTI, CARLO AUGUSTO ; COSSARIZZA, ANDREA ; PINTI, MARCELLO: Chapter One The biology of Lonp1: More than a mitochondrial protease. In: *International Review of Cell and Molecular Biology* vol. 354 (2020), pp. 1–61
- [119] BOGENHAGEN, DANIEL F.: Mitochondrial DNA nucleoid structure. In: *Biochimica et Biophysica Acta (BBA) - Gene Regulatory Mechanisms* vol. 1819 (2012), Nr. 9–10, pp. 914–920
- [120] SZCZEPANOWSKA, KAROLINA ; SENFT, KATHARINA ; HEIDLER, JULIANA ; HERHOLZ, MARIJA ; KUKAT, ALEXANDRA ; HÖHNE, MICHAELA NICOLE ; HOFSETZ, EDUARD ; BECKER, CHRISTINA ; ET AL.: A salvage pathway maintains highly functional respiratory complex I. In: *Nature Communications* vol. 11 (2020), Nr. 1, p. 1643
- [121] SZCZEPANOWSKA, KAROLINA ; MAITI, PRIYANKA ; KUKAT, ALEXANDRA ; HOFSETZ, EDUARD ; NOLTE, HENDRIK ; SENFT, KATHARINA ; BECKER, CHRISTINA ; RUZZENENTE, BENEDETTA ; ET AL.: CLPP coordinates mitoribosomal assembly

- through the regulation of ERAL1 levels. In: *The EMBO Journal* vol. 35 (2016), Nr. 23, pp. 2566–2583
- [122] RAPE, MICHAEL: Ubiquitylation at the crossroads of development and disease. In: *Nature Reviews Molecular Cell Biology* vol. 19 (2018), Nr. 1, pp. 59–70
- [123] SHIIBA, ISSHIN ; TAKEDA, KEISUKE ; NAGASHIMA, SHUN ; YANAGI, SHIGERU: Overview of Mitochondrial E3 Ubiquitin Ligase MITOL/MARCH5 from Molecular Mechanisms to Diseases. In: *International Journal of Molecular Sciences* vol. 21 (2020), Nr. 11, p. 3781
- [124] CHEN, ZIHENG ; LIU, LEI ; CHENG, QI ; LI, YANJUN ; WU, HAO ; ZHANG, WEILIN ; WANG, YUEYING ; SEHGAL, SHEIKH ARSLAN ; ET AL.: Mitochondrial E3 ligase MARCH5 regulates FUNDC1 to fine-tune hypoxic mitophagy. In: *EMBO reports* vol. 18 (2017), Nr. 3, pp. 495–509
- [125] BRAGOSZEWSKI, PIOTR ; WASILEWSKI, MICHAL ; SAKOWSKA, PAULINA ; GORNICKA, AGNIESZKA ; BÖTTINGER, LENA ; QIU, JIAN ; WIEDEMANN, NILS ; CHACINSKA, AGNIESZKA: Retro-translocation of mitochondrial intermembrane space proteins. In: *Proceedings of the National Academy of Sciences* vol. 112 (2015), Nr. 25, pp. 7713–7718
- [126] MCLELLAND, GIAN-LUCA ; SOUBANNIER, VINCENT ; CHEN, CAROL X ; MCBRIDE, HEIDI M ; FON, EDWARD A: Parkin and PINK1 function in a vesicular trafficking pathway regulating mitochondrial quality control. In: *The EMBO Journal* vol. 33 (2014), Nr. 4, pp. 282–295
- [127] KÖNIG, TIM ; NOLTE, HENDRIK ; AALTONEN, MARI J. ; TATSUTA, TAKASHI ; KROLS, MICHIEL ; STROH, THOMAS ; LANGER, THOMAS ; MCBRIDE, HEIDI M.: MIROs and DRP1 drive mitochondrial-derived vesicle biogenesis and promote quality control. In: *Nature Cell Biology* vol. 23 (2021), Nr. 12, pp. 1271–1286
- [128] SOUBANNIER, VINCENT ; MCLELLAND, GIAN-LUCA ; ZUNINO, RODOLFO ; BRASCHI, EMELIE ; RIPPSTEIN, PETER ; FON, EDWARD A. ; MCBRIDE, HEIDI M.: A Vesicular Transport Pathway Shuttles Cargo from Mitochondria to Lysosomes. In: *Current Biology* vol. 22 (2012), Nr. 2, pp. 135–141
- [129] MCLELLAND, GIAN-LUCA ; LEE, SYDNEY A. ; MCBRIDE, HEIDI M. ; FON, EDWARD A.: Syntaxin-17 delivers PINK1/parkin-dependent mitochondrial vesicles to the endolysosomal system. In: *Journal of Cell Biology* vol. 214 (2016), Nr. 3, pp. 275–291
- [130] RYAN, THOMAS A ; PHILLIPS, ELLIOTT O ; COLLIER, CHARLOTTE L ; ROBINSON, ALICE JB ; ROUTLEDGE, DANIEL ; WOOD, REBECCA E ; ASSAR, EMELIA A ; TUMBARELLO, DAVID A: Tollip coordinates Parkin-dependent trafficking of

- mitochondrial-derived vesicles. In: *The EMBO Journal* vol. 39 (2020), Nr. 11, p. e102539
- [131] TODKAR, KIRAN ; CHIKHI, LILIA ; DESJARDINS, VÉRONIQUE ; EL-MORTADA, FIRAS ; PÉPIN, GENEVIÈVE ; GERMAIN, MARC: Selective packaging of mitochondrial proteins into extracellular vesicles prevents the release of mitochondrial DAMPs. In: *Nature Communications* vol. 12 (2021), Nr. 1, p. 1971
- [132] NEUSPIEL, MARGARET ; SCHAUSS, ASTRID C. ; BRASCHI, EMELIE ; ZUNINO, RODOLFO ; RIPPSTEIN, PETER ; RACHUBINSKI, RICHARD A. ; ANDRADE-NAVARRO, MIGUEL A. ; MCBRIDE, HEIDI M.: Cargo-Selected Transport from the Mitochondria to Peroxisomes Is Mediated by Vesicular Carriers. In: *Current Biology* vol. 18 (2008), Nr. 2, pp. 102–108
- [133] SUGIURA, AYUMU ; MATTIE, SEVAN ; PRUDENT, JULIEN ; MCBRIDE, HEIDI M.: Newly born peroxisomes are a hybrid of mitochondrial and ER-derived pre-peroxisomes. In: *Nature* vol. 542 (2017), Nr. 7640, pp. 251–254
- [134] POPOV, LUCIA-DOINA: Mitochondrial-derived vesicles: Recent insights. In: *Journal of Cellular and Molecular Medicine* vol. 26 (2022), Nr. 12, pp. 3323–3328
- [135] ESCOLL, PEDRO ; SONG, OK-RYUL ; VIANA, FLÁVIA ; STEINER, BERNHARD ; LAGACHE, THIBAUT ; OLIVO-MARIN, JEAN-CHRISTOPHE ; IMPENS, FRANCIS ; BRODIN, PRISCILLE ; ET AL.: Legionella pneumophila Modulates Mitochondrial Dynamics to Trigger Metabolic Repurposing of Infected Macrophages. In: *Cell Host & Microbe* vol. 22 (2017), Nr. 3, pp. 302-316.e7
- [136] LUM, MABEL ; MORONA, RENATO: Dynamin-related protein Drp1 and mitochondria are important for Shigella flexneri infection. In: *International Journal of Medical Microbiology* vol. 304 (2014), Nr. 5–6, pp. 530–541
- [137] JAIN, PRASHANT ; LUO, ZHAO-QING ; BLANKE, STEVEN R: Helicobacter pylori vacuolating cytotoxin A (VacA) engages the mitochondrial fission machinery to induce host cell death. In: *Proceedings of the National Academy of Sciences of the United States of America* vol. 108 (2011), Nr. 38, pp. 16032–7
- [138] STAVRU, FABRIZIA ; RIEMER, JAN ; JEX, AARON ; SASSERA, DAVIDE: When bacteria meet mitochondria: The strange case of the tick symbiont Midichloria mitochondrii†. In: *Cellular Microbiology* vol. 22 (2020), Nr. 4, p. e13189
- [139] CHATEL-CHAIX, LAURENT ; CORTESE, MIRKO ; ROMERO-BREY, INÉS ; BENDER, SILKE ; NEUFELDT, CHRISTOPHER JOHN ; FISCHL, WOLFGANG ; SCATURRO, PIETRO ; SCHIEBER, NICOLE ; ET AL.: Dengue Virus Perturbs Mitochondrial Morphodynamics to Dampen Innate Immune Responses. In: *Cell Host & Microbe* vol. 20 (2016), Nr. 3, pp. 342–356

- [140] TO, EUNICE E. ; ERLICH, JONATHAN R. ; LIONG, FELICIA ; LUONG, RAYMOND ; LIONG, STELLA ; ESAQ, FARISHA ; OSEGHAE, OSEZUA ; ANTHONY, DESIREE ; ET AL.: Mitochondrial Reactive Oxygen Species Contribute to Pathological Inflammation During Influenza A Virus Infection in Mice. In: *Antioxidants & Redox Signaling* vol. 32 (2020), Nr. 13, pp. 929–942
- [141] WANG, RUIFANG ; ZHU, YINXING ; LIN, XIAN ; REN, CHENWEI ; ZHAO, JIACHANG ; WANG, FANGFANG ; GAO, XIAOCHEN ; XIAO, RONG ; ET AL.: Influenza M2 protein regulates MAVS-mediated signaling pathway through interacting with MAVS and increasing ROS production. In: *Autophagy* vol. 15 (2019), Nr. 7, pp. 1163–1181
- [142] MEHRZADI, SAEED ; KARIMI, MOHAMMAD YAHYA ; FATEMI, ALIREZA ; REITER, RUSSEL J. ; HOSSEINZADEH, AZAM: SARS-CoV-2 and other coronaviruses negatively influence mitochondrial quality control: beneficial effects of melatonin. In: *Pharmacology & Therapeutics* vol. 224 (2021), p. 107825
- [143] SHI, CHONG-SHAN ; QI, HAI-YAN ; BOULARAN, CEDRIC ; HUANG, NING-NA ; ABU-ASAB, MONES ; SHELHAMER, JAMES H. ; KEHRL, JOHN H.: SARS-Coronavirus Open Reading Frame-9b Suppresses Innate Immunity by Targeting Mitochondria and the MAVS/TRAF3/TRAF6 Signalosome. In: *The Journal of Immunology* vol. 193 (2014), Nr. 6, pp. 3080–3089
- [144] KIM, SEONG-JUN ; SYED, GULAM H. ; SIDDIQUI, ALEEM: Hepatitis C Virus Induces the Mitochondrial Translocation of Parkin and Subsequent Mitophagy. In: *PLoS Pathogens* vol. 9 (2013), Nr. 3, p. e1003285
- [145] KIM, SEONG-JUN ; KHAN, MOHSIN ; QUAN, JUN ; TILL, ANDREAS ; SUBRAMANI, SURESH ; SIDDIQUI, ALEEM: Hepatitis B Virus Disrupts Mitochondrial Dynamics: Induces Fission and Mitophagy to Attenuate Apoptosis. In: *PLoS Pathogens* vol. 9 (2013), Nr. 12, p. e1003722
- [146] LENTINI, GAELLE ; PACHECO, NICOLAS DOS SANTOS ; BURLEIGH, BARBARA A.: Targeting host mitochondria: A role for the *Trypanosoma cruzi* amastigote flagellum. In: *Cellular Microbiology* vol. 20 (2018), Nr. 2, p. e12807
- [147] KAUSHANSKY, A ; METZGER, P G ; DOUGLASS, A N ; MIKOLAJCZAK, S A ; LAKSHMANAN, V ; KAIN, H S ; KAPPE, S HI: Malaria parasite liver stages render host hepatocytes susceptible to mitochondria-initiated apoptosis. In: *Cell Death & Disease* vol. 4 (2013), Nr. 8, p. e762
- [148] HAN, BING ; MA, YANFEN ; TU, VINCENT ; TOMITA, TADAKIMI ; MAYORAL, JOSHUA ; WILLIAMS, TERE ; HORTA, ALINE ; HUANG, HUAN ; ET AL.: Microsporidia Interact with Host Cell Mitochondria via Voltage-Dependent Anion Channels Using Sporoplasm Surface Protein 1. In: *mBio* vol. 10 (2019), Nr. 4, pp. e01944-19

- [149] HERAS, NATALIA DE LAS ; GIMÉNEZ, VIRNA MARGARITA MARTÍN ; FERDER, LEÓN ; MANUCHA, WALTER ; LAHERA, VICENTE: Implications of Oxidative Stress and Potential Role of Mitochondrial Dysfunction in COVID-19: Therapeutic Effects of Vitamin D. In: *Antioxidants* vol. 9 (2020), Nr. 9, p. 897
- [150] GAO, XIAOPAN ; ZHU, KAIXIANG ; QIN, BO ; OLIERIC, VINCENT ; WANG, MEITIAN ; CUI, SHENG: Crystal structure of SARS-CoV-2 Orf9b in complex with human TOM70 suggests unusual virus-host interactions. In: *Nature Communications* vol. 12 (2021), Nr. 1, p. 2843
- [151] ABDUL-SATER, ALI A. ; SAÏD-SADIER, NAJWANE ; LAM, VERISSA M. ; SINGH, BHAVNI ; PETTENGILL, MATTHEW A. ; SOARES, FRASER ; TATTOLI, IVAN ; LIPINSKI, SIMONE ; ET AL.: Enhancement of Reactive Oxygen Species Production and Chlamydial Infection by the Mitochondrial Nod-like Family Member NLRX1. In: *Journal of Biological Chemistry* vol. 285 (2010), Nr. 53, pp. 41637–41645
- [152] MOREIRA, DIANA ; RODRIGUES, VASCO ; ABENGOZAR, MARIA ; RIVAS, LUIS ; RIAL, EDUARDO ; LAFORGE, MIREILLE ; LI, XIAOLING ; FORETZ, MARC ; ET AL.: Leishmania infantum Modulates Host Macrophage Mitochondrial Metabolism by Hijacking the SIRT1-AMPK Axis. In: *PLoS Pathogens* vol. 11 (2015), Nr. 3, p. e1004684
- [153] SHIVAPPAGOWDAR, ABHISHEK ; GARG, SWATI ; SRIVASTAVA, AKRITI ; HADA, RAHUL S. ; KALIA, INDERJEET ; SINGH, AGAM P. ; GARG, LALIT C. ; PATI, SOUMYA ; ET AL.: Pathogenic Pore Forming Proteins of Plasmodium Triggers the Necrosis of Endothelial Cells Attributed to Malaria Severity. In: *Toxins* vol. 13 (2021), Nr. 1, p. 62
- [154] GUPTA, SHIVALI ; BHATIA, VANDANAJAY ; WEN, JIAN-JUN ; WU, YEWEN ; HUANG, MING-HE ; GARG, NISHA JAIN: Trypanosoma cruzi infection disturbs mitochondrial membrane potential and ROS production rate in cardiomyocytes. In: *Free Radical Biology and Medicine* vol. 47 (2009), Nr. 10, pp. 1414–1421
- [155] DUBEY, J P ; LINDSAY, D S ; SPEER, C A: Structures of Toxoplasma gondii Tachyzoites, Bradyzoites, and Sporozoites and Biology and Development of Tissue Cysts. In: *Clinical Microbiology Reviews* vol. 11 (1998), Nr. 2, pp. 267–299
- [156] GENOVA, BRUNO MARTORELLI DI ; WILSON, SARAH K. ; DUBEY, J. P. ; KNOLL, LAURA J.: Intestinal delta-6-desaturase activity determines host range for Toxoplasma sexual reproduction. In: *PLoS Biology* vol. 17 (2019), Nr. 8, p. e3000364

- [157] HOWE, D K ; SIBLEY, L D: Toxoplasma gondii Comprises Three Clonal Lineages: Correlation of Parasite Genotype with Human Disease. In: *Journal of Infectious Diseases* vol. 172 (1995), Nr. 6, pp. 1561–1566
- [158] SHEINER, LILACH ; VAIDYA, AKHIL B ; MCFADDEN, GEOFFREY I: The metabolic roles of the endosymbiotic organelles of Toxoplasma and Plasmodium spp. In: *Current Opinion in Microbiology* vol. 16 (2013), Nr. 4, pp. 452–458
- [159] BLANCHARD, NICOLAS ; GONZALEZ, FEDERICO ; SCHAEFFER, MARIE ; JONCKER, NATHALIE T ; CHENG, TIFFANY ; SHASTRI, ANJALI J ; ROBNEY, ELLEN A ; SHASTRI, NILABH: Immunodominant, protective response to the parasite Toxoplasma gondii requires antigen processing in the endoplasmic reticulum. In: *Nature Immunology* vol. 9 (2008), Nr. 8, pp. 937–944
- [160] DEBIERRE-GROCKIEGO, FRANÇOISE ; CAMPOS, MARCO A. ; AZZOUZ, NAHID ; SCHMIDT, JÖRG ; BIEKER, ULRIKE ; RESENDE, MARIANNE GARCIA ; MANSUR, DANIEL SANTOS ; WEINGART, RALF ; ET AL.: Activation of TLR2 and TLR4 by Glycosylphosphatidylinositols Derived from Toxoplasma gondii. In: *The Journal of Immunology* vol. 179 (2007), Nr. 2, pp. 1129–1137
- [161] HÅKANSSON, SEBASTIAN ; CHARRON, AUDRA J. ; SIBLEY, L.DAVID: Toxoplasma evacuoles: a two-step process of secretion and fusion forms the parasitophorous vacuole. In: *The EMBO Journal* vol. 20 (2001), Nr. 12, pp. 3132–3144
- [162] SCHWAB, J C ; BECKERS, C J ; JOINER, K A: The parasitophorous vacuole membrane surrounding intracellular Toxoplasma gondii functions as a molecular sieve. In: *Proceedings of the National Academy of Sciences* vol. 91 (1994), Nr. 2, pp. 509–513
- [163] CYGAN, ALICJA M. ; THEISEN, TERENCE C. ; MENDOZA, ALMA G. ; MARINO, NICOLE D. ; PANAS, MICHAEL W. ; BOOTHROYD, JOHN C.: Coimmunoprecipitation with MYR1 Identifies Three Additional Proteins within the Toxoplasma gondii Parasitophorous Vacuole Required for Translocation of Dense Granule Effectors into Host Cells. In: *mSphere* vol. 5 (2020), Nr. 1, pp. e00858-19
- [164] GOLD, DANIEL A. ; KAPLAN, AARON D. ; LIS, AGNIESZKA ; BETT, GLENNA C.L. ; ROSOWSKI, EMILY E. ; CIRELLI, KIMBERLY M. ; BOUGDOUR, ALEXANDRE ; SIDIK, SAIMA M. ; ET AL.: The Toxoplasma Dense Granule Proteins GRA17 and GRA23 Mediate the Movement of Small Molecules between the Host and the Parasitophorous Vacuole. In: *Cell Host & Microbe* vol. 17 (2015), Nr. 5, pp. 642–652
- [165] PIRO, FEDERICA ; FOCAIA, RICCARDO ; DOU, ZHICHENG ; MASCI, SILVIA ; SMITH, DAVID ; CRISTINA, MANLIO DI: An Uninvited Seat at the Dinner Table:

- How Apicomplexan Parasites Scavenge Nutrients from the Host. In: *Microorganisms* vol. 9 (2021), Nr. 12, p. 2592
- [166] COPPENS, ISABELLE: Exploitation of auxotrophies and metabolic defects in *Toxoplasma* as therapeutic approaches. In: *International Journal for Parasitology* vol. 44 (2014), Nr. 2, pp. 109–120
- [167] BLUME, MARTIN ; SEEBER, FRANK: Metabolic interactions between *Toxoplasma gondii* and its host. In: *F1000Research* vol. 7 (2018), p. F1000 Faculty Rev-1719
- [168] SINAI, A P ; WEBSTER, P ; JOINER, K A: Association of host cell endoplasmic reticulum and mitochondria with the *Toxoplasma gondii* parasitophorous vacuole membrane: a high affinity interaction. In: *Journal of cell science* vol. 110 (Pt 17) (1997), pp. 2117–28
- [169] JONES, THOMAS C ; HIRSCH, JAMES G: THE INTERACTION BETWEEN TOXOPLASMA GONDII AND MAMMALIAN CELLS. In: *The Journal of Experimental Medicine* vol. 136 (1972), Nr. 5, pp. 1173–1194
- [170] PERNAS, LENA ; ADOMAKO-ANKOMAH, YAW ; SHASTRI, ANJALI J ; EWALD, SARAH E ; TREECK, MORITZ ; BOYLE, JON P ; BOOTHROYD, JOHN C: *Toxoplasma* effector MAF1 mediates recruitment of host mitochondria and impacts the host response. In: *PLoS biology* vol. 12 (2014), Nr. 4, p. e1001845
- [171] BLANK, MATTHEW L. ; PARKER, MICHELLE L. ; RAMASWAMY, RAGHAVENDRAN ; POWELL, CAMERON J. ; ENGLISH, ELIZABETH D. ; ADOMAKO-ANKOMAH, YAW ; PERNAS, LENA F. ; WORKMAN, SEAN D. ; ET AL.: A *Toxoplasma gondii* locus required for the direct manipulation of host mitochondria has maintained multiple ancestral functions. In: *Molecular Microbiology* vol. 108 (2018), Nr. 5, pp. 519–535
- [172] ADOMAKO-ANKOMAH, YAW ; ENGLISH, ELIZABETH D. ; DANIELSON, JEFFREY J. ; PERNAS, LENA F. ; PARKER, MICHELLE L. ; BOULANGER, MARTIN J. ; DUBEY, JITENDER P. ; BOYLE, JON P.: Host Mitochondrial Association Evolved in the Human Parasite *Toxoplasma gondii* via Neofunctionalization of a Gene Duplicate. In: *Genetics* vol. 203 (2016), Nr. 1, pp. 283–298
- [173] KELLY, FELICE D. ; WEI, BRIAN M. ; CYGAN, ALICJA M. ; PARKER, MICHELLE L. ; BOULANGER, MARTIN J. ; BOOTHROYD, JOHN C.: *Toxoplasma gondii* MAF1b Binds the Host Cell MIB Complex To Mediate Mitochondrial Association. In: *mSphere* vol. 2 (2017), Nr. 3, pp. e00183-17
- [174] BLANK, MATTHEW L. ; XIA, JING ; MORCOS, MARY M. ; SUN, MAI ; CANTRELL, PAMELA S. ; LIU, YANG ; ZENG, XUEMEI ; POWELL, CAMERON J. ; ET AL.: *Toxoplasma gondii* association with host mitochondria requires key mitochondrial

protein import machinery. In: *Proceedings of the National Academy of Sciences* vol. 118 (2021), Nr. 12, p. e2013336118

- [175] FUKUMOTO, JUNPEI ; SAKURA, TAKAYA ; MATSUBARA, RYUMA ; TAHARA, MICHIRU ; MATSUZAKI, MOTOMICHI ; NAGAMUNE, KISABURO: Rhoptry kinase protein 39 (ROP39) is a novel factor that recruits host mitochondria to the parasitophorous vacuole of *Toxoplasma gondii*. In: *Biology Open* vol. 10 (2021), Nr. 9, p. bio058988
- [176] FU, YONG ; CUI, XIA ; FAN, SAI ; LIU, JING ; ZHANG, XIAO ; WU, YIHAN ; LIU, QUN: Comprehensive Characterization of *Toxoplasma* Acyl Coenzyme A-Binding Protein TgACBP2 and Its Critical Role in Parasite Cardiolipin Metabolism. In: *mBio* vol. 9 (2018), Nr. 5, pp. e01597-18
- [177] BENDRIS, NAWAL ; SCHMID, SANDRA L.: Endocytosis, Metastasis and Beyond: Multiple Facets of SNX9. In: *Trends in Cell Biology* vol. 27 (2017), Nr. 3, pp. 189–200
- [178] CHENETTE, EMILY J.: A mitochondria–lysosome transport pathway. In: *Nature Cell Biology* vol. 14 (2012), Nr. 2, pp. 130–130
- [179] XU, FANG ; DU, WANQING ; ZOU, QIN ; WANG, YUTING ; ZHANG, XIN ; XING, XUDONG ; LI, YING ; ZHANG, DACHUAN ; ET AL.: COPII mitigates ER stress by promoting formation of ER whorls. In: *Cell Research* (2020), pp. 1–16
- [180] SCHUCK, SEBASTIAN ; GALLAGHER, CIARA M. ; WALTER, PETER: ER-phagy mediates selective degradation of endoplasmic reticulum independently of the core autophagy machinery. In: *Journal of Cell Science* vol. 127 (2014), Nr. 18, pp. 4078–4088
- [181] DERRÉ, ISABELLE ; PYPART, MARC ; DAUTRY-VARSAT, ALICE ; AGAÏSSE, HERVÉ: RNAi Screen in *Drosophila* Cells Reveals the Involvement of the Tom Complex in Chlamydia Infection. In: *PLoS Pathogens* vol. 3 (2007), Nr. 10, p. e155
- [182] NIU, HUA ; KOZJAK-PAVLOVIC, VERA ; RUDEL, THOMAS ; RIKIHISA, YASUKO: *Anaplasma phagocytophilum* Ats-1 Is Imported into Host Cell Mitochondria and Interferes with Apoptosis Induction. In: *PLoS Pathogens* vol. 6 (2010), Nr. 2, p. e1000774
- [183] KOZJAK-PAVLOVIC, VERA ; DIAN-LOTHROP, ELKE A. ; MEINECKE, MICHAEL ; KEPP, OLIVER ; ROSS, KATHARINA ; RAJALINGAM, KRISHNARAJ ; HARSMAN, ANKE ; HAUF, EVA ; ET AL.: Bacterial Porin Disrupts Mitochondrial Membrane Potential and Sensitizes Host Cells to Apoptosis. In: *PLoS Pathogens* vol. 5 (2009), Nr. 10, p. e1000629

7. Acknowledgements

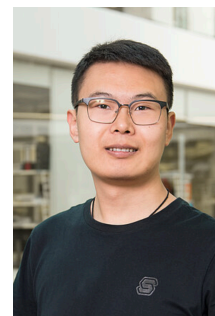
Forever grateful to my parents for bringing me into this world! They raised me up, they taught me how to explore the world, how to get along with people, and how to be peaceful inside. Their behaviors example to me how to be a man, instead of words. Maybe the Chinese poetry “谁言寸草心， 报得三春晖” (Such kindness of warm sun, can't be repaid by grass) is able to express one ten-thousandth of my love.

Thanks to my childhood in the village, tons of happiness and learning in the field, in the river, and in the lake, from grass, flowers, tree, ant, bugs, dragonflies, fish, ducks, birds, cats, dogs, and playmates. Recalling my education, my first literature teacher Xi-Feng Chen (陈希峰) made me realize that I am able to be better one. Thanks to all teachers and professors, who let me pass the examinations. Thanks to everyone in my life, who does not kill a soul by accidental behavior or words. Thanks to professor Xi-Chen Zhang (张西臣), who opened the window of science and trained me to be a researcher. Thanks for Dr. Lena Pernas! She is my supervisor, my friend and my lucky star! She brought me fantastic scientific training, research experience and a great life in Köln! It is sehr fortunate to meet her in my life!

Thanks to all my friends, our story is recalled in my heart again and again, when I typed the words. You know it you are here!

Xianhe Li 李显赫

Max Planck Institute for Biology of Ageing
Joseph Stelzmann Str. 9b, Cologne, Germany
+49 15224029837 • lxianhe@age.mpg.de



Education

Max Planck Institute for Biology of Aging & Cologne University, Ph.D. Lena Pernas Lab & Graduate School for Biological Sciences, Cologne University	05/2019–Now
Max Planck Institute for Infection Biology Thomas F. Meyer Lab	09/2018–04/2019
Jilin University, China M.S. College of Veterinary Medicine	09/2015–06/2018
Jilin University, China B.S. College of Veterinary Medicine	09/2010–06/2015

Experience

04/2013-08/2014

“Evaluation of treatment effect of Herbaceous peony Decoction on Chicken Coccidiosis”

Jilin university students innovative experimental project [grant numbers 2013B81369]

02/2016-02/2017

“Effect of Giardia Virus on the molecular mechanism of Giardiasis”

(Engaged in identification functional mRNA from Giardia Virus)

National Natural Science Foundation of China [grant numbers 31772732].

02/2017-06/2018

“Screening of telomerase-associated proteins and its localization and function in Giardia”

(Engaged in research for telomerase-associated proteins localization and function)

National Natural Science Foundation of China [grant numbers 31672288].

01/2020-Now

“MITO vs TOXO” (Engaged in research for host mitochondrial sense and response to Toxoplasma infection)

European Research Council (ERC) Horizon 2020 action [grant numbers 852457].

Grants, Fellowships, and Awards

National Scholarship in Master (10/2017)

PhD fellowship from China Scholarship Council (09/2018-09/2022)

Boehringer Scholarships (Germany) for FEBS/EMBO summer school (05/2022)

Scientific Conferences and Seminars

Outstanding Oral Report Award (11/2017)

International Symposium on Biodiversity and Evolution of Protozoa (ISBEP) - Guangzhou, China

Poster presentation (09/2021)

EMBO workshop of Mitochondrial homeostasis and human disease - Barcelona, Spain

Selected short scientific talk and poster presentation (05/2022)

EMBO / FEBS Advanced Lecture Course “Lipids, proteins and their interactions in organelle biology” - Athens, Greece

Research Interest

Xianhe Li, was trained as molecular biologist and pathologist. With his research, he aims to translate results from the work probing the role of organelles in the cellular response to an understanding of how cellular metabolism and integrity influence the progression of infectious and degenerative diseases.

Language

Fluency in English

Publications

1. **Li, X.**, Straub, J., Medeiros, T. C., Mehra, C., den Brave, F., Peker, E., ... & Pernas, L. F. (2022). Mitochondria shed their outer membrane in response to infection-induced stress. **Science**, 375(6577), eabi4343.

2. Gong P, **Li X**, Wu W, et al. A novel microRNA from the translated region of the Giardavirus rdrp gene governs virus copy number in *Giardia duodenalis*[J]. **Frontiers in microbiology**, 2020, 11
3. **Li X**, Zhang N, Wu N, et al. Identification of GdRFC1 as a novel regulator of telomerase in *Giardia duodenalis*[J]. **Parasitology research**, 2020, 119(3): 1035-1041.
4. Wang X, Li J, Gong P, **Li X**, et al. Detection of *Neospora caninum* DNA by polymerase chain reaction in bats from Southern China[J]. **Parasitology international**, 2018, 67(4): 389-391.
5. **Li X**, Li J, Zhang X, et al. Prevalence of *Pentatrichomonas hominis* infections in six farmed wildlife species in Jilin, China[J]. **Veterinary parasitology**, 2017, 244: 160-163.
6. Zhang B, Teng Z, **Li X**, et al. Chalcone attenuates *Staphylococcus aureus* virulence by targeting sortase A and alpha-hemolysin[J]. **Frontiers in microbiology**, 2017, 8: 1715.

References

Dr. Pernas Lena

Group Leader, Metabolism of Infection

Max Planck Institute for Biology of Ageing

Phone: +49(0)22137970770

Email: Lena.Pernas@age.mpg.de

Professor Dr. Thomas Langer

Managing Director

Max Planck Institute for Biology of Ageing

Phone: +49 221 37970 88501

Email: langer@age.mpg.de

Professor Dr. Xu-Ming Deng

Veterinary Medicine College, Jilin University

Phone: +86 0431-87836161

Email: dengxm@jlu.edu.cn

Professor Dr. Xi-Chen Zhang

Veterinary Medicine College, Jilin University

Phone: +86 0431-87836155

Email: xc Zhang@jlu.edu.cn

Erklärung zur Dissertation

gemäß der Promotionsordnung vom 12. März 2020

Diese Erklärung muss in der Dissertation enthalten sein. (This version must be included in the doctoral thesis)

„Hiermit versichere ich an Eides statt, dass ich die vorliegende Dissertation selbstständig und ohne die Benutzung anderer als der angegebenen Hilfsmittel und Literatur angefertigt habe. Alle Stellen, die wörtlich oder sinngemäß aus veröffentlichten und nicht veröffentlichten Werken dem Wortlaut oder dem Sinn nach entnommen wurden, sind als solche kenntlich gemacht. Ich versichere an Eides statt, dass diese Dissertation noch keiner anderen Fakultät oder Universität zur Prüfung vorgelegen hat; dass sie - abgesehen von unten angegebenen Teilpublikationen und eingebundenen Artikeln und Manuskripten - noch nicht veröffentlicht worden ist sowie, dass ich eine Veröffentlichung der Dissertation vor Abschluss der Promotion nicht ohne Genehmigung des Promotionsausschusses vornehmen werde. Die Bestimmungen dieser Ordnung sind mir bekannt. Darüber hinaus erkläre ich hiermit, dass ich die Ordnung zur Sicherung guter wissenschaftlicher Praxis und zum Umgang mit wissenschaftlichem Fehlverhalten der Universität zu Köln gelesen und sie bei der Durchführung der Dissertation zugrundeliegenden Arbeiten und der schriftlich verfassten Dissertation beachtet habe und verpflichte mich hiermit, die dort genannten Vorgaben bei allen wissenschaftlichen Tätigkeiten zu beachten und umzusetzen. Ich versichere, dass die eingereichte elektronische Fassung der eingereichten Druckfassung vollständig entspricht.“

Teilpublikationen:

Li, X., Straub, J., Medeiros, T. C., Mehra, C., den Brave, F., Peker, E., ... & Pernas, L. F. (2022). Mitochondria shed their outer membrane in response to infection-induced stress. *Science*, 375(6577), eabi4343.

Datum, Name und Unterschrift

25.08.2022 Xianhe Li (李显赫)



Erklärung zum Gesuch um Zulassung zur Promotion

gemäß der Promotionsordnung vom 12. März 2020

1. Zugänglichkeit von Daten und Materialien

Die Dissertation beinhaltet die Gewinnung von Primärdaten oder die Analyse solcher Daten oder die Reproduzierbarkeit der in der Dissertation dargestellten Ergebnisse setzt die Verfügbarkeit von Datenanalysen, Versuchsprotokollen oder Probenmaterial voraus.

Trifft nicht zu

Trifft zu.

In der Dissertation ist dargelegt wie diese Daten und Materialien gesichert und zugänglich sind (entsprechend den Vorgaben des Fachgebiets beziehungsweise der Betreuerin oder des Betreuers).

2. Frühere Promotionsverfahren

Ich habe bereits einen Dokortitel erworben oder ehrenhalber verliehen bekommen. Oder: Für mich ist an einer anderen Fakultät oder Universität ein Promotionsverfahren eröffnet

worden, aber noch nicht abgeschlossen.

Oder: Ich bin in einem Promotionsverfahren gescheitert.

Trifft nicht zu

Zutreffend

Erläuterung:

3. Straftat

Ich bin nicht zu einer vorsätzlichen Straftat verurteilt worden, bei deren Vorbereitung oder Begehung der Status einer Doktorandin oder eines Doktoranden missbraucht wurde.

Ich versichere, alle Angaben wahrheitsgemäß gemacht zu haben.

Datum 25.08.2022 Name Xianhe Li (李显赫) Unterschrift 